

University of Nevada, Reno

**The Impact of Fines on AC Mixtures Passing Sieve #200 using
Marshall Mix Design**

A thesis submitted in partial fulfillment of the
requirements for the degree of Master of Science in
Civil and Environmental Engineering

by

Mohammad Mehedi Hasan

Dr. Peter E. Sebaaly/Thesis Advisor

May, 2025



THE GRADUATE SCHOOL

We recommend that the thesis
prepared under our supervision by

Mohammad Mehedi Hasan

entitled

**The Impact of Fines on AC Mixtures Passing Sieve #200
using Marshall Mix Design**

be accepted in partial fulfillment of the
requirements for the degree of

Master of Science

Peter E. Sebaaly, Ph.D.
Advisor

Adam J.T. Hand, Ph.D.
Committee Member

Elie Y. Hajj, Ph.D.
Committee Member

Anna Panorska, Ph.D.
Graduate School Representative

Markus Kemmelmeier, Ph.D., Dean
Graduate School

May 2025

Abstract

Asphalt pavements are constantly subjected to the damaging effects of traffic and weather. Fine aggregates play a significant role in the overall performance and durability of asphalt concrete. This research investigates the impact of the percentage of fines passing sieve #200 using the Marshall Mix Design method and evaluates how the varying percentages fine aggregate passing sieve #200 influences the mechanical properties and overall performance of the mixture. The aggregates consisted of sampling from three different sources and two different mix types, each mixtures having a 2% added and reduced fine content to compare with the control mix. The mixture design were conformed to the “Standard Specifications for Public Works Construction” by Regional Transportation Commission (RTC). By adjusting the fines contents p#200 by +2% and -2% from the control mix fines, this study aims to assess its effect on key performance criteria, including cracking resistance, rutting susceptibility, and stiffness. Although some mixtures required binder adjustments to meet the air voids specification of $4 \pm 1.5\%$, most of the mixtures still performed within acceptable limits.

The mixtures underwent performance testing including the Ideal Cracking Test (IDEAL-CT), Hamburg Wheel Tracking Test (HWTT), and Dynamic Modulus (E^*) testing using the Asphalt Mixture Performance Tester (AMPT), under both short-term and mid-term aging conditions. The results revealed that increasing P200 content generally led to higher rutting susceptibility and reduced dynamic modulus, particularly in Type 3 mixtures, indicating decreased stiffness and structural performance. Mixtures with lower

P200 showed a higher CTindex value due to increased binder film thickness because of less amount of fine contents in the mix. Findings emphasize that precise control of fines and binder content is essential to ensure performance, especially under changing field conditions. Overall, this research confirms that even small changes in fine aggregate content can significantly affect asphalt mix behavior and highlights the importance of performance-based mix design for long-term pavement reliability. The study supports the growing shift toward performance-based specifications by demonstrating how fine aggregate content influences key mechanical properties.

ACKNOWLEDGEMENTS

I would like to begin by expressing my deep gratitude to the Pavement Engineering and Science (PES) program, for providing me with the resources and support essential to completing this study. The access to state-of-the-art facilities and expertise within the program has been invaluable throughout my research journey.

My sincerest gratitude goes to my advisor, Dr. Peter E. Sebaaly, for his unwavering support, enthusiasm, and trust in me over the past years. Due to his dedication to research and expertise, working under his supervision has been a rewarding experience and his encouragement has been a true source of motivation. I extend my sincere thanks to Dr. Elie Hajj and Dr. Adam Hand for their invaluable advice and support throughout my graduate studies. I am also thankful to Dr. Anna Panorska for her willingness to serve on my committee and for her thoughtful feedback.

My appreciation also extends to the Regional Transportation Commission (RTC) of Washoe, who made this research possible and who were actively involved and shared their thoughts and knowledge.

I am especially thankful to Dr. Ashraf Alrajhi and Siththarththan Arunthavabalan, our current and past laboratory manager, for their incredible assistance and expertise over the past two years. I am also grateful to my colleagues Dr. Nicole Elias, Bipin Khanal, Mahmoud Khadem, Rita Nasr and others for generously sharing their knowledge and support with laboratory activities whenever needed.

Finally, I would like to thank my family and my friends for their endless love, encouragement and patience. Their support has been my foundation throughout this journey, and I am forever grateful for their unwavering belief in me. I am grateful beyond words to the Almighty for blessing us with health, protection and everything.

Table of Contents

Chapter 1: Introduction	1
1.1 Background	1
1.2 Research Objectives	2
Chapter 2: Literature Review.....	4
2.1 Influence of Gradation on Mixture Properties	4
2.2 Marshall Mix Design.....	5
2.3 Influence of Fines Passing #200 on Mixture Properties	5
2.4 Impact of Fine Content on Rutting and Cracking Resistance	7
2.5 Influence of Fine Content on Dynamic Modulus (E^*).....	8
2.6 Influence of Dust Proportion on Mixture Properties.....	8
Chapter 3: Materials and Mix Design.....	9
3.1 Asphalt Binder Properties	9
3.2 Aggregate Properties.....	11
3.3 Reclaimed Asphalt Pavement (RAP)	13
3.4 MIX DESIGN	15
3.4.1 Aggregate Gradation.....	15
3.4.2 Selection of Optimum Binder Content (OBC)	21
3.4.3 Moisture Sensitivity Test.....	22
3.4.4 Adjustment of Binder Content.....	22
3.4.5 Summary of OBC, VMA and DP for All Mixtures.....	26
Chapter 4: Mixture Performance Test Methods.....	29
4.1 Moisture Sensitivity Testing by Tensile Strength Ratio (TSR)	29
4.1.1 Sample Preparation.....	29
4.1.2 Testing and Evaluation	30
4.2 Engineering Properties: Dynamic Modulus	31
4.2.1 Specimen Preparation	32
4.2.2 Test Matrix	32
4.2.3 Master Curve Development.....	33
4.2.4 Precision and Acceptance.....	34
4.3 Resistance to Rutting: Hamburg Wheel Tracking Test.....	34

4.3.1 Test Apparatus and Procedure.....	35
4.3.2 Performance Metrics and Analysis.....	37
4.3.3 Limitations and Considerations.....	38
4.4 Resistance to Cracking: Indirect Tensile Cracking Test (IDEAL-CT).....	39
4.4.1 Sample Preparation and Test Conditions.....	39
4.4.2 CT _{index} Calculation.....	41
4.4.3 Variability and Repeatability.....	42
Chapter 5: Performance Test Results and Analysis	44
5.1 Tensile Strength Ratio (TSR) Test.....	44
5.2 Engineering Properties: Dynamic Modulus	45
5.3 Resistance to Rutting: Hamburg Wheel Tracking Test.....	53
5.3.1 Stripping Inflection Points (SIP)	60
5.4 Resistance to Cracking: Indirect Tensile Cracking Test (IDEAL-CT).....	64
5.4.1 Conditioning of Specimens	65
5.4.2 CT _{index} after MTOA vs OBC	71
5.4.3 CT _{index} after MTOA vs VMA	72
5.4.4 CT _{index} after MTOA vs DP	73
5.4.5 Interaction Plot for IDEAL-CT Test	75
Chapter 6: Mechanistic Empirical Pavement Modeling	82
6.1 Introduction to Pavement ME Design.....	82
6.2 AASHTOWare Pavement ME Design Software	82
6.3 Model Calibration for Nevada Conditions	83
6.4 Simulation of Mix Performance.....	83
6.5 Key Modeling Insights.....	84
6.6 Future Application of Pavement ME in Fine Content Research.....	85
Chapter 7: Findings, Conclusions, and Recommendations	87
7.1 Findings and Conclusions	87
7.2 Recommendations	88
Chapter 8: References	91

List of Tables

Table 1: Summary of PG Specifications as per AASHTO M320 and M332	10
Table 2: Summary of Aggregate Quality Test Data	12
Table 3: RAP Aggregate Gradations	14
Table 4: RAP Materials Properties	14
Table 5: Aggregate Gradation: Lockwood Type 2	16
Table 6: Aggregate Gradation: Lockwood Type 3	16
Table 7: Aggregate Gradation: Spanish Spring Type 2	17
Table 8: Aggregate Gradation: Spanish Spring Type 3	17
Table 9: Aggregate Gradation: Mustang Type 2	18
Table 10: Aggregate Gradation: Mustang Type 3	18
Table 11: Marshall Mix Design for Lockwood Type 2 Mixtures.....	23
Table 12: Marshall Mix Design for Lockwood Type 3 Mixtures.....	23
Table 13: Marshall Mix Design for Spanish Spring Type 2 Mixtures	24
Table 14: Marshall Mix Design for Spanish Spring Type 3 Mixtures	24
Table 15: Marshall Mix Design for Mustang Type 2 Mixtures.....	25
Table 16: Marshall Mix Design for Mustang Type 3 Mixtures.....	25
Table 17: Summary of Optimum Binder Content for All Mix Designs	26
Table 18: Dynamic Modulus Test Acceptance Limits	34
Table 19: Dynamic Modulus Results for Lockwood Type 2 and Type 3.....	47
Table 20: Dynamic Modulus Results for Spanish Spring Type 2 and Type 3	47
Table 21: Dynamic Modulus Results for Mustang Type 2 and Type 3.....	48
Table 22: HWTT Specifications Used (AASHTO T324).....	54

Table 23: HWTT Results for Lockwood Type 2 at 50°C.....	55
Table 24: HWTT Results for Lockwood Type 3 at 50°C.....	55
Table 25: HWTT Results for Spanish Spring Type 2 at 50°C.....	55
Table 26: HWTT Results for Spanish Spring Type 3 at 50°C.....	56
Table 27: HWTT Results for Mustang Type 2 at 50°C.....	56
Table 28: HWTT Results for Mustang Type 3 at 50°C.....	56
Table 29: IDEAL-CT Specifications (ASTM D8225-19).....	66
Table 30: IDEAL-CT Results for Lockwood Type 2 @ 25C.....	67
Table 31: IDEAL-CT Results for Lockwood Type 3 @ 25C.....	67
Table 32: IDEAL-CT Results for Spanish Spring Type 2 @ 25C.....	68
Table 33: IDEAL-CT Results for Spanish Spring Type 3 @ 25C.....	68
Table 34: IDEAL-CT Results for Mustang Type 2 @ 25C.....	69
Table 35: IDEAL-CT Results for Mustang Type 3 @ 25C.....	69
Table 36: Comparison of Average Performance Test Results Between Pavement ME Output and Laboratory Test	85

List of Figures

Figure 1. Blend gradation chart for Lockwood Type 2: control, -2% and +2% P200.....	19
Figure 2. Blend gradation chart for Lockwood Type 3: control, -2% and +2% P200.....	19
Figure 3. Blend gradation chart for Spanish Spring Type 2: control, -2% and +2% P200.	20
Figure 4. Blend gradation chart for Spanish Spring Type 3: control, -2% and +2% P200.	20
Figure 5. Blend gradation chart for Mustang Type 2: control, -2% and +2% P200.....	21
Figure 6. Blend gradation chart for Mustang Type 2: control, -2% and +2% P200.....	21
Figure 7. Optimum binder content comparison for all 18 asphalt mixtures.	27
Figure 8. Comparison of all mixtures' VMA.....	27
Figure 9. Comparison of DP for all mixtures.	28
Figure 10. Comparison of specification on P200.....	28
Figure 11. Dynamic Modulus Test Setup.	32
Figure 12. Dynamic Modulus Test Specimen Inside the Chamber.	33
Figure 13. Hamburg Wheel Track Machine Setup Before Testing.	36
Figure 14. Sample with Rutting After Hamburg Wheel Track Testing.....	36
Figure 15. HWTT deformation output curve [38].	38
Figure 16. IDEAL-CT Testing Setup with Sample Alignment.	40
Figure 17. Specimen with Cracking Surface after the IDEAL-CT Testing.....	40
Figure 18. IDEAL-CT load vs. displacement data [40].....	42
Figure 19. Tensile strength ratio results for all mixtures.	45
Figure 20. Dynamic modulus master curve for Lockwood Type 2 mixtures.	49
Figure 21. Dynamic modulus master curve for Lockwood Type 3 mixtures.	49
Figure 22. Dynamic modulus master curve for Spanish Spring Type 2 mixtures.....	50
Figure 23. Dynamic modulus master curve for Spanish Spring Type 3 mixtures.....	50
Figure 24. Dynamic modulus master curve for Mustang Type 2 mixtures.	51
Figure 25. Dynamic modulus master curve for Mustang Type 3 mixtures.	51
Figure 26. Comparison of dynamic modulus at 20°C and 10Hz for -2%, control and +2% P200 mix.	52

Figure 27. Comparison of dynamic modulus at 40°C and 10Hz for -2%, control and +2% P200 mix.	53
Figure 28. Rut depth (mm) vs number of passes for Lockwood Type 2 mixtures @ 50°C.	57
Figure 29. Rut depth (mm) vs number of passes for Lockwood Type 3 mixtures @ 50°C.	57
Figure 30. Rut depth (mm) vs number of passes for Spanish Spring Type 2 mixtures @ 50°C.	58
Figure 31. Rut depth (mm) vs number of passes for Spanish Spring Type 3 mixtures @ 50°C.	58
Figure 32. Rut depth (mm) vs number of passes for Mustang Type 2 mixtures @ 50°C.	59
Figure 33. Rut depth (mm) vs number of passes for Mustang Type 3 mixtures @ 50°C.	59
Figure 34. Comparison of rut depth (mm) for -2% p200, control and +2% p200 mixtures at 50°C.	60
Figure 35. SIP for Spanish Spring Type 3 control mixture left wheel.	62
Figure 36. SIP for Lockwood Type 2 +2% P200 left wheel.	62
Figure 37. SIP for Lockwood Type 3 +2% P200 left (a) and right (b) wheel.	63
Figure 38. SIP for Spanish Spring Type 3 +2% P200 left (a) and right (b) wheel.	63
Figure 39. SIP for Mustang Type 3 +2% P200 right wheel.	64
Figure 40. Comparison of Average CTIndex for -2% p200, control and +2% p200 short-term aged mix @ 25°C.	70
Figure 41. Comparison of Average CTIndex for -2% p200, control and +2% p200 mid-term aged mix @ 25°C.	70
Figure 42. CTindex vs OBC.	72
Figure 43. CTindex vs VMA.	73
Figure 44. CTindex vs DP.	74
Figure 45. Interaction plots for Lockwood mid-term aged mix @ 25°C.	77
Figure 46. Interaction plots for Spanish Spring mid-term aged mix @ 25°C.	79
Figure 47. Interaction plots for Mustang mid-term aged mix @ 25°C.	81

Chapter 1: Introduction

1.1 Background

The performance of asphalt mixtures is highly dependent on the gradation and composition of aggregates, particularly the fraction of fines passing the No. 200 sieve (0.075 mm) (P200). These fine aggregates influence the important characteristics of asphalt mix such as workability, moisture susceptibility, and overall durability of the mix. Asphalt concrete pavements, constantly subjected to the combined actions of traffic and weather, must exhibit sufficient durability and resistances to rutting and cracking to maintain their structural integrity and functionality over their intended service life [1]. The durability, cracking, and rutting resistances of asphalt mixtures are essential in determining the longevity and resilience of asphalt pavements. Given the critical role of fines P#200 in asphalt mix behavior, it is essential to understand how varying fine content influences durability, cracking and rutting performance under different loading conditions.

Recent research has highlighted the importance of fine aggregate content and suggested that this fraction plays a significant role in determining mixture characteristics such as stiffness, moisture susceptibility, and resistance to deformation [2]. As a result, adjusting the level of fines has become a focus in optimizing asphalt mixture designs, especially when the objective is to enhance performance and minimize maintenance costs over time. Different State Departments of Transportation (DOTs) have employed various index-based performance tests to assess the laboratory performance of mix designs and impact of material modifications on the durability and cracking and rutting resistance of the mixtures.

This research effort conducted a comprehensive investigation on the impact of P200 content on the performance and durability of AC mixtures. To evaluate the impact of gradations with three different percentages of P200, this study developed 18 different gradation blends from three aggregate sources (Lockwood, Spanish Spring, and Mustang). Two laboratory-mix laboratory-compacted (LMLC) mixtures meeting Type 2 and Type 3 specification limits were utilized as per the Standard Specifications of Public Works Construction, also known as The Orange Book [3]. The Marshall mix design method was used with 15% reclaimed asphalt pavement (RAP), PG64-28NV asphalt binder, and 1.5% hydrated lime. In addition to moisture sensitivity as an indicator of durability, performance tests were conducted to evaluate the mechanical properties of the mixtures, including the Hamburg Wheel Tracking Test (HWTT) for rutting resistance, the Ideal Cracking Test (IDEAL-CT) for cracking susceptibility, and the Dynamic Modulus (E^*) Test to assess stiffness and viscoelastic properties. These tests provide a comprehensive assessment of how fine content variations affect the durability and structural performance of asphalt pavements.

1.2 Research Objectives

The primary objective of this research is to evaluate the influence of different fine content levels on the behavior of asphalt mixtures, particularly in terms of durability, rutting resistance, cracking potential, and stiffness. By analyzing the relationship between P200 and mix performance, this study aims to provide insights that can contribute to improved mix design practices, ensuring better pavement longevity and resistance to environmental and traffic-induced distresses.

To achieve the objectives of the study, the research covered the following tasks:

- Review existing literature to understand the role of gradation in asphalt mixtures and its impact on mechanical properties, drawing insights from current and relevant research.
- Design AC mixtures following the Marshall Method [11] with varying levels of P200 in accordance with the Washoe Regional Transportation Commission (RTC) standard specifications [3] to assess the effects of varying fine aggregate content on mixture performance.
- Evaluate the engineering properties of the mixtures in terms of dynamic modulus (E^*). Conduct performance testing to analyze the rutting and cracking resistance of the mixtures using the Hamburg Wheel Tracking Test (HWTT) and the Ideal Cracking Test (IDEAL-CT) for rutting and cracking resistance, respectively.
- Assess the impact of different P200 levels on the performance properties of the AC mixtures in terms of engineering property, durability, resistance to cracking and resistance to rutting.
- Provide recommendations concerning the control of P200 during construction.

Chapter 2: Literature Review

The performance of asphalt mixtures is highly dependent on the selection and proportioning of materials, particularly the aggregate gradation. This chapter summarizes past research efforts that evaluated the impact of aggregate gradation on the performance of asphalt mixtures.

2.1 Influence of Gradation on Mixture Properties

Several studies have highlighted that aggregate gradation impacts the mixture properties and various pavement performance characteristics, including rutting resistance, workability, and cracking susceptibility [4, 5, 6]. Both coarse and fine aggregates, which make up nearly 95% of the mixture by weight, play important roles in determining key properties such as air voids, voids in mineral aggregate (VMA), stability, and resistances to rutting, cracking and moisture damage. Achieving an optimum blend of aggregates ensures that the mix meets durability and performance requirements. Variations in aggregate gradation during production due to handling, crushing methods, and source variations can significantly affect the final mix properties [7]. Thus, maintaining consistency in aggregate processing is essential for ensuring consistent performance between laboratory mix and plant mix. Some states adopt coarse-graded asphalt mixtures on high-traffic pavements, citing their more durable structure and resistance to rutting [8, 9], but achieving the target density in the field remains a challenge for these mixtures, as they need higher compaction energy to reach the desired level of density. Also, the quality of aggregate is important; weaker aggregates may break down under the impact of the

Marshall hammer during the mix design process, leading to an increase in fines and filler content, which can potentially result in an unusually high Marshall stability [10].

2.2 Marshall Mix Design

The Marshall mix design method is widely used for designing asphalt mixtures by optimizing aggregate gradation and binder content to achieve the desired performance characteristics, performed as per ASTM D6927 [11]. This method evaluates properties such as stability, flow, air voids, VMA, and voids filled with asphalt (VFA) to ensure a balance between strength and durability. Studies have shown that P200 in the mix significantly affects Marshall properties, particularly stability and flow. Higher fines can improve cohesion but may also lead to excessive binder demand, affecting the overall workability and compactability of the mix [17].

2.3 Influence of Fines Passing #200 on Mixture Properties

The P200 fines fraction in the asphalt mix, often referred to as particles passing the No. 200 sieve (0.075 mm), plays a significant role in asphalt mixture performance. While an optimum fine percentage improves cohesion and asphalt binder adhesion, excessive fines can lead to problems, affecting the long-term performance of the pavement. The presence of excessive P200 in asphalt mixtures can significantly impact the mixture performance, influencing key properties such as stiffness, workability, compaction, moisture susceptibility, and long-term durability [9]. Higher amounts of P200 tend to increase mixture stiffness, increase the demand for asphalt content, and enhance moisture sensitivity. However, higher P200 may accelerate oxidation and aging, ultimately reducing

the durability of the pavement [10]. If the fines are smaller than the asphalt film thickness, they may increase the binder volume, reducing binder demand. Sebaaly et al. found that excessive P200 material can affect the fatigue life and thermal cracking of the mix [5].

Researchers have conducted extensive investigations into the effects of fines in hot mix asphalt highlighting that their role varies depending on particle size, composition, and interaction with the binder. The influence of fines on asphalt binders is highly dependent on their particle size and distribution, playing a crucial role in determining the mechanical and durability properties of asphalt mixtures. Fines can act as either fillers or extenders, contributing to the mixture's overall stiffness and workability. However, an excessive quantity of fines can affect the balance of the mixture, causing potential issues such as flushing, bleeding, and rutting [12]. One of the most significant impacts of P200 material is its effect on VMA, which can lower asphalt film thickness, affect the aging of the binder and increase the risk of premature failure [10]. To mitigate these adverse effects, sometimes adjustments in the asphalt binder content may be necessary to maintain the appropriate balance between durability and flexibility. Kandhal et al. suggested that maintaining an asphalt film thickness between 9-10 microns is essential for ensuring higher mix stiffness while thinner films accelerate the aging process, leading to premature pavement deterioration [7].

Excessive P200 can also impact the viscoelastic behavior of the asphalt binder, making it stiffer, which negatively impacts fracture resistance and increases susceptibility to cracking, particularly under thermal stresses [8]. Brian et al. found that certain fines, especially those with high surface area and clay content, can significantly affect moisture susceptibility leading to stripping and weakening of the asphalt-aggregate bond [8]. The

role of fines in HMA is further influenced by their mineralogical composition, which determines their ability to absorb binder and influence mix stiffness. Fines with high methylene blue values tend to retain more moisture, making the mixture more prone to stripping and reducing long-term performance. To ensure the effectiveness of the mixture, fines must be carefully evaluated through particle size analysis, Rigden voids, and other characterization methods [8]. The influence of P200 materials is evident in various asphalt performance tests, including HWTT for rutting, Texas Overlay Test for reflective cracking, IDEAL-CT for cracking, and tensile strength ratio [5]. Proper gradation control and quality assessment of fines are essential for achieving an optimal balance in asphalt mixtures, minimizing premature failures, and enhancing pavement longevity.

2.4 Impact of Fine Content on Rutting and Cracking Resistance

Rutting, or permanent deformation, is a critical distress mode in asphalt pavements, particularly in regions with high traffic loads and elevated temperatures. The HWTT is commonly used to evaluate the rutting resistance of asphalt mixtures. Research has found that excessive fines may lead to binder over-reliance, which could reduce mixture stiffness and lead to premature deformation under repeated loading [13]. A study by Kim et al. found that increasing fine content beyond the limit (above 8% P200) led to a noticeable reduction in the performance of asphalt mixtures in the HWTT [15].

Cracking resistance is another major performance criterion in asphalt pavements, particularly in colder climates or areas with significant thermal fluctuations. The IDEAL-CT has been widely used to evaluate the fracture resistance of asphalt mixtures. Studies suggest that an increase in fine content generally enhances mixture cohesion, which can

improve crack resistance under tensile stresses. However, excessive fines may reduce flexibility and increase brittleness, making the mix more prone to thermal and fatigue cracking [19].

2.5 Influence of Fine Content on Dynamic Modulus (E^*)

Dynamic modulus is a fundamental property used to characterize the viscoelastic behavior of asphalt mixtures under different loading and temperature conditions. The relationship between fine content and dynamic modulus is complex. A higher dynamic modulus generally indicates improved stiffness and load-bearing capacity, which is beneficial for high-traffic pavements. Studies have shown that fine content significantly influences E^* , with excessive fines leading to reduced flexibility [19]. Brown et al. stated that fine content in the range of 5-7% P200 provides an optimal balance between stiffness and fatigue resistance [20].

2.6 Influence of Dust Proportion on Mixture Properties

The dust proportion, defined as the ratio of P200 to the effective binder content of the mix, is a critical parameter affecting asphalt mix performance. Studies have indicated that the optimal dust proportion typically ranges between 0.6 and 1.2, depending on the mix type and expected traffic conditions [21]. Properly managing the dust proportion ensures balanced performance in terms of stability, durability, and resistance to environmental factors.

Chapter 3: Materials and Mix Design

3.1 Asphalt Binder Properties

The performance of asphalt mixtures is highly dependent on the properties of the asphalt binder, which serves as the primary binding agent. Asphalt binders are categorized based on their performance grading (PG), which is determined by evaluating their rheological and mechanical properties under varying temperature and loading conditions.

For this study, a styrene-butadiene-styrene (SBS) polymer-modified asphalt binder was used with a grade of PG64-28NV. The asphalt binder used in this research was obtained from a local supplier located in Fernley, NV. The addition of SBS enhances the binder's elasticity, improving its resistance to rutting at high temperatures while maintaining flexibility at lower temperatures, which is important in preventing fatigue and thermal cracking. The performance grade of the binder was verified using the Superpave Performance Grading system. First, the flashpoint and viscosity tests were conducted to ensure the binder's safety and constructability at production temperatures. Next, the binder was subjected to short-term aging using the Rolling Thin Film Oven, followed by long-term aging in the Pressurized Aging Vessel. The original, short-term aged, and long-term aged binder were tested using the Dynamic Shear Rheometer (DSR) to determine the high and intermediate temperature grades. The Bending Beam Rheometer (BBR) test was performed on the long-term aged binder to evaluate its low-temperature performance. Table 1 summarizes the verification results per AASHTO M320 [25] and M332 [26]. The binder is graded as PG64-28 according to AASHTO M320 and PG 64H-28 according to AASHTO M332.

Table 1: Summary of PG Specifications as per AASHTO M320 and M332.

Test	Units	Test Method	Test Temperature (°C)	Average value	PG Criteria	Met Criteria
Tests on Original Asphalt						
Flash Point, Cleveland Open Cup	°C	AASHTO T 48	-	305.5	230 Minimum	Yes
Rotational Viscosity	Pa.s	AASHTO T316	135	0.59	3.00 Maximum	Yes
Dynamic Shear, $G^*/\sin\delta$ @10 rads/sec	kPa	AASHTO T315	58	3.04	1.00 Minimum	Yes
			64	1.35		Yes
			70	0.65		No
Tests on Residue from Rolling Thin Film Oven						
Dynamic Shear, $G^*/\sin\delta$ @10 rads/sec	kPa	AASHTO T315	58	6.13	2.20 Min.	Yes
			64	3.69		Yes
			70	1.71		No
Average Mass Change	%	AASHTO T240	163	-0.46	1.00 Max.	Yes
Tests on Residue from Pressure Aging Vessel @100 °C (AASHTO R 28)						
Dynamic Shear, $G^*\sin\delta$ @10 rads/sec	kPa	AASHTO T315	22	1325	5,000 Max.	Yes
			19	1930		Yes
			16	2771		Yes
			13	3930		Yes
			10	5510		No
Stiffness modulus, S @ t = 60 sec	MPa	AASHTO T313	-18	140	300 Max.	Yes
			-24	307		No
m-value @ t = 60 sec	-	AASHTO T313	-18	0.31	0.30 Min.	Yes
			-24	0.29		No
MSCR, T350 'H' Traffic Designation	kPa ⁻¹	AASHTO T350	64	$J_{nr\ 3.2} = 1.67$	$J_{nr\ 3.2}$ Max. = 2	Yes
				$J_{nr\ diff.} = 66\%$	$J_{nr\ diff.}$ Max.=75%	Yes
PG 64-28 (per AASHTO M320)						
PG 64H-28 (per AASHTO M332)						

3.2 Aggregate Properties

The aggregates used in this study were sampled from three different local sources: Lockwood, Spanish Spring, and Mustang. Each source was evaluated for compliance with gradation and properties specifications. Gradation analysis was conducted per AASHTO T 11 [27] and AASHTO T 27 [28] to determine the distribution of particle sizes within each stockpile. The evaluation included aggregates meeting Type 2 and Type 3 gradations per the Orange Book for Washoe Regional Transportation Commission projects [3].

To ensure the sampled aggregates met the required quality standards, a comprehensive series of laboratory tests were conducted following standardized procedures. All aggregate properties were measured in accordance with the Orange Book Specifications [3] to verify compliance with standard quality criteria. The evaluation focused on assessing the physical and mechanical properties of the aggregates, including bulk specific gravity, absorption rates for coarse and fine aggregates, and plasticity characteristics. Durability assessments were performed through Los Angeles (L.A.) abrasion and soundness tests to determine resistance to wear and weathering effects. Additionally, fractured face analysis ensured angularity of aggregate to produce sufficient interlock and stability within the mix.

Table 2 summarizes the measured properties of the aggregates from the three sources, along with the corresponding specification limits. The results indicate that all tested aggregates met the applicable requirements for both Type 2 and Type 3 gradations and compliance with standard quality criteria and suitability for asphalt applications.

Table 2: Summary of Aggregate Quality Test Data.

Tests	RTC Criteria	ASTM Method	Test Properties					
			Lock-wood Type 2	Lock-wood Type 3	Spanish Spring Type 2	Spanish Spring Type 3	Mus-tang Type 2	Mus-tang Type 3
Bulk specific gravity of aggregate blend (Gsb Dry)	-	C127	2.622	2.619	2.631	2.624	2.646	2.632
Coarse aggregate absorption, %	4 Max.	C127	2.4	2.2	0.8	0.9	1.1	1.6
Fine aggregate absorption, %	-	C128	2.8	2.9	1.6	1.8	2.2	2.4
Liquid limit of fine aggregate	35 Max.	D4318	0	0	0	0	0	0
Plasticity index of fine aggregate	6 Max.	D1073	NP	NP	NP	NP	NP	NP
L.A. abrasion (500 rev.), %	37% Max.	C131	13.2	17.6	16.9	21.4	14.1	16.5
Fractured Faces, %		D5821						
Fractured, 1 face, %	80% Min.		96	99	100	100	95	99
Fractured, 2 faces, %	50% Min.		93	97	98	99	91	96
Soundness, % loss		C88						
Coarse Aggregate	12% Max.		4.6	2.7	3.2	2.9	2.4	1.9
Fine Aggregate	15% Max.		9.3	6.5	7.6	7.3	5.7	5.1

3.3 Reclaimed Asphalt Pavement (RAP)

RAP is widely used in asphalt mixtures as a sustainable and cost-effective material, that reduces the demand for virgin aggregates and binder, making it an environmentally friendly option while maintaining pavement performance. RAP offers significant environmental and economic advantages by reducing the need for new materials and lowering construction costs [29].

However, careful evaluation of RAP properties is necessary to ensure proper blending with virgin materials and to mitigate potential issues related to mix workability, durability, and cracking susceptibility.

For this study, RAP materials were collected from the three aggregate sources: Lockwood, Spanish Spring, and Mustang. To perform gradation analysis and test the aggregate quality, the RAP aggregates were extracted following AASHTO T 319, the standard method for asphalt binder extraction and recovery [30]. The gradation analysis of RAP aggregates was performed to blend with virgin aggregates. The binder content of the RAP was determined to account for its contribution to the total binder content in the final asphalt mix. Tables 3 and 4 summarize the gradation of RAP aggregate, specific gravity, and the binder contents for all three RAP sources, respectively.

Table 3: RAP Aggregate Gradations.

Sieve Size	Source of RAP		
	Lockwood	Spanish Spring	Mustang
	NMAS		
	1/2"	1/2"	3/8"
1"	100.0	100	100.0
3/4"	100.0	100	100.0
1/2"	100.0	100	100.0
3/8"	97.8	97	99.7
#4	71.8	68	72.6
#8	53.9	50	51.3
#10	50.3	48	45.7
#16	40.5	39	39.0
#30	30.6	35	30.3
#40	25.8	31	24.6
#50	21.4	23	18.8
#100	13.41	18	14.7
#200	9.5	11.8	7.8

Table 4: RAP Materials Properties.

Source	Parameters	
Lockwood	RAP Aggregate Bulk Specific Gravity (dry)	2.6
	RAP Binder Content (TWM)	4.6
	RAP Aggregate: % of Total Aggregate	15
	Type 2: RAP % of Total Mix	14.9
	Type 3: RAP % of Total Mix	14.8
Spanish Spring	RAP Aggregate Bulk Specific Gravity (dry)	2.6
	RAP Binder Content (TWM)	4.3
	RAP Aggregate: % of Total Aggregate	15
	Type 2: RAP % of Total Mix	14.9
	Type 3: RAP % of Total Mix	14.9
Mustang	RAP Aggregate Bulk Specific Gravity (dry)	2.6
	RAP Binder Content (TWM)	5
	RAP Aggregate: % of Total Aggregate	15
	Type 2: RAP% of Total Mix	15.1
	Type 3: RAP% of Total Mix	15

3.4 MIX DESIGN

Mix design is the process of selecting and proportioning asphalt binder and aggregates to produce a mixture that meets specific performance requirements for pavement construction. A well-designed asphalt mix ensures durability, stability, resistance to deformation and adequate flexibility to withstand traffic loads and environmental conditions. The mix design process involves optimizing the blend of aggregates and binder to achieve the desired volumetric and mechanical properties.

The Marshall mix design method is one of the most widely used techniques for designing asphalt mixtures. It was developed by Bruce Marshall in the 1930s and later standardized by the ASTM D6926 [31] and AASHTO T 245 [32] procedures. This method evaluates the strength and stability of asphalt mixtures through volumetric analysis and mechanical testing. It involves compacting asphalt samples using a standard number of hammer blows and measuring properties including stability, flow, air voids (AV), VMA and VFA. The mix design process ensures that the selected asphalt mixture meets the necessary durability, strength, and flexibility requirements, optimizing pavement performance under traffic and environmental conditions.

3.4.1 Aggregate Gradation

Gradation analysis for each aggregate stockpile of the three sources and two types were conducted following the standard procedures outlined in AASHTO T 11 [27] and AASHTO T 27 [28] to assess the particle size distribution. The gradations were evaluated for compliance with Type 2 and Type 3 mix specifications to ensure they conform the required standards outlined in the Orange Book Specifications [3].

To achieve the required gradation for Type 2 and Type 3 mixtures, the blend composition was adjusted by modifying stockpile percentages while maintaining control point restrictions on key sieve sizes. Six mix gradations were developed from the three aggregate sources, each meeting the designated specification limits. Tables 5 to 10 provides a summary of the blend gradations.

Table 5: Aggregate Gradation: Lockwood Type 2.

Sieve Size	Stockpile Percentages							RTC Specification
	17	16	16	16.74	19.26	15	100	
	3/4"	1/2"	3/8"	Crusher Fines	Washed Sand	RAP 1/2"	Combined	
1"	100.0	100.0	100.0	100.0	100.0	100.0	100.00	100
3/4"	99.7	100.0	100.0	100.0	100.0	100.0	99.94	90-100
1/2"	44.8	99.2	100.0	100.0	100.0	100.0	90.49	
3/8"	8.5	65.4	100.0	100.0	99.8	97.8	78.54	63-85
#4	2.2	2.2	37.5	99.9	89.9	71.8	51.54	45-63
#8	1.7	1.5	4.6	73.7	81.8	54.0	37.46	
#10	1.6	1.4	3.8	65.7	59.0	50.3	30.99	30-44
#16	1.4	1.2	3.0	47.2	37.8	40.5	22.16	
#30	1.3	1.1	2.4	33.0	27.2	30.6	16.14	
#40	1.3	1.1	2.2	28.6	17.7	25.8	12.82	12-22
#50	1.3	1.0	2.0	25.5	5.5	21.4	9.25	
#100	1.3	1.0	1.8	21.5	2.1	13.4	6.67	
#200	1.1	0.9	1.5	18.0	1.1	9.5	5.23	3-8

Table 6: Aggregate Gradation: Lockwood Type 3.

Sieve Size	Stockpile Percentages						RTC Specification
	23.76	20.79	20.58	18.62	15	100	
	1/2"	3/8"	Crusher Fines	Washed Sand	RAP 1/2"	Combined	
1/2"	99.2	100.0	100.0	100.0	100.0	99.80	100
3/8"	65.4	100.0	100.0	99.8	97.8	91.41	85-100
#4	2.2	37.5	99.9	89.9	71.8	57.65	50-75
#8	1.5	4.6	73.7	81.8	4.0	41.07	
#10	1.4	3.8	65.7	59.0	50.3	34.41	32-52
#16	1.2	3.0	47.2	37.8	40.5	24.97	
#30	1.1	2.4	33.0	27.2	30.6	18.44	
#40	1.1	2.2	28.6	17.8	25.8	15.00	12-26
#50	1.0	2.0	25.5	5.5	21.4	11.39	
#100	1.0	1.8	21.5	2.1	13.4	8.67	
#200	0.9	1.5	18.0	1.1	9.5	6.75	3-8

Table 7: Aggregate Gradation: Spanish Spring Type 2.

Sieve Size	Stockpile Percentages							RTC Specification
	20	10	10	35	10	15	100	
	3/4"	1/2"	3/8"	Washed AC Sand	Washed Natural Sand	1/2" Rap	Combined	
1"	100	100	100	100	100	100	100.00	100
3/4"	99	100	100	100	100	100	99.80	90-100
1/2"	41	100	100	100	100	100	88.20	
3/8"	12	73	100	100	100	97	79.25	63-85
#4	6	8	23	98	99	68	58.70	45-63
#8	3	3	8	67	91	50	41.75	
#10	2	2	6	57	87	48	37.05	30-44
#16	2	2	6	41	65	39	27.90	
#30	2	1	5	26	36	35	18.95	
#40	1	1	4	20	26	31	14.95	12-22
#50	1	1	4	17	13	23	11.40	
#100	1	1	3	10	7	18	7.50	
#200	1.0	0.8	3.4	5.6	4.6	11.8	4.81	3-8

Table 8: Aggregate Gradation: Spanish Spring Type 3.

Sieve Size	Stockpile Percentages							RTC Specification
	30	10	35	5	5	15	100	
	1/2"	3/8"	W.AC Sand	Crusher Dust	W. Natural Sand	1/2" Rap	Combined	
3/4"	100	100	100	100	100	100	100.00	
1/2"	100	100	100	100	100	100	100.00	100
3/8"	73	100	100	100	100	97	91.45	85-100
#4	8	23	98	100	99	68	59.15	50-75
#8	3	8	67	68	91	50	40.60	
#10	2	6	57	65	87	48	35.95	32-52
#16	2	6	41	38	65	39	26.55	
#30	1	5	26	34	36	35	18.65	
#40	1	4	20	33	26	31	15.30	12-26
#50	1	4	17	21	13	23	11.80	
#100	1	3	10	17	7	18	8.00	
#200	0.8	3.4	5.6	15.8	4.6	11.3	5.3	3-8

Table 9: Aggregate Gradation: Mustang Type 2.

Sieve Size	Stockpile Percentages						RTC Specification
	13	32	33	7	15	100	
	3/4"	1/2"	Crusher Fines	Sand	RAP 3/8"	Combined	
1"	100.0	100.0	100.0	100.0	100.0	100.0	100
3/4"	68.2	99.3	100.0	100.0	100.0	95.6	90-100
1/2"	6.1	64.6	100.0	100.0	100.0	76.5	
3/8"	4.1	23.4	100.0	100.0	99.7	63.0	63-85
#4	2.7	2.4	89.8	100.0	72.6	48.6	45-63
#8	1.4	2.1	57.3	99.7	51.3	34.4	
#10	1.1	1.8	53.9	99.5	45.7	32.3	30-44
#30	1.0	1.3	21.7	87.2	30.3	18.4	
#40	1.0	1.0	18.5	72.1	24.6	15.3	12-22
#100	1.0	1.0	10.4	23.2	14.7	7.7	
#200	1.0	1.0	8.8	9.5	7.8	5.2	3-8

Table 10: Aggregate Gradation: Mustang Type 3.

Sieve Size	Stockpile Percentages					RTC Specification
	43	32	10	15	100	
	3/8"	Crusher Fines	Sand	RAP 3/8"	Combined	
1/2"	100.0	100.0	100.0	100.0	100.00	100
3/8"	96.7	100.0	100.0	99.7	98.54	85-100
#4	6.9	89.8	100.0	72.6	52.59	50-75
#8	2.3	57.3	99.7	51.3	36.99	
#10	1.5	53.9	99.5	45.7	34.70	32-52
#30	1.1	21.7	87.2	30.3	20.68	
#40	1.0	18.5	72.1	24.6	17.25	12-26
#100	1.0	10.4	23.2	14.7	8.28	
#200	0.6	8.8	9.5	7.8	5.19	3-8
Pan	0	0	0	0		

Figures 1-6 present the gradation chart for the aggregates, with the minimum and maximum control points for each sieve size, denoted in red triangles. The bin percentage were adjusted by trials based on control points on several sieve sizes as per the specification to ensure compliance with the Orange book standards. All the aggregate blends are within the control points, specified for Type 2 and Type 3 mixtures.

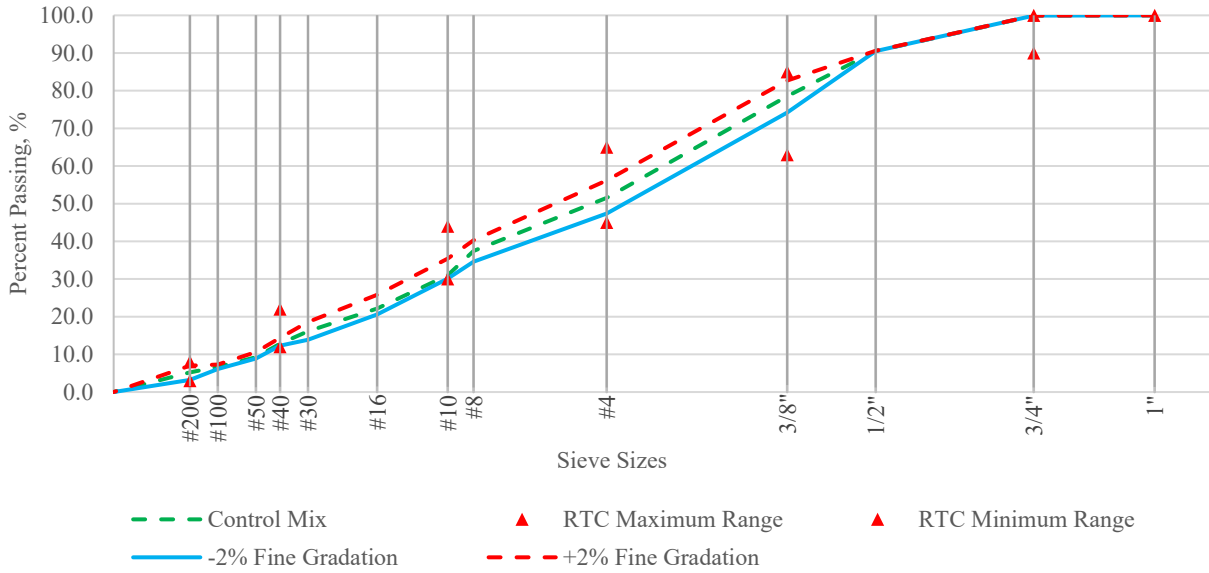


Figure 1. Blend gradation chart for Lockwood Type 2: control, -2% and +2% P200.

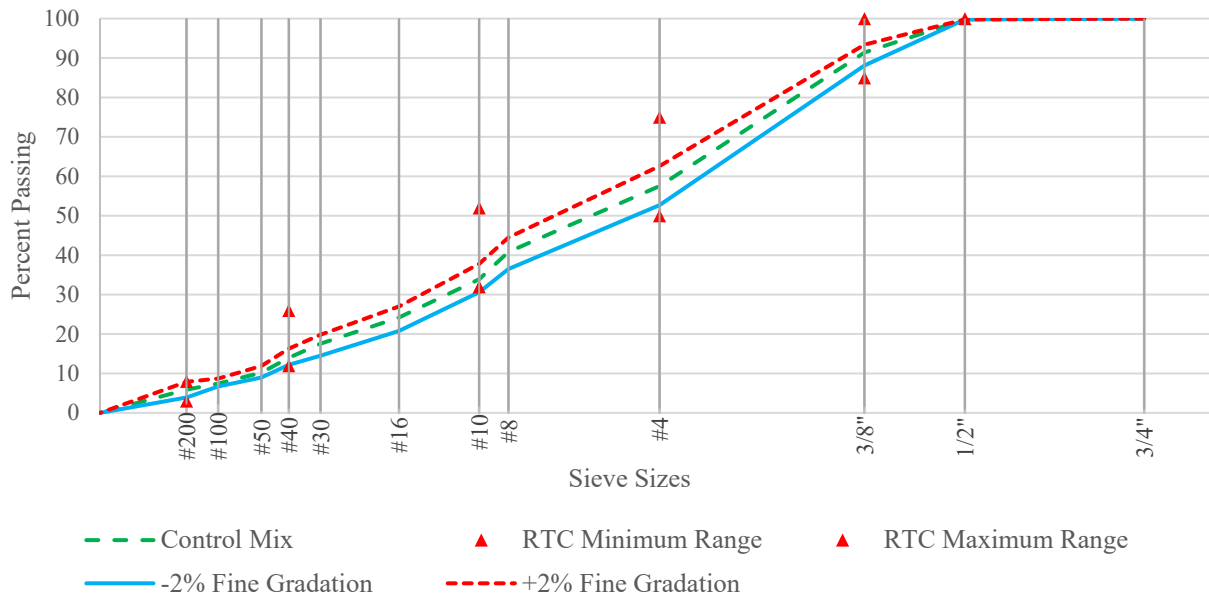


Figure 2. Blend gradation chart for Lockwood Type 3: control, -2% and +2% P200.

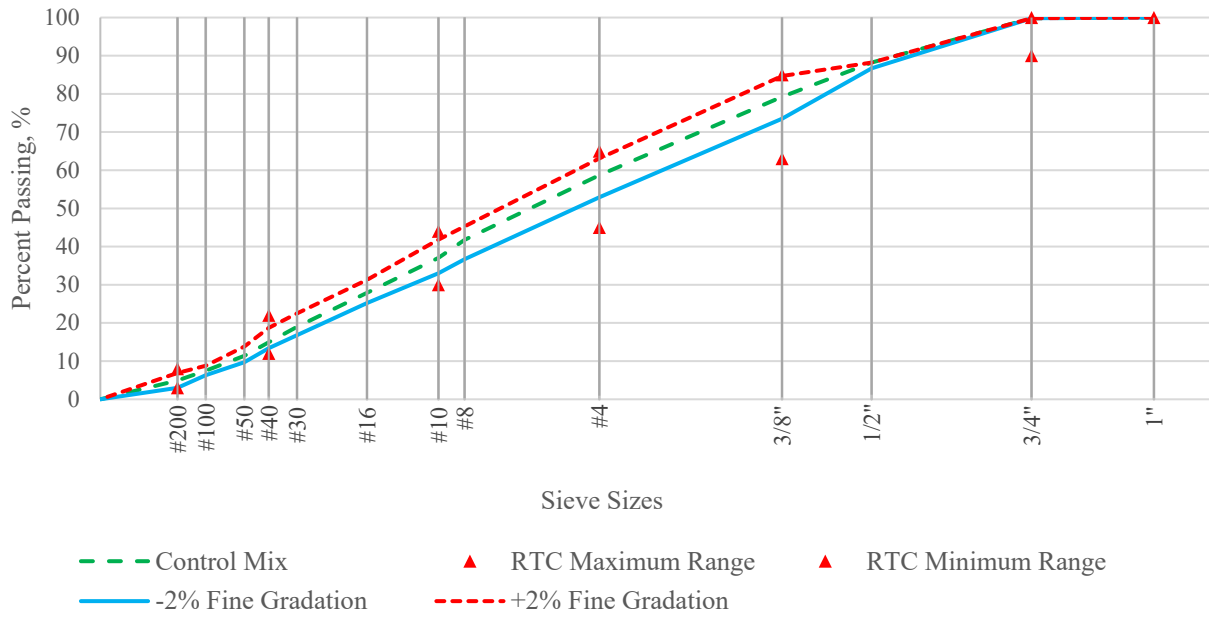


Figure 3. Blend gradation chart for Spanish Spring Type 2: control, -2% and +2% P200.

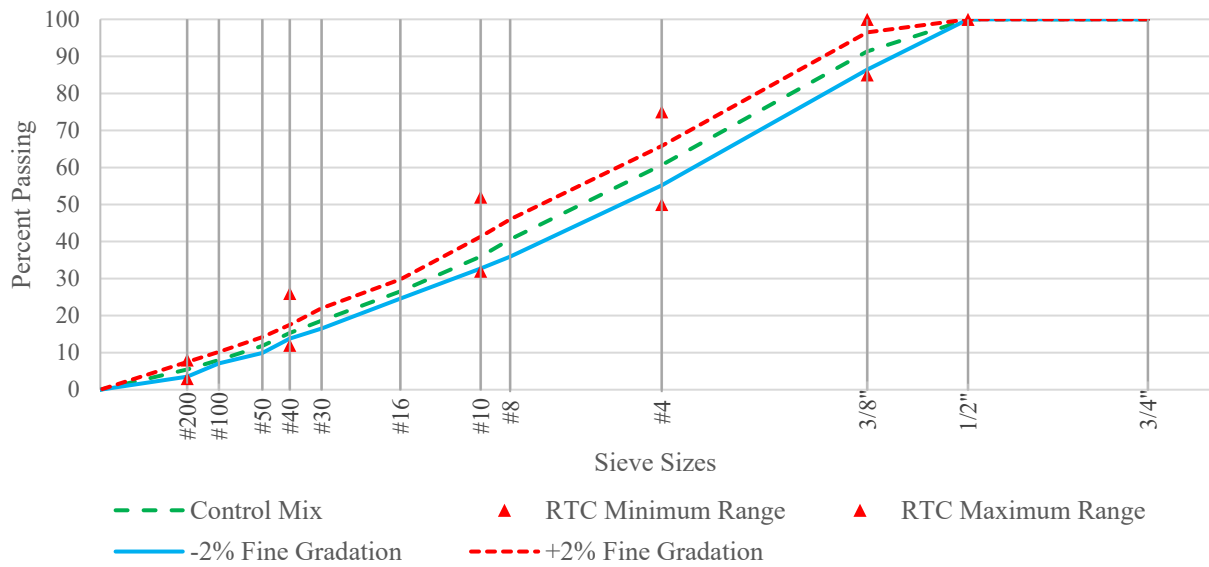


Figure 4. Blend gradation chart for Spanish Spring Type 3: control, -2% and +2% P200.

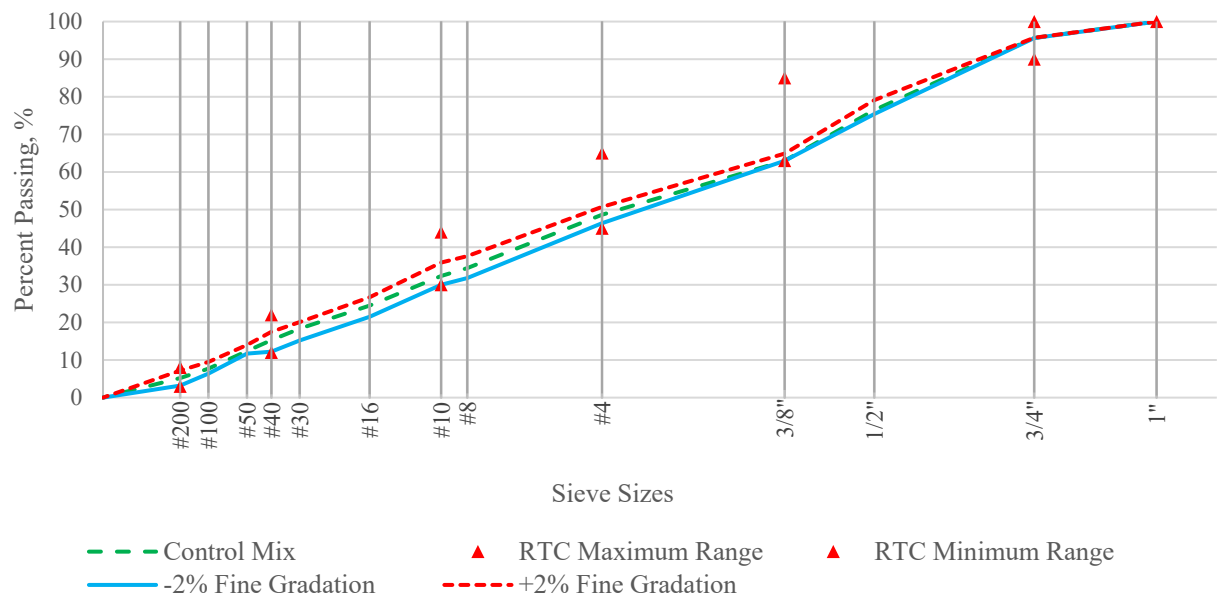


Figure 5. Blend gradation chart for Mustang Type 2: control, -2% and +2% P200.

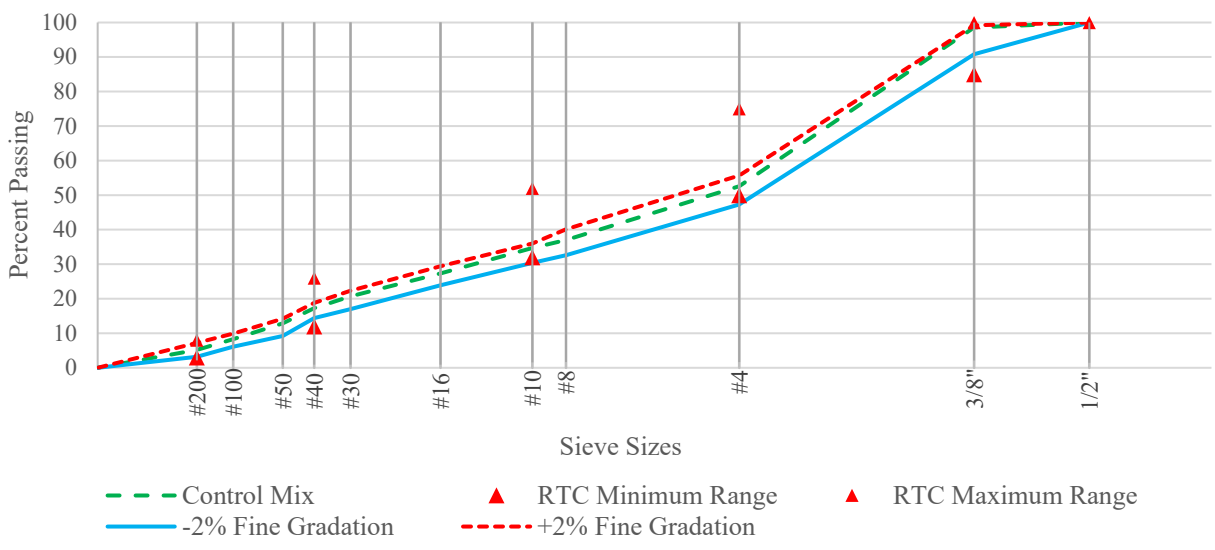


Figure 6. Blend gradation chart for Mustang Type 2: control, -2% and +2% P200.

3.4.2 Selection of Optimum Binder Content (OBC)

Optimum binder content ensures a balanced mix with adequate strength, durability, and flexibility. Mix designs were performed following the Marshall Mix Design method to determine the OBC for all eighteen mixtures. The process began with aggregate gradation analysis, followed by batching and preparation where aggregates and RAP were proportioned and preheated. From each

aggregate source, two mixture types: Type 2 and Type 3 were initially designed to meet the specifications, all with 15% RAP. The mixtures were considered as the “control mixtures.” Subsequently, the P200 content for each mix was adjusted by $\pm 2\%$, resulting in three distinct mixtures for each source and type. This approach allowed for evaluating the impact of fine content variation on the performance of asphalt mixtures.

Mixing with asphalt binder was performed with proper conditioning at the target temperature to ensure uniform coating. The prepared mixtures were then compacted using the Marshall hammer with standard blows per face. The specimens were compacted by applying 75 blows for Type 2 and 50 blows for Type 3 mix on each side of the specimen. Theoretical maximum specific gravity (G_{mm}) and bulk specific gravity (G_{mb}) were determined to assess density and air voids. For each gradation, four different binder contents were used to evaluate properties including air voids, stability, and flow. The optimum binder content was chosen at 4% air voids. Marshall stability and flow tests were conducted to measure load-bearing capacity and resistance to deformation. Finally, the OBC was determined by balancing air voids, VMA, VFA and stability values.

3.4.3 Moisture Sensitivity Test

Moisture Sensitivity Test of the Marshall compacted specimens were performed at air void of $7 \pm 0.5\%$. The tensile strength ratio (TSR) was calculated as the ratio of the average tensile strength of the conditioned specimens over the average tensile of the unconditioned specimens.

3.4.4 Adjustment of Binder Content

When the P200 percentage was adjusted by $\pm 2\%$, some mixtures failed to meet the air voids criterion of $4 \pm 1.5\%$. To address this, the binder content was adjusted accordingly to bring the air voids within the acceptable range. In some cases, the OBC was modified to ensure compliance with the allowable air voids requirement during construction. These adjustments were necessary

to maintain the desired mix performance and durability.

The detailed mix designs including the optimum binder content, VMA%, VFA%, dust proportion, and TSR are presented in Tables 11 – 16.

Table 11: Marshall Mix Design for Lockwood Type 2 Mixtures.

Marshall Mix Design for PG 64-28NV and Lockwood Type 2 Aggregate				
Property	Control Mix	-2% Fines	+2% Fines	RTC Specification
Hydrated Lime, %	1.5			1.5
Mixing Temperature, °F	315			310-320
Compaction Temperature, °F	295			293-300
Optimum Binder (OBC), % TWM	4.7	4.7	4.7	-
Air Voids, % TWM	4.0	4.1	2.9	4 (JMF ± 1.5)
VMA, %	13.4	13.4	13.4	13 Min
VFA, %	70.1	70.1	70.1	65 - 75
Dust Proportion, P _{0.075} /P _{be}	1.2	1.2	1.2	0.8 - 1.2
Gmm at OBC	2.48	2.49	2.48	-
Pbe at OBC, %	3.6	3.6	3.6	-
Unconditioned Tensile Strength at OBC @77F, psi	187.8	175.8	192.4	65
Conditioned Tensile Strength at OBC @77F, psi	162.0	161.3	180.5	-
Tensile Strength Ratio at OBC @77F, %	86.3	85.2	93.8	70% Min

Table 12: Marshall Mix Design for Lockwood Type 3 Mixtures.

Marshall Mix Design for PG 64-28NV and Lockwood Type 3 Aggregate				
Property	Control Mix	-2% Fines	+2% Fines	RTC Specification
Hydrated Lime, %	1.5			1.5
Mixing Temperature, °F	315			310-320
Compaction Temperature, °F	295			293-300
Optimum Binder (OBC), % TWM	5.9	5.9	5.7	-
Air Voids, % TWM	4.0	4.0	2.5	4 (JMF ± 1.5)
VMA, %	14.9	14.9	15.2	14 Min
VFA, %	75.5	75.5	69	65 - 78
Dust Proportion, P _{0.075} /P _{be}	1.2	1.2	1.2	0.6 – 1.2
Gmm at OBC	2.43	2.42	2.43	-
Pbe at OBC, %	4.7	4.7	4.7	-
Unconditioned Tensile Strength at OBC @77F, psi	121.9	131.6	147.4	65
Conditioned Tensile Strength at OBC @77F, psi	111.0	103.2	143.3	-
Tensile Strength Ratio @77F, %	91.1	78.4	97.3	70% Min

Table 13: Marshall Mix Design for Spanish Spring Type 2 Mixtures.

Marshall Mix Design for PG 64-28NV and Spanish Spring Type 2 Aggregate				
Property	Control Mix	-2% Fines	+2% Fines	RTC Specification
Hydrated Lime, %		1.5		1.5
Mixing Temperature, °F		315		310-320
Compaction Temperature, °F		295		293-300
Optimum Binder (OBC), % TWM		4.4		-
Air Voids, % TWM	4.0	4.0	3.3	4 (JMF ± 1.5)
VMA, %	13.0	13.0	13.0	13 Min
VFA, %	68	68	68	65 - 75
Dust Proportion, $P_{0.075}/P_{be}$	1.2	1.2	1.2	0.8 - 1.2
Gmm at OBC	2.50	2.51	2.49	-
Pbe at OBC, %	3.3	3.3	3.3	-
Unconditioned Tensile Strength at OBC @77F, psi	192.3	176.8	190.2	65
Conditioned Tensile Strength at OBC @77F, psi	177.5	161.6	167.6	-
Tensile Strength Ratio at OBC @77F, %	92	91.4	88.1	70% Min

Table 14: Marshall Mix Design for Spanish Spring Type 3 Mixtures.

Marshall Mix Design for PG 64-28NV and Spanish Spring Type 3 Aggregate				
Property	Control Mix	-2% Fines	+2% Fines	RTC Specification
Hydrated Lime, %		1.5		1.5
Mixing Temperature, °F		315		310-320
Compaction Temperature, °F		295		293-300
Optimum Binder (OBC), % TWM	4.9	4.9	4.7	-
Air Voids, % TWM	4.0	4.0	2.5	4 (JMF ± 1.5)
VMA, %	14	14	14.2	14 Min
VFA, %	72.1	72.1	68	65 - 78
Dust Proportion, $P_{0.075}/P_{be}$	1.1	1.1	1.1	0.6 - 1.2
Gmm at OBC	2.47	2.47	2.47	-
Pbe at OBC, %	4.3	4.3	4.3	-
Unconditioned Tensile Strength at OBC @77F, psi	170.8	155.4	167	65
Conditioned Tensile Strength at OBC @77F, psi	159.6	132.7	146.8	-
Tensile Strength Ratio at OBC @77F, %	93.4	75.4	87.9	70% Min

Table 15: Marshall Mix Design for Mustang Type 2 Mixtures.

Marshall Mix Design for PG 64-28NV and Spanish Mustang Type 2 Aggregate				
Property	Control Mix	-2% Fines	+2% Fines	RTC Specification
Hydrated Lime, %	1.5			1.5
Mixing Temperature, °F	315			310-320
Compaction Temperature, °F	295			293-300
Optimum Binder (OBC), % TWM	4.6			-
Air Voids, % TWM	4.0	4.0	3.1	4 (JMF ± 1.5)
VMA, %	13.2	13.2	13.2	13 Min
VFA, %	70	70	70	65 - 75
Dust Proportion, $P_{0.075}/P_{bc}$	1.2	1.2	1.2	0.8 - 1.2
Gmm at OBC	2.51	2.52	2.51	-
Pbe at OBC, %	3.5	3.5	3.5	-
Unconditioned Tensile Strength at OBC @77F, psi	176.6	172.1	179.9	65
Conditioned Tensile Strength at OBC @77F, psi	169.5	160.4	159.2	-
Tensile Strength Ratio at OBC @77F, %	96	93.2	88.5	70% Min

Table 16: Marshall Mix Design for Mustang Type 3 Mixtures.

Marshall Mix Design for PG 64-28NV and Spanish Mustang Type 3 Aggregate				
Property	Control Mix	-2% Fines	+2% Fines	RTC Specification
Hydrated Lime, %	1.5			1.5
Mixing Temperature, °F	315			310-320
Compaction Temperature, °F	295			293-300
Optimum Binder (OBC), % TWM	5.6	5.6	5.3	-
Air Voids, % TWM	4.0	4.1	2.6	4 (JMF ± 1.5)
VMA, %	14.1	14.1	14.3	14 Min
VFA, %	72	72	67.5	65 - 78
Dust Proportion, $P_{0.075}/P_{bc}$	1.2	1.2	1.2	0.6 - 1.2
Gmm at OBC	2.49	2.49	2.48	-
Pbe at OBC, %	4.3	4.3	4.3	-
Unconditioned Tensile Strength at OBC @77F, psi	170.8	155.4	167	65
Conditioned Tensile Strength at OBC @77F, psi	159.6	132.7	146.8	-
Tensile Strength Ratio at OBC @77F, %	93.4	75.4	87.9	70% Min

3.4.5 Summary of OBC, VMA and DP for All Mixtures

Table 17 summarizes the OBC determined for all 18 asphalt mix designs, considering three aggregate sources (Lockwood, Spanish Spring, and Mustang), two mix types (Type 2 and Type 3), and three levels of P200 content (-2%, Control, and +2%). In accordance with the RTC job control grading brand [3], the acceptable air void range is $4\% \pm 1.5\%$. When P200 content was adjusted by $\pm 2\%$, some mixtures failed to meet this air void criterion, necessitating adjustments to the binder content to ensure compliance. However, for Type 2 mixtures across all sources, the OBC remained unchanged, indicating that the air voids were still within acceptable limits and no modification to the binder content was required. For Type 3 mixtures, slight reductions in OBC were observed as P200 increased in some cases, which suggests that higher fines content may reduce the binder demand due to increase air voids. Figure 7 provides a visual comparison of these values across all mix configurations.

Table 17: Summary of Optimum Binder Content for All Mix Designs.

Aggregate Source	Mix Type	P200	OBC (%)
Lockwood	Type 2	-2%	4.7
		Control	4.7
		+2%	4.7
	Type 3	-2%	5.9
		Control	5.9
		+2%	5.7
Spanish Spring	Type 2	-2%	4.4
		Control	4.4
		+2%	4.4
	Type 3	-2%	4.9
		Control	4.9
		+2%	4.7
Mustang	Type 2	-2%	4.6
		Control	4.6
		+2%	4.6
	Type 3	-2%	5.6
		Control	5.6
		+2%	5.3

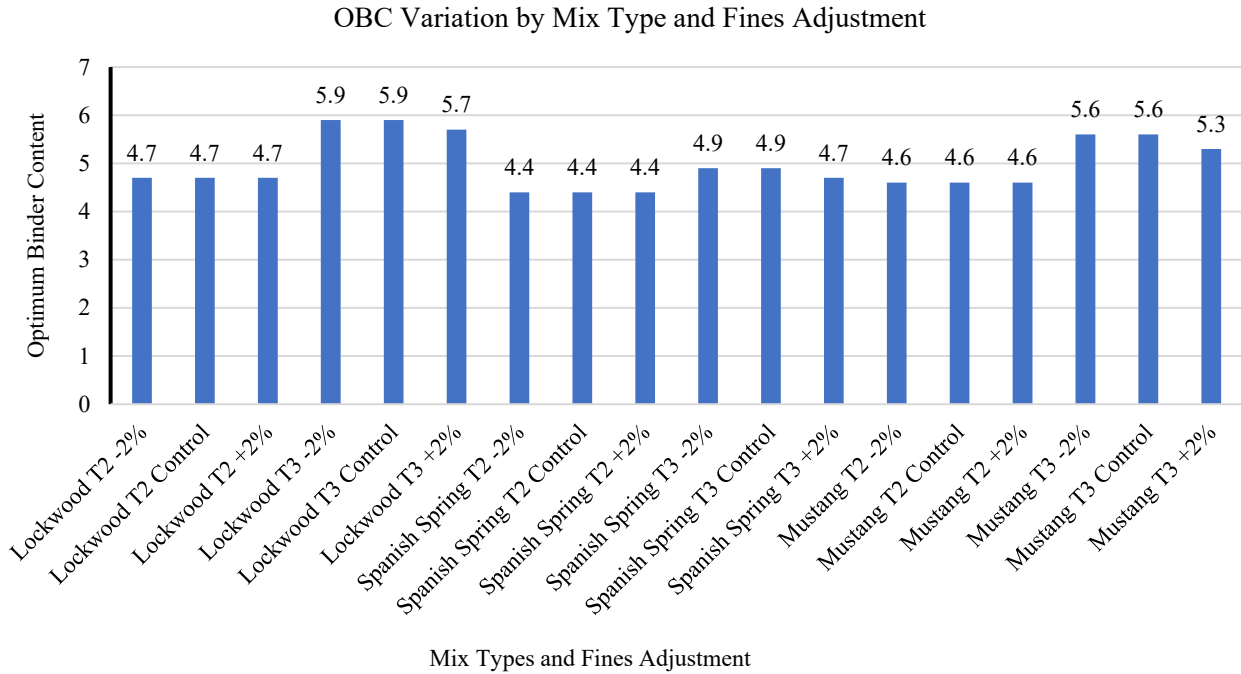


Figure 7. Optimum binder content comparison for all 18 asphalt mixtures.

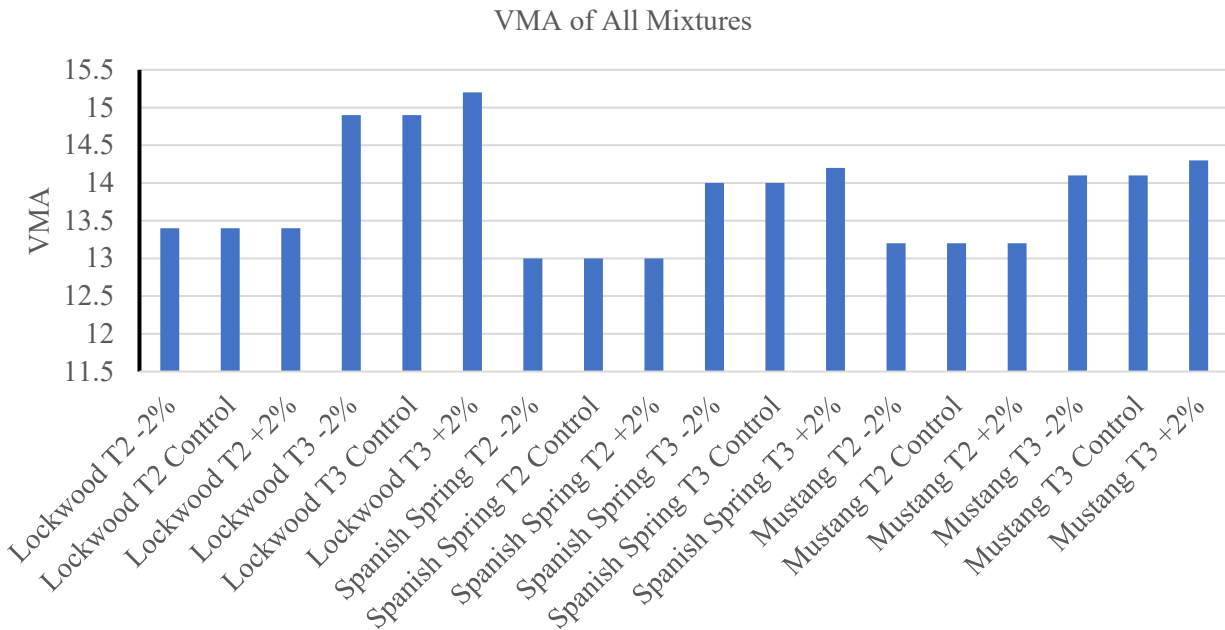


Figure 8. Comparison of all mixtures' VMA.

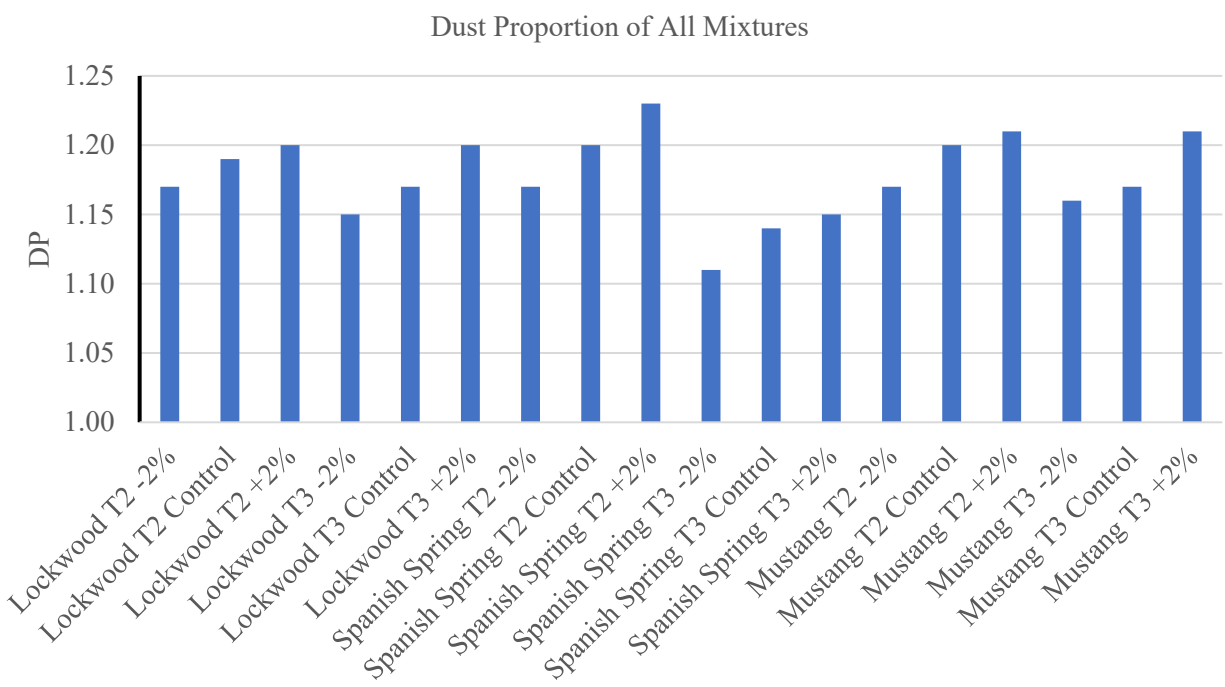


Figure 9. Comparison of DP for all mixtures.

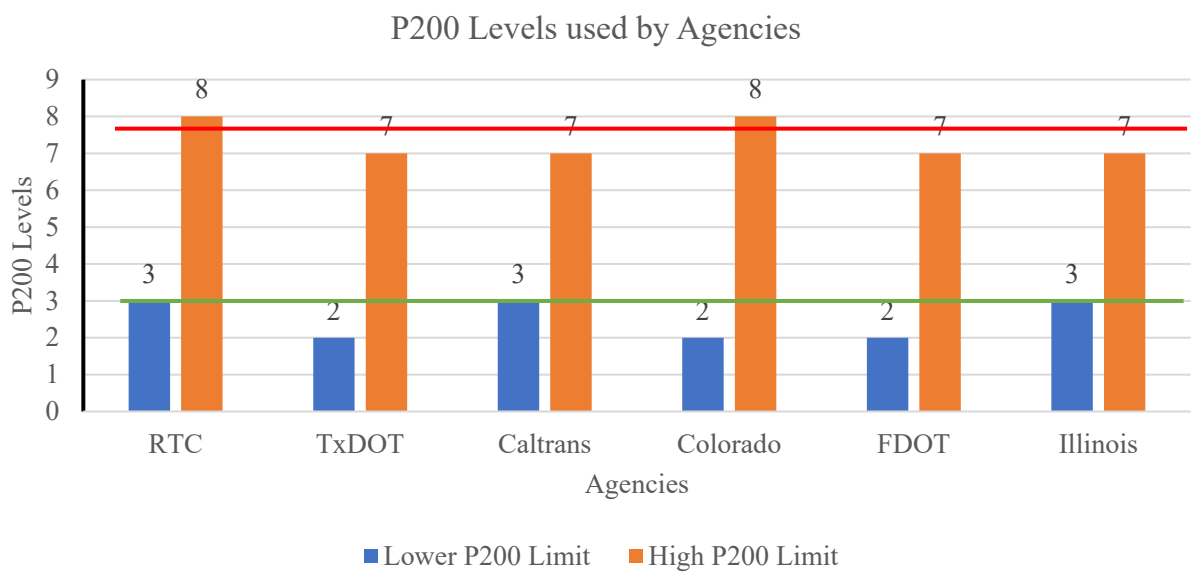


Figure 10. Comparison of specification on P200.

Chapter 4: Mixture Performance Test Methods

4.1 Moisture Sensitivity Testing by Tensile Strength Ratio (TSR)

Moisture-induced damage is one of the leading causes of premature distress in asphalt pavements [33]. The Tensile Strength Ratio (TSR) test is commonly used, in accordance with AASHTO T 283-22 and was used in this research [34] to evaluate the moisture sensitivity of asphalt mixtures. This test is designed to assess the potential for moisture-related stripping by comparing the tensile strength of asphalt specimens under dry and moisture-conditioned states. The TSR is calculated as the ratio of average tensile strength of moisture-conditioned specimens over the average tensile strength of the unconditioned specimens times 100. A higher TSR value indicates greater resistance to moisture-induced damage, while a lower value implies vulnerability to stripping and weakening under wet conditions. Typically, a minimum TSR value is recommended for satisfactory moisture resistance, though this threshold may vary based on local standards or performance specifications. The TSR data has been included as part of the mix designs for the 18 mixtures in Chapter 3. The moisture sensitivity data will be further used in Chapter 5 to evaluate the impact of P200 on the tensile strength properties of the mixtures.

4.1.1 Sample Preparation

Test specimens were prepared using a Marshall compactor, resulting in cylindrical samples with a nominal diameter of 4 inches (101.6 mm) and a height of 2.5 inches (63.5 ± 2.5 mm). The compacted samples were prepared to have an average air void content of $7 \pm 0.5\%$, which is considered ideal for simulating field conditions while maintaining test consistency.

Two groups of specimens are prepared:

- Unconditioned (Dry) Set: These are stored at room temperature in a dry environment until testing.
- Conditioned (Wet) Set: These undergo a carefully controlled moisture conditioning process to simulate field exposure to moisture and freeze-thaw cycles.

The conditioning process is designed to replicate environmental factors that cause stripping. Specimens were saturated to a target range of 70%–80% saturation. The saturated samples were wrapped in plastic film to reduce direct water loss and placed in sealed plastic bags containing distilled water to maintain a moist environment during freezing. The wrapped specimens were frozen at $0 \pm 5^\circ\text{F}$ ($-18 \pm 3^\circ\text{C}$) for a minimum of 16 hours to simulate frost-induced cracking and binder-aggregate debonding. Following freezing, the specimens are thawed in a water bath maintained at $140 \pm 2^\circ\text{F}$ ($60 \pm 1^\circ\text{C}$) for 24 ± 1 hours. Finally, before testing, the samples were submerged in a $77 \pm 1^\circ\text{F}$ ($25 \pm 0.5^\circ\text{C}$) water bath for 2 ± 0.5 hours to ensure uniform testing temperature across all specimens.

4.1.2 Testing and Evaluation

The indirect tensile strength was determined by applying diametral loading at a constant deformation rate of 2 in/min until failure occurs. The tensile strength is calculated using the following formula:

$$\text{ITS} = 2P / (\pi tD)$$

Where; ITS is in psi. P is the maximum load at failure (lbf), t is the specimen thickness (in) and D is the specimen diameter (in).

The Tensile Strength Ratio (TSR) is then computed as:

$$\text{TSR} = (\text{ITS Conditioned} / \text{ITS Unconditioned}) \times 100\%$$

TSR test supports material selection decisions, such as the use of anti-stripping agents (e.g., hydrated lime, liquid additives) or modification of binder type to improve moisture resistance. The results can indicate the need for aggregate source changes or adjustments in gradation to enhance long-term pavement durability. Poor adhesion or the presence of water-sensitive aggregates may lead to rapid deterioration under traffic loading and environmental stressors. The test results are often used as a quality control measure in mix design evaluations and are required for moisture sensitivity approval in many state and national specifications.

4.2 Engineering Properties: Dynamic Modulus

The Dynamic Modulus (E^*) is a fundamental property characterizing the viscoelastic behavior of asphalt mixtures and is a key input for advanced pavement design methodologies, particularly within the Mechanistic-Empirical Pavement Design Guide (MEPDG) framework. This test evaluates the stiffness of asphalt mixtures under cyclic loading across a range of temperatures and loading frequencies, enabling the prediction of mixture performance under field-like conditions. It provides a measure of the asphalt mixture's ability to resist deformation under traffic loading, with time and temperature effects. As asphalt behaves as a viscoelastic material, its stiffness (modulus) varies significantly with temperature and loading rate.

The development of a mixture master curve from dynamic modulus test data allows to model this complex behavior for a continuous spectrum of conditions. This master curve provides a comprehensive output of the material's response, supporting long-term performance prediction, pavement structure optimization, and mixture design improvement.

The Dynamic Modulus Test was conducted according to AASHTO T 378-22 [35]. Cylindrical specimens of the mixtures were subjected to sinusoidal axial compressive loads at various controlled temperatures and frequencies. The applied load is typically a haversine waveform.

4.2.1 Specimen Preparation

After compacted using Superpave Gyrotory Compactor (SGC), the compacted samples (initially 5.9 inches in diameter and 6.7 inches in height) were cored and sawed to a diameter of 3.9 inches and a height of 5.9 inches. The target air void content after coring is $7.0 \pm 0.5\%$.

4.2.2 Test Matrix

Testing was conducted at 39.2°F, 68°F, and 104°F (4°C, 20°C, and 40°C) temperatures representing cold, intermediate, and high pavement service conditions. 10 Hz, 1 Hz, and 0.1 Hz frequencies were used, with an additional frequency of 0.01 Hz at 104°F (40°C) to capture low-frequency behavior at elevated temperatures. Both axial stress and axial strain are recorded using LVDTs.



Figure 11. Dynamic Modulus Test Setup.



Figure 12. Dynamic Modulus Test Specimen Inside the Chamber.

The phase lag (ϕ) between stress and strain is used to calculate the dynamic modulus ($|E^*|$), and to understand the viscoelastic phase behavior of the material.

Here,

$$|E^*| = \text{Peak Stress} / \text{Peak Strain}$$

$$\phi = \text{Phase Angle}$$

4.2.3 Master Curve Development

To generalize the test results across a wider spectrum of frequencies and temperatures, the time-temperature superposition principle is applied. This approach shifts modulus data measured at various temperatures horizontally along the frequency axis to create a single, continuous master curve at a chosen reference temperature of 20°C. This process was completed as per AASHTO R

84 [36], which defines the mathematical standard for fitting and shifting the modulus values. A sigmoidal function is typically used to represent the shape of the master curve.

$$\log |E^*| = \delta + \frac{Max - \delta}{1 + e^{\beta + \gamma \log fr}}$$

The reduced frequency (fr) accounts for temperature shift using a shift factor (a_T), typically derived using the Arrhenius or Williams-Landel-Ferry (WLF) equation, depending on the temperature range and behavior of the binder. Fitting parameters α , β , γ and δ define the shape and curvature of the model.

4.2.4 Precision and Acceptance

Per AASHTO R 84, test results are considered valid only if they meet specified precision and acceptance criteria. This includes checks on data repeatability, linear viscoelasticity, and specimen uniformity. Deviations may indicate problems such as non-uniform compaction, material segregation, or equipment calibration errors.

Table 18: Dynamic Modulus Test Acceptance Limits.

Data Quality Parameters	Acceptance Limit
Load Standard Error	10%
Deformation Standard Error	10%
Deformation Uniformity	30%
Phase Uniformity	3 degrees

4.3 Resistance to Rutting: Hamburg Wheel Tracking Test

The Hamburg Wheel Tracking Test (HWTT) is a performance-based laboratory test used to evaluate the rutting resistance and moisture susceptibility of HMA. This test simulates the combined effects of repetitive traffic loading and environmental moisture exposure, providing a

comprehensive measure of an asphalt mixture's structural and moisture-related durability. The test was performed as per AASHTO T 324 [37]. The test simulates the field conditions of heavy axle loads and prolonged moisture infiltration. The objective is to measure rut depth over a specified number of wheel passes, determining two key performance parameters: permanent deformation (rutting) due to repetitive load applications and moisture-induced damage (stripping) resulting from the loss of binder-aggregate adhesion under wet conditions.

4.3.1 Test Apparatus and Procedure

The HWT device consists of a steel wheel with a diameter of 8 inches (203 mm) and a width of 1.85 inches (47 mm), which moves over the surface of two compacted HMA slab specimens simultaneously. Samples were compacted using the Superpave Gyratory Compactor (SGC) and cut to fit standardized dimensions for the HWT mold. The applied load was 158 ± 1.0 lb (705 ± 4.5 N), intended to replicate the loading of commercial traffic. The testing was performed within a water bath maintained at $122 \pm 1^\circ\text{F}$ ($50 \pm 1^\circ\text{C}$), ensuring consistent thermal conditioning throughout the experiment. The total number of loading cycles was 20,000 passes, or until a critical failure threshold of 12.5 mm of rut depth was reached.



Figure 13. Hamburg Wheel Track Machine Setup Before Testing.



Figure 14. Sample with Rutting After Hamburg Wheel Track Testing.

4.3.2 Performance Metrics and Analysis

The Hamburg Wheel Tracking Test yields three critical performance indicators:

- **Creep Slope:** Represents the rate of rutting in the early linear deformation phase, associated with the rutting resistance of the mixture under continuous loading in the absence of moisture-induced failure.
- **Stripping Slope:** Measured after the initiation of moisture-induced damage. This indicates the rate of rutting progression in the presence of stripping (loss of cohesion within the mixture due to water infiltration). Steeper stripping slopes suggest greater vulnerability to moisture damage.
- **Stripping Inflection Point (SIP):** Defined as the number of wheel passes at which the creep slope and stripping slope intersect. This point marks the transition from stable deformation to rapid structural degradation caused by stripping.

SIP = Intersection of Creep and Stripping Slope Regression Lines

Figure 8 represents the HWTT deformation output curve at the testing temperature.

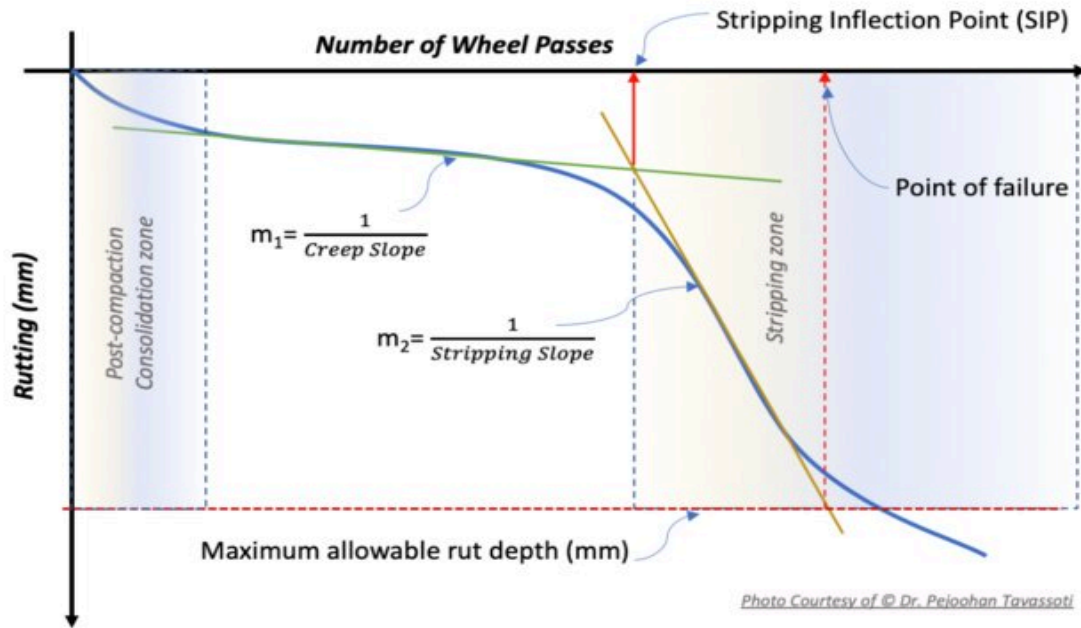


Figure 15. HWTT deformation output curve [38].

In well-performing mixtures, rutting progresses gradually, and stripping may never initiate within the test duration. In contrast, mixtures with poor moisture resistance often show a distinct change in the deformation rate, which is indicative of rapid deterioration [37]. Because of its ability to detect both rutting and moisture damage in a single test, the HWT is often considered a better alternative to separate rutting or stripping tests. The results play an important role in mix design acceptance, field performance prediction, and research evaluations of new materials like warm-mix asphalt (WMA), polymer-modified binders, and balanced mix designs (BMD).

4.3.3 Limitations and Considerations

Despite its many strengths, the HWT test has certain limitations. It may not fully represent long-term aging effects or performance under varying field drainage conditions. Additionally, the test is more suitable for surface mixtures rather than base courses, and the water bath temperature may need to be adjusted in regions with extreme climates.

4.4 Resistance to Cracking: Indirect Tensile Cracking Test (IDEAL-CT)

The Indirect Tensile Cracking Test (IDEAL-CT) is used to evaluate the cracking resistance of asphalt mixtures. As pavement structures are increasingly exposed to dynamic traffic loads and environmental aging, fatigue and thermal cracking have become critical distress mechanisms, especially in the absence of proper mix design adjustments. The test is currently standardized under ASTM D8225 [39], titled Standard Test Method for Determination of Cracking Tolerance Index of Asphalt Mixtures Using the Indirect Tensile Cracking Test at Intermediate Temperature. The primary objective of the IDEAL-CT test is to generate a Cracking Tolerance Index (CT_{index}) that measures the ability of an asphalt mixture to resist fracture propagation under tensile stresses. A higher CT_{index} value usually indicates better cracking resistance, implying that the pavement will better withstand traffic-induced fatigue and thermal contraction without significant cracking over its design life.

4.4.1 Sample Preparation and Test Conditions

Cylindrical specimens are compacted using the Superpave Gyratory Compactor (SGC), with a diameter of 5.9 ± 0.08 inches (150 ± 2 mm) and a height of 2.44 ± 0.08 inches (62 ± 2 mm). The targeted air void is $7 \pm 0.5\%$, consistent with field compaction levels. No coring or trimming is required before testing. The specimen is conditioned at a temperature of 25°C for 2 hours before the testing and the test is performed at 25°C .

A monotonic vertical load is applied to the specimen at a constant displacement rate of 50 mm/min until failure occurs. This loading configuration induces tensile stress perpendicular to the loading direction, similar to the tensile stresses experienced by pavements under service conditions.

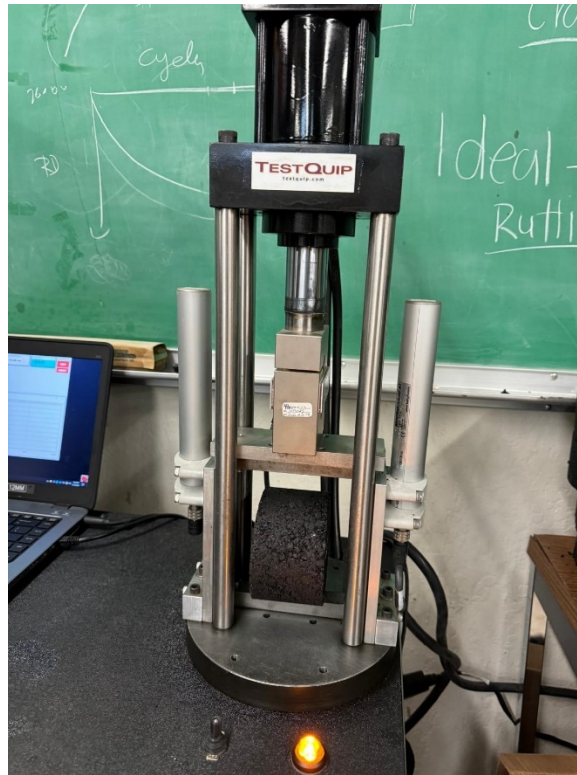


Figure 16. IDEAL-CT Testing Setup with Sample Alignment.



Figure 17. Specimen with Cracking Surface after the IDEAL-CT Testing.

4.4.2 CT_{index} Calculation

During the test, a load-displacement curve is generated in real time, showing key indicators of mixture behavior during crack initiation and propagation. From this curve, the following parameters are obtained:

- Peak Load (P_{\max}): The maximum load before failure
- Post-Peak Slope ($|m_{75}|$): Slope of the load-displacement curve after the peak, measured between peak load and 75% of the peak
- Displacement at 75% Peak Load (l_{75}): Corresponds to the deformation tolerance after peak load
- Work of Failure (W_f): The area under the load-displacement curve, representing the total energy absorbed until failure
- Failure Energy (G_f): Computed by normalizing W_f over the specimen's cross-sectional area

$$G_f = W_f / (\pi D^2 t / 4)$$

Where;

G_f : Failure energy (J/m²)

D: Specimen diameter (mm)

t: Specimen thickness (mm)

Using these values, the Cracking Tolerance Index is calculated as:

$$CT_{index} = \frac{t}{62} \times \frac{l_{75}}{D} \times \frac{G_f}{|m_{75}|} \times 10^6$$

Where,

$|m_{75}|$: the absolute value of the post-peak slope m_{75} (N/m)

l_{75} : displacement at 75% of the peak load after the peak (mm)

This index provides a comprehensive measure of both energy dissipation (resistance to cracking) and deformation tolerance (resilience after initial cracking). Figure 9 illustrates the graphical representation of these calculations.

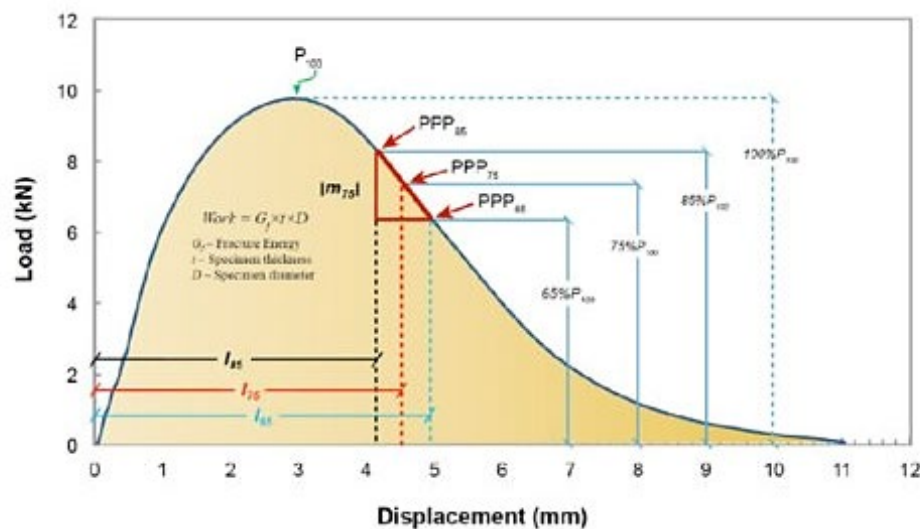


Figure 18. IDEAL-CT load vs. displacement data [40].

4.4.3 Variability and Repeatability

According to the ASTM D8225 standard, the within-laboratory standard deviation for the CT_{index} is reported to be approximately 13.5. However, several studies have explored the repeatability and

robustness of the test further. For example: West et al. reported coefficient of variation (COV) values ranging from 10% to 25%, depending on material type and testing consistency [41]. Hierholzer observed a COV range between 10.8% and 20% under controlled lab conditions [42]. Romero-Zambrana found COV values of 15%–22%, confirming moderate variability within acceptable limits for quality assurance purposes [43]. The CT_{index} is significantly influenced by asphalt binder properties, aggregate structure, air void content, and inclusion of recycled materials. Additives such as polymers, fibers, or rejuvenators can improve the CT_{index} by increasing energy absorption and controlling crack propagation.

Chapter 5: Performance Test Results and Analysis

5.1 Tensile Strength Ratio (TSR) Test

TSR test was performed following AASHTO T283 [34] standard procedure to evaluate the moisture susceptibility of asphalt mixtures in this study. The test measures both dry and conditioned (wet) tensile strengths, the TSR is calculated as the ratio of wet to dry tensile strength, expressed as a percentage:

$$\text{TSR} = (\text{Tensile Strength (Dry)} / \text{Tensile Strength (Wet)}) * 100$$

According to the RTC Orange Book specifications, a minimum TSR value of 70% and a minimum dry tensile strength of 65 psi are required to ensure satisfactory resistance to moisture damage [3].

It is important to note that aggregates commonly used in Nevada are known to have high water absorption characteristics, which inherently increases the potential for moisture damage. To mitigate this issue, all mixtures in this study were subjected to a hydrated lime marination process, where the wet aggregates are mixed with lime and left to cure for 48 hours prior to mixing. This treatment has been shown to be effective in enhancing the bond between the aggregate and binder, thereby improving resistance to stripping. Studies have shown that hydrated lime not only improves adhesion but also reduces the effects of aging and oxidation within the binder film [44]. The results in this study strongly support this approach, as all mixtures met or exceeded the required TSR and dry strength thresholds.

Figure 10 presents the TSR values for all gradations tested in this study. It can be observed that all mixtures exceeded the 70% TSR threshold and most of the gradations had a TSR value close to 100% indicating good resistance to moisture-induced damage. In particular, the control mixtures

demonstrated the highest TSR value among all, suggesting a strong balance between dry and wet tensile strengths.

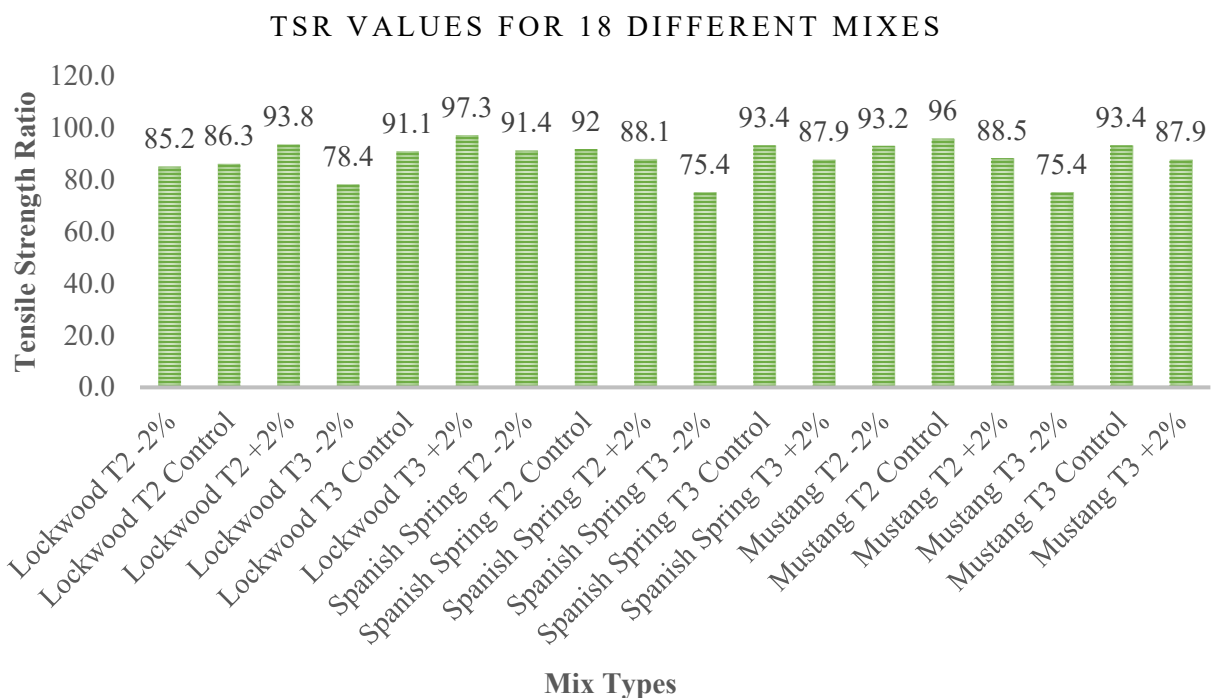


Figure 19. Tensile strength ratio results for all mixtures.

5.2 Engineering Properties: Dynamic Modulus

The Dynamic Modulus Test was conducted using the Asphalt Mixture Performance Tester (AMPT) as per AASHTO T378 to evaluate the stiffness of asphalt mixtures under varying conditions. Dynamic modulus (E^*) is a fundamental parameter in evaluating the structural performance of asphalt concrete (AC) mixtures, as it reflects the stiffness of the material under cyclic loading. In this study, dynamic modulus testing was conducted using a uniaxial cyclic compression test setup on a cylindrical specimen to characterize the viscoelastic behavior of the mixture.

The test was performed on asphalt mixtures with three levels of P200 content (Control, -2%, +2%) and two gradation types (Type 2 and Type 3), compacted using the Superpave Gyratory Compactor. Each specimen was subjected to sinusoidal loading at four frequencies: 10 Hz, 1 Hz, 0.1 Hz, and 0.01 Hz and at three different temperatures: 4°C, 20°C, and 40°C with an additional frequency of 0.01 Hz at 40°C to capture low-frequency behavior at elevated temperatures. These combinations were selected to simulate a range of field conditions, from cold weather stiffness to high temperature softening behavior. The data were later used to construct dynamic modulus master curves using a sigmoidal function at a reference temperature of 20°C, following the principles of time–temperature superposition.

The analysis indicates dynamic modulus decreased with increasing temperature and decreasing loading frequency, which is characteristic of viscoelastic materials. However, the influence of P200 content was particularly noteworthy. Mixtures with higher fine content (+2%) consistently exhibited lower stiffness, especially at lower frequencies (0.1 Hz and 0.01 Hz) and elevated temperatures (40°C). This suggests a reduced capacity to resist slow moving or static loads, making such mixtures more susceptible to permanent deformation under repeated traffic loads. Some high P200 mixtures approached the lower end of the performance spectrum, signaling potential concerns for heavy-load applications. On the other hand, mixtures with reduced P200 content and control mixtures displayed higher E^* values, indicating enhanced structural stiffness and better load-bearing potential.

The test results indicate the critical role that fine aggregate content plays in mix stiffness and overall pavement performance. While fines contribute to mix cohesion and workability, excessive P200 can disrupt the mix performance, increase binder demand, and reduce internal friction, leading to a softer, more deformation-prone mixture. The results are summarized in Tables 19 - 22 and in Figures 10 - 16.

Table 19: Dynamic Modulus Results for Lockwood Type 2 and Type 3.

Aggregate Source: Lockwood													
Conditions		Mix Type 2						Mix Type 3					
Temperature	Frequency	-2%		Control		+2%		-2%		Control		+2%	
		Average Modulus	Average Phase Angle	Average Modulus	Average Phase Angle	Average Modulus	Average Phase Angle	Average Modulus	Average Phase Angle	Average Modulus	Average Phase Angle	Average Modulus	Average Phase Angle
C	Hz	ksi	Degree	ksi	Degree	ksi	Degree	ksi	Degree	ksi	Degree	ksi	Degree
4.0	0.1	744.3	24.5	667.4	25.7	595.7	25.3	578.4	25.3	723.0	43.3	495.2	23.7
4.0	1.0	1242.6	17.8	1147.1	20.2	996.9	20.2	1003.5	19.4	1287.2	31.3	826.6	20.4
4.0	10.0	1804.1	12.9	1748.3	14.7	1501.6	14.7	1509.2	13.9	2048.0	40.8	1277.2	16.4
20.0	0.1	173.4	35.6	172.6	32.2	101.8	31.8	113.6	33.6	112.8	33.5	123.5	28.4
20.0	1.0	409.5	31.7	406.1	30.8	239.0	32.6	275.4	32.6	279.3	32.3	250.4	29.0
20.0	10.0	805.1	24.9	818.1	25.9	522.9	29.9	585.8	27.7	584.5	27.2	495.8	26.9
40.0	0.01	10.4	22.8	20.7	19.1	10.7	26.7	12.8	20.7	12.3	20.8	15.5	19.1
40.0	0.1	19.9	31.7	31.7	25.4	17.8	29.6	19.1	27.1	18.5	28.5	21.7	23.0
40.0	1.0	54.0	38.2	62.0	32.1	41.4	34.1	40.0	34.0	39.3	35.3	35.4	27.9
40.0	10.0	163.2	39.6	163.3	36.5	149.4	39.9	110.3	37.8	111.2	38.5	73.6	32.4

Table 20: Dynamic Modulus Results for Spanish Spring Type 2 and Type 3.

Aggregate Source: Spanish Spring													
Conditions		Mix Type 2						Mix Type 3					
Temperature	Frequency	-2%		Control		+2%		-2%		Control		+2%	
		Average Modulus	Average Phase Angle	Average Modulus	Average Phase Angle	Average Modulus	Average Phase Angle	Average Modulus	Average Phase Angle	Average Modulus	Average Phase Angle	Average Modulus	Average Phase Angle
C	Hz	ksi	Degree	ksi	Degree	ksi	Degree	ksi	Degree	ksi	Degree	ksi	Degree
4.0	0.1	922.8	22.2	1060.0	22.5	779.5	22.1	734.9	20.4	761.5	24.3	702.4	23.6
4.0	1.0	1444.1	17.3	1607.5	17.6	1240.3	16.9	1168.3	15.3	1260.6	18.6	1129.1	18.5
4.0	10.0	2063.4	12.8	2206.0	13.0	1768.3	12.4	1690.7	11.1	1844.5	13.5	1653.4	13.8
20.0	0.1	213.3	30.9	244.6	30.9	109.4	33.0	191.2	32.8	149.5	32.9	160.2	26.4
20.0	1.0	444.7	29.5	516.9	28.5	254.0	32.6	407.1	30.1	355.4	31.8	346.4	30.5
20.0	10.0	843.3	25.5	946.6	24.0	541.0	28.8	757.6	26.0	729.2	27.2	668.3	32.0
40.0	0.0	28.2	23.3	19.4	9.3	16.8	22.2	29.6	23.5	14.9	21.2	22.9	23.4
40.0	0.1	48.5	28.5	39.9	41.6	25.5	27.6	49.4	29.0	23.5	27.0	40.4	29.8
40.0	1.0	106.9	32.2	97.9	15.6	55.2	33.3	106.8	32.4	49.6	31.8	92.2	33.6
40.0	10.0	258.7	34.1	251.1	29.1	147.0	36.3	242.5	34.1	137.2	37.3	230.0	34.7

Table 21: Dynamic Modulus Results for Mustang Type 2 and Type 3.

Aggregate Source: Mustang													
Conditions		Mix Type 2						Mix Type 3					
Temperature	Frequency	-2%		Control		+2%		-2%		Control		+2%	
		Average Modulus	Average Phase Angle	Average Modulus	Average Phase Angle	Average Modulus	Average Phase Angle	Average Modulus	Average Phase Angle	Average Modulus	Average Phase Angle	Average Modulus	Average Phase Angle
C	Hz	ksi	Degree	ksi	Degree	ksi	Degree	ksi	Degree	ksi	Degree	ksi	Degree
4.0	0.1	726.2	25.4	937.3	23.1	722.4	22.9	605.1	21.6	555.8	24.2	506.3	24.3
4.0	1.0	1222.5	20.7	1503.9	17.8	1149.3	17.6	961.6	16.9	947.0	18.6	861.9	20.7
4.0	10.0	1860.6	15.2	2175.9	12.9	1627.3	12.1	1384.3	12.8	1437.1	13.6	1343.1	16.4
20.0	0.1	206.3	31.2	240.3	31.4	151.8	36.8	127.1	32.5	112.0	33.3	115.3	28.6
20.0	1.0	467.2	29.7	528.5	29.7	371.8	32.2	274.6	30.2	267.8	32.0	236.2	29.6
20.0	10.0	896.4	25.8	1007.9	25.2	735.6	25.0	530.1	25.7	557.8	27.6	479.5	27.8
40.0	0.0	21.9	21.5	21.4	22.8	8.5	24.4	15.7	24.6	10.9	20.5	19.2	19.5
40.0	0.1	33.0	28.7	34.8	29.5	15.9	31.6	28.0	31.1	16.3	27.8	24.3	22.8
40.0	1.0	76.0	33.5	77.9	29.7	43.0	38.1	64.5	35.1	34.2	32.0	36.3	27.3
40.0	10.0	208.2	35.9	210.8	37.0	133.5	40.1	163.9	35.5	93.5	37.9	71.7	32.1

The master curves were plotted at a reference temperature of 20°C for six different mix types, with each mix featuring three variations in fine P200 percentages: -2%, control and +2%.

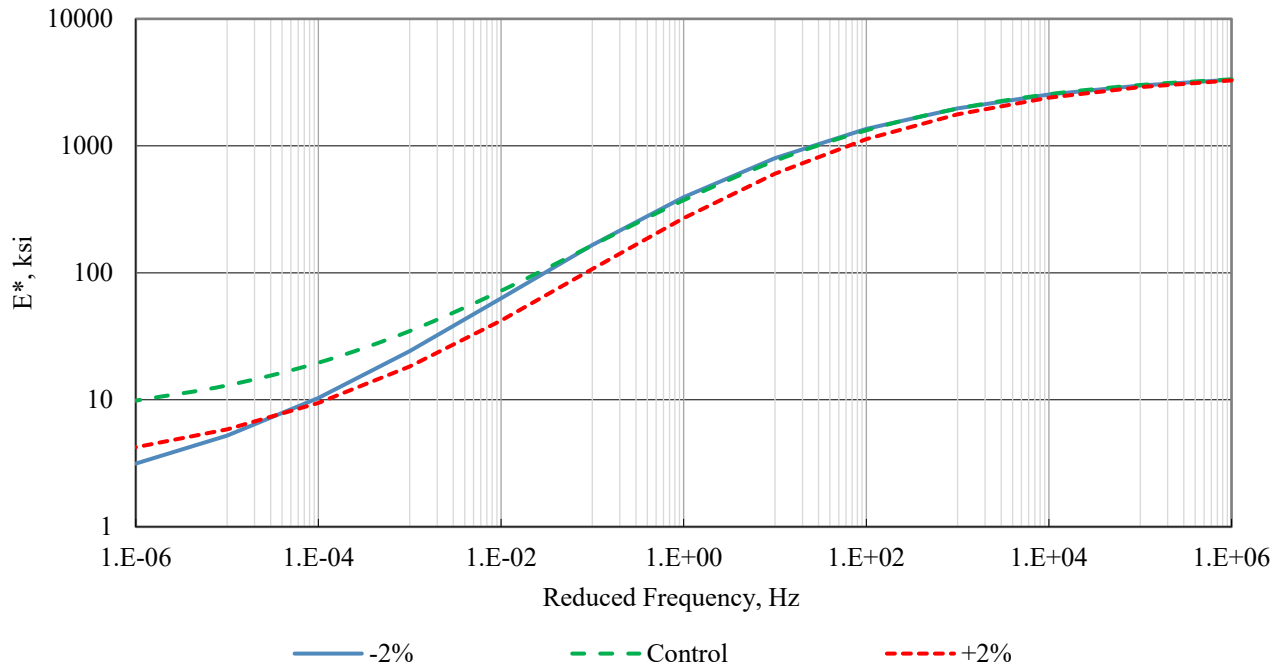


Figure 20. Dynamic modulus master curve for Lockwood Type 2 mixtures.

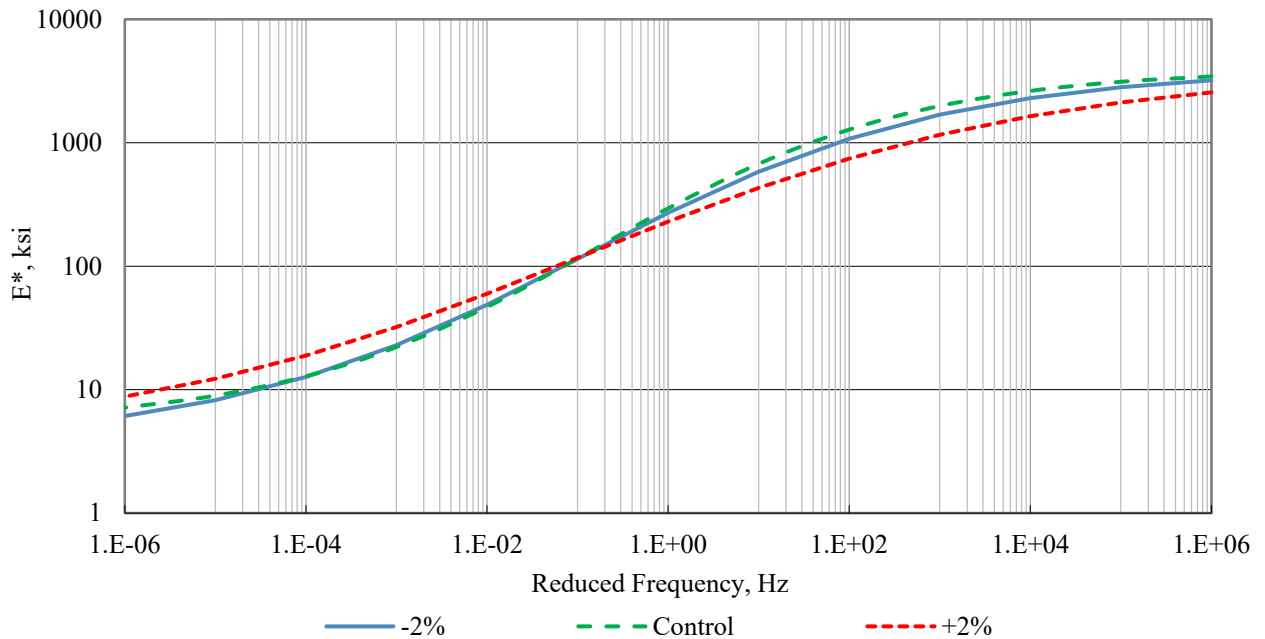


Figure 21. Dynamic modulus master curve for Lockwood Type 3 mixtures.

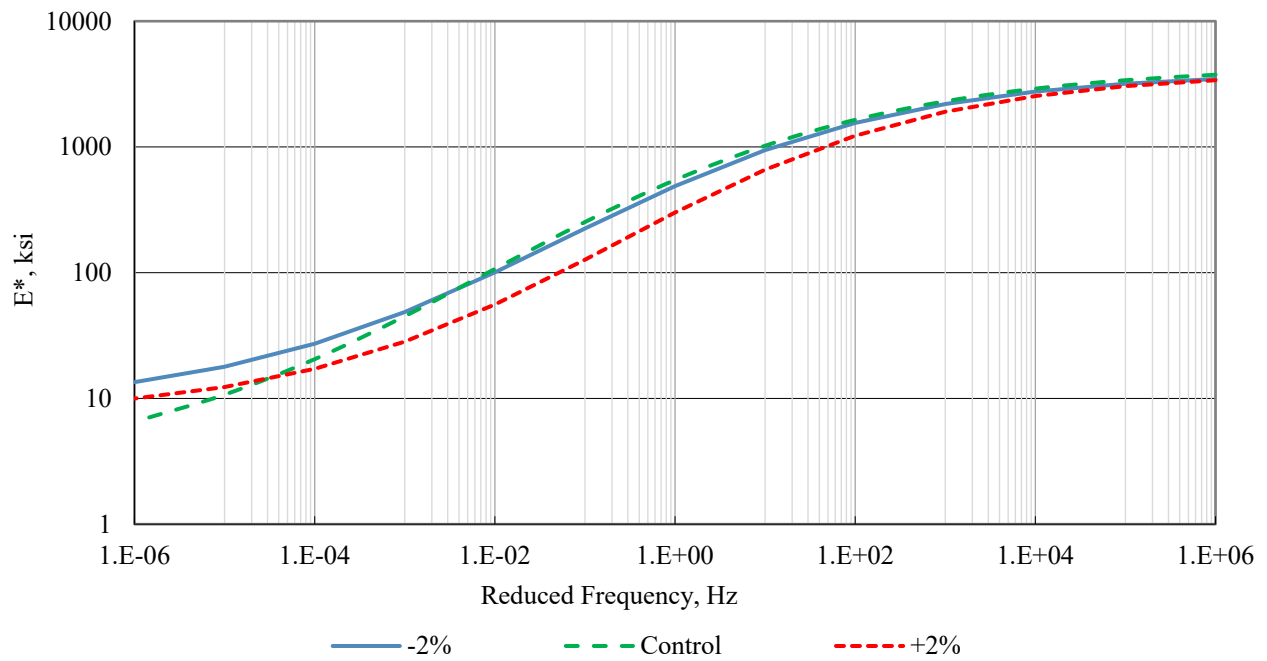


Figure 22. Dynamic modulus master curve for Spanish Spring Type 2 mixtures.

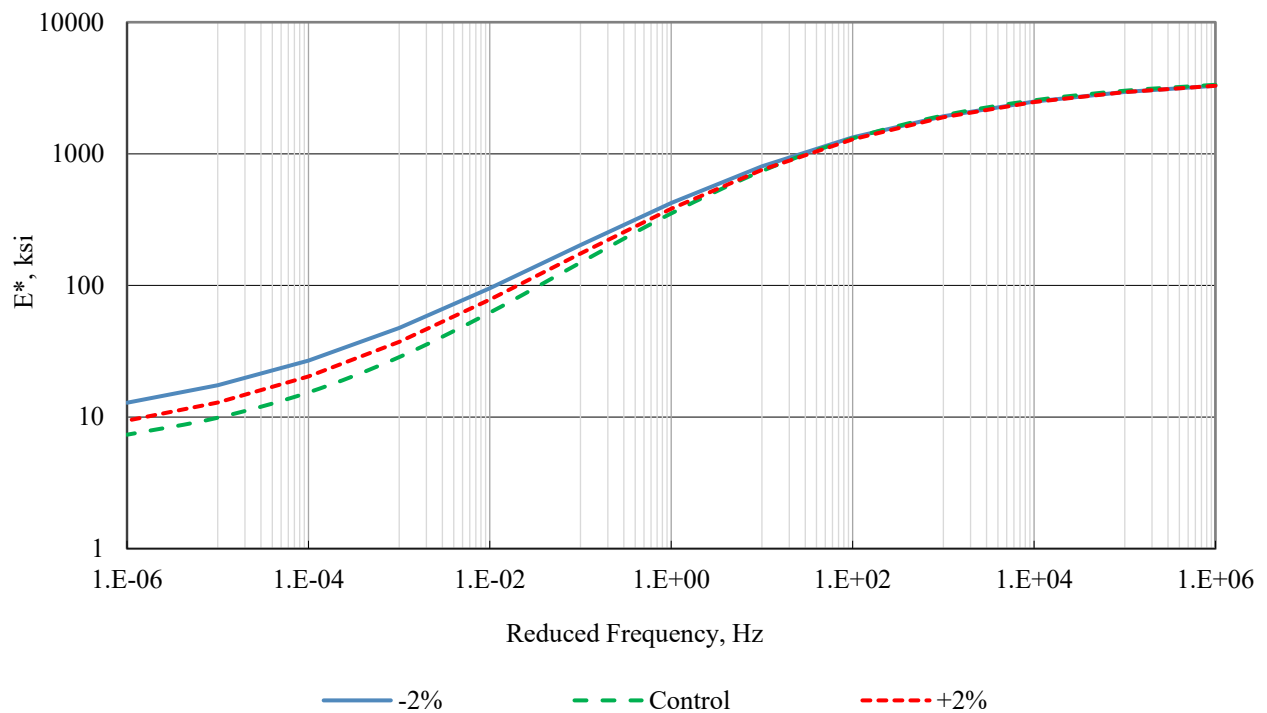


Figure 23. Dynamic modulus master curve for Spanish Spring Type 3 mixtures.

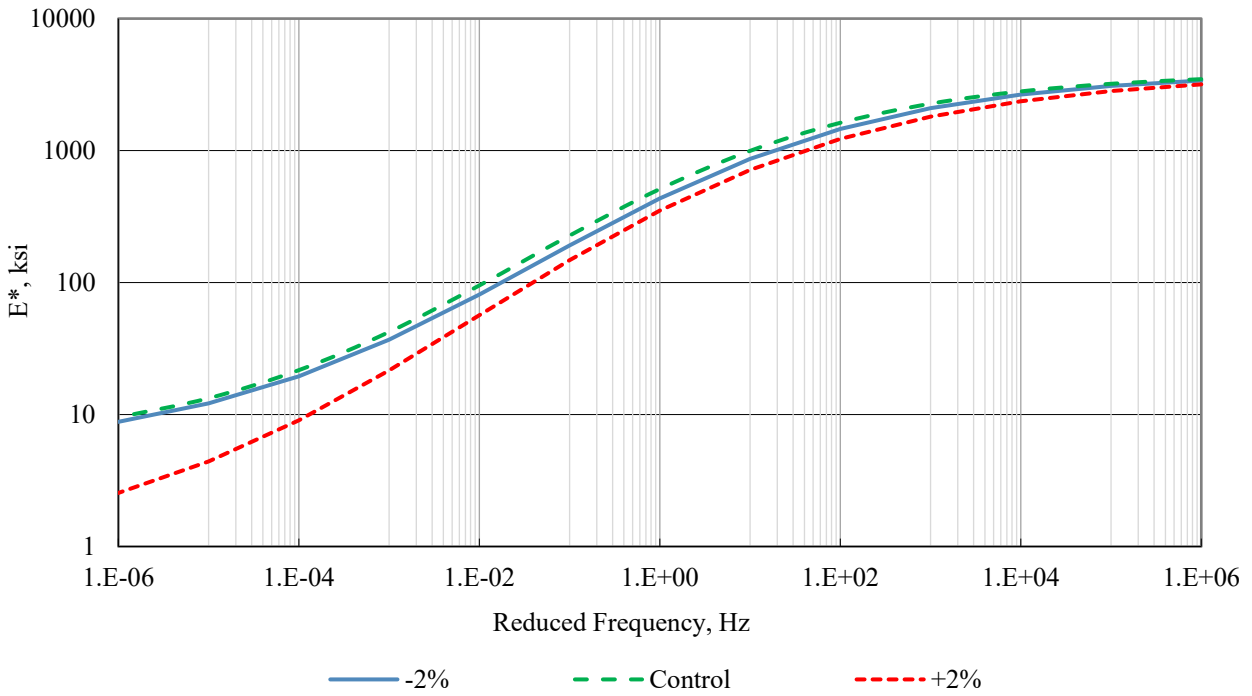


Figure 24. Dynamic modulus master curve for Mustang Type 2 mixtures.

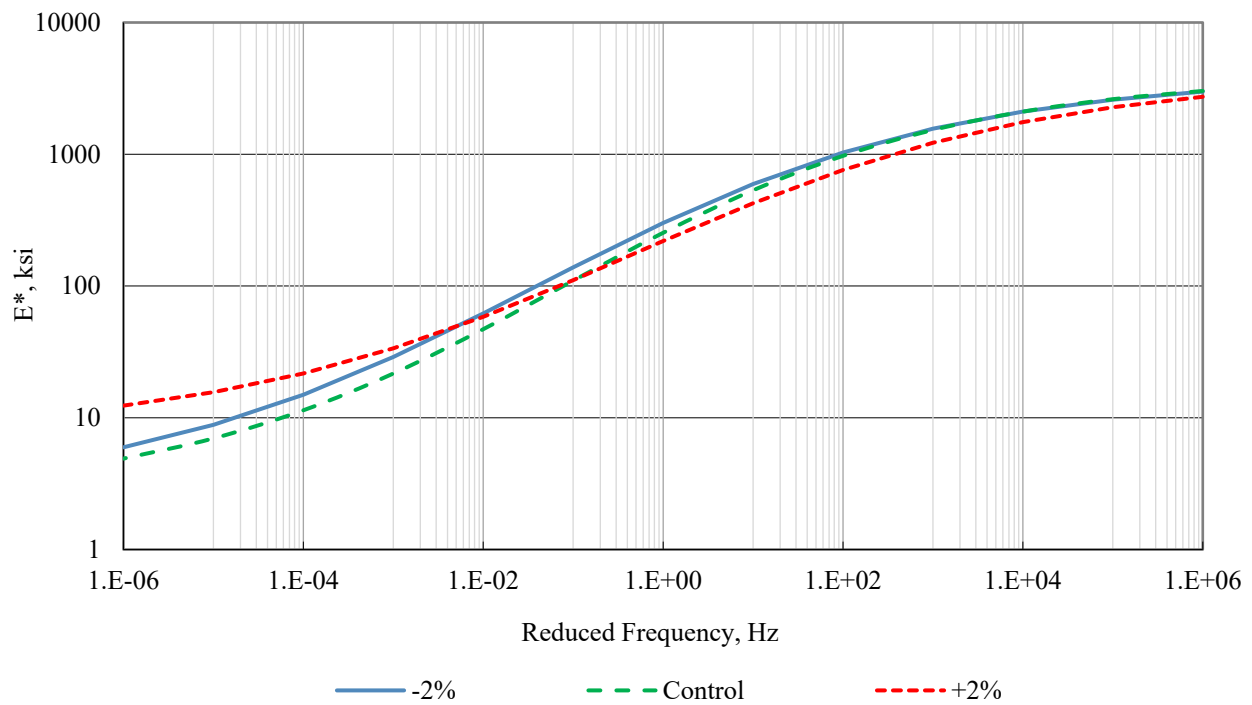


Figure 25. Dynamic modulus master curve for Mustang Type 3 mixtures.

The dynamic modulus values showed that at 40°C, the stiffness (E^*) decreased for all asphalt mixtures, highlighting the temperature sensitivity of the materials. As temperature increased, the modulus values dropped, and the average phase angle increased, indicating a shift toward more viscous behavior. Mixtures with higher fine content (+2% P200) consistently showed lower modulus values, especially at low frequencies, suggesting a reduced stiffness. In contrast, control and -2% P200 mixtures maintained higher modulus values, reflecting better load-bearing capacity and structural performance. These results emphasize the impact of fine aggregate content on the stiffness and overall mechanical behavior of asphalt mixtures under varying thermal conditions. The comparison of the modulus values at 20°C and 40°C among the mixtures are presented in figure 16 and 17.

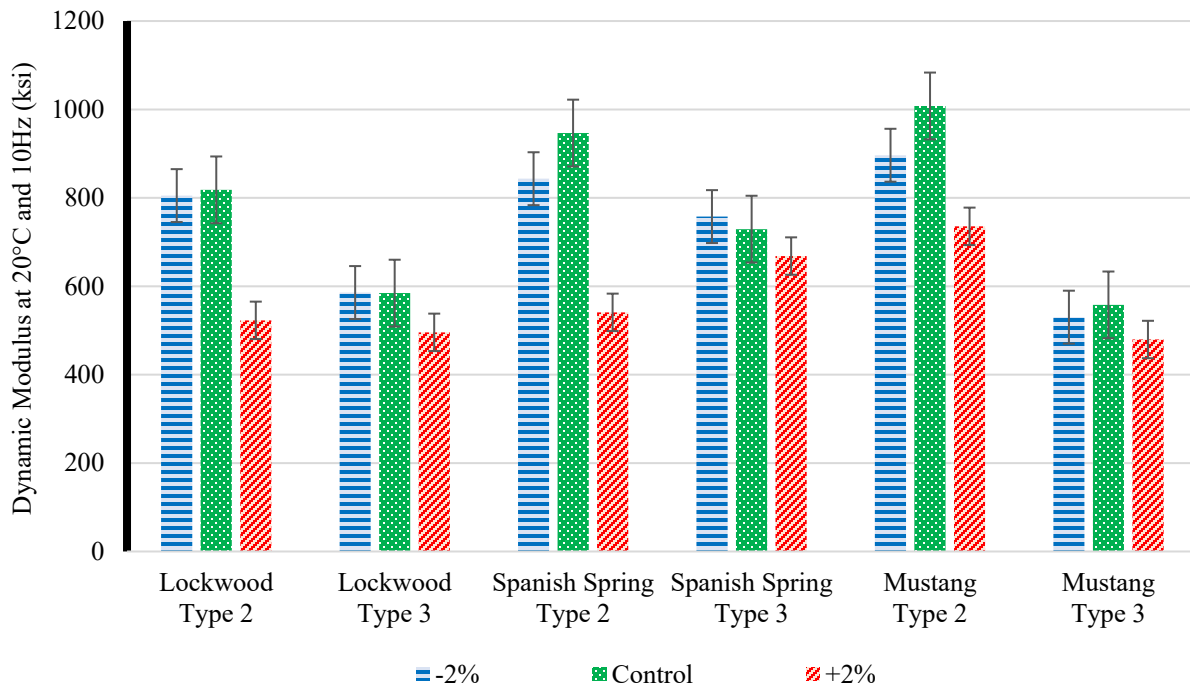


Figure 26. Comparison of dynamic modulus at 20°C and 10Hz for -2%, control and +2% P200 mix.

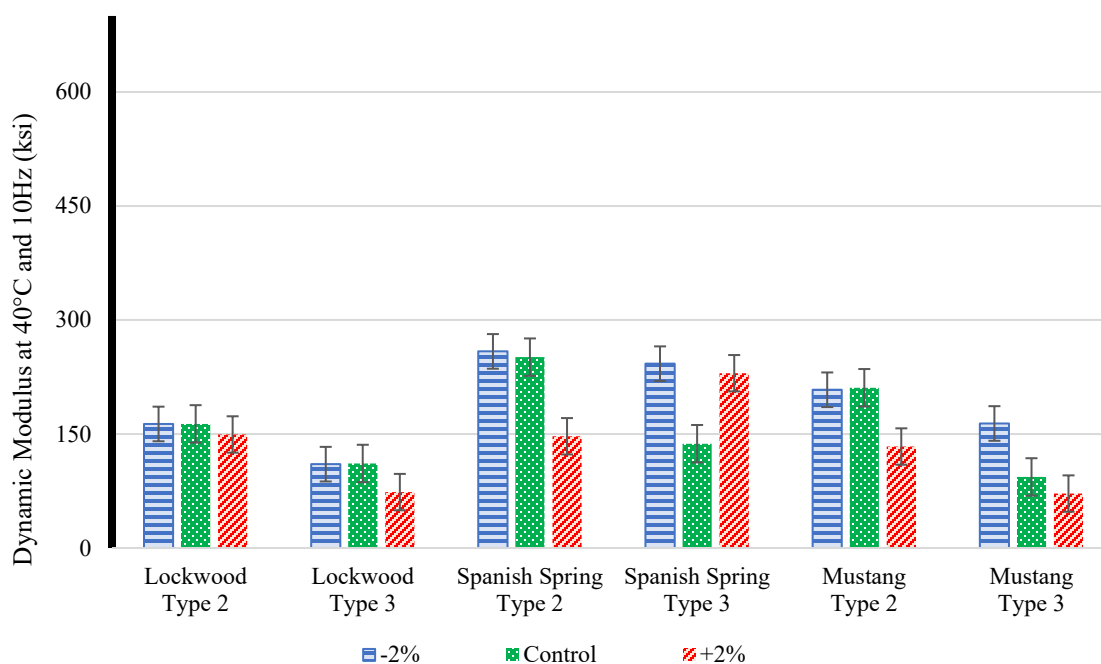


Figure 27. Comparison of dynamic modulus at 40°C and 10Hz for -2%, control and +2% P200 mix.

5.3 Resistance to Rutting: Hamburg Wheel Tracking Test

The rutting performance of asphalt concrete mixtures was evaluated using the Hamburg Wheel Tracking Test (HWTT) in accordance with the AASHTO T 324-22 [37] standard. This test simulates the impact of both traffic loading and moisture on pavement performance by subjecting compacted samples to repeated wheel passes while submerged in water. All tests were conducted at a water temperature of 50°C, with a rut depth failure threshold set at 12.5 mm or a maximum of 20,000 loading cycles, whichever occurred first.

For each mix variant defined by P200 content adjustment (-2%, Control, +2%) and gradation type (Type 2 or Type 3) four replicate specimens were prepared. All specimens were compacted to target air voids within $7 \pm 0.5\%$, ensuring comparability of rutting behavior across different fine content levels and aggregate sources. The results from the HWTT revealed a clear trend: rutting resistance decreased with an increase in P200 content. Mixtures containing higher percentages of

fine aggregates exhibited greater deformation under wheel loading, indicating reduced resistance to permanent deformation. This trend was particularly evident in type 3 mixtures, where rut depths approached or exceeded the 12.5 mm threshold before reaching the 20,000-cycle limit, suggesting these mixtures are more sensitive to fine content variation in terms of structural stability.

In contrast, mixtures with reduced P200 content (-2%) and control mixtures demonstrated superior rutting resistance, maintaining lower rut depths well below the failure threshold throughout the test duration. Furthermore, no distinct stripping inflection points were observed, indicating that moisture-induced damage was not a dominant failure mechanism in these mixtures during the HWTT procedure. The HWTT results provide strong evidence that increased P200 content compromises the rutting resistance of asphalt mixtures, particularly in finer gradations. These findings emphasize the need for tight construction control over fine aggregate content, especially when producing dense-graded mixtures for regions susceptible to high temperatures and heavy traffic loading. Future specifications may benefit from incorporating performance-based criteria that consider the rutting sensitivity of mixtures to fine content variations. The results are summarized in Tables 23 - 28 and Figures 17 - 23.

Table 22: HWTT Specifications Used (AASHTO T324).

Standard	AASHTO T324
Aging	Short Term (2h+2h)
Compaction Method	Superpave Gyrotory
Target Air Voids%	7 ± 0.5 %
Test Temperature	50°C
Conditioning	45 minutes
Wheel Load	703 ± 4.5 N (158 ± 1 lb)

Table 23: HWTT Results for Lockwood Type 2 at 50°C.

Lockwood Type 2									
Parameters	-2% P200			Control Mix			+2% P200		
Passes	Left	Right	Average 2 Wheels	Left	Right	Average 2 Wheels	Left	Right	Average 2 Wheels
5000	-3.47	-3.28	-3.38	-3.22	-3.06	-3.14	-3.45	-3.46	-3.45
10000	-4.03	-4.58	-4.31	-3.78	-3.53	-3.66	-4.17	-4.13	-4.15
15000	-4.36	-4.76	-4.56	-4.22	-4.04	-4.13	-5.07	-4.85	-4.96
20000	-4.57	-4.95	-4.76	-4.65	-4.27	-4.46	-6.37	-5.75	-6.06
Failure (12.5 mm)	Not Reached			Not Reached			Not Reached		
Stripping Inflection Point, cycles	Not Reached			Not Reached			17060	Not Reached	-

Table 24: HWTT Results for Lockwood Type 3 at 50°C.

Lockwood Type 3									
Parameters	-2% P200			Control Mix			+2% P200		
Passes	Left	Right	Average 2 Wheels	Left	Right	Average 2 Wheels	Left	Right	Average 2 Wheels
5000	-4.25	-1.49	-2.87	-4.85	-4.63	-4.74	-4.75	-3.53	-4.14
10000	-5.27	-2.49	-3.88	-5.82	-5.51	-5.66	-7.46	-6.13	-6.79
15000	-6.51	-5.44	-5.97	-6.86	-6.69	-6.77	-11.80	-10.88	-11.34
20000	-8.18	-8.37	-8.28	-8.54	-8.10	-8.32	-12.50	-12.50	-12.50
Failure (12.5 mm)	Not Reached			Not Reached			15.7	16.7	
Stripping Inflection Point, cycles	Not Reached			Not Reached			12061	11859	11960

Table 25: HWTT Results for Spanish Spring Type 2 at 50°C.

Spanish Spring Type 2									
Parameters	-2% P200			Control Mix			+2% P200		
Passes	Left	Right	Average 2 Wheels	Left	Right	Average 2 Wheels	Left	Right	Average 2 Wheels
5000	-2.40	-2.42	-2.41	-2.24	-2.05	-2.14	-2.92	-3.16	-3.04
10000	-2.74	-2.73	-2.74	-2.58	-2.35	-2.47	-3.52	-3.65	-3.58
15000	-2.96	-2.90	-2.93	-2.78	-2.67	-2.72	-3.87	-4.01	-3.94
20000	-3.25	-3.02	-3.14	-3.00	-2.89	-2.94	-4.13	-4.40	-4.27
Failure (12.5 mm)	Not Reached			Not Reached			Not Reached		
Stripping Inflection Point, cycles	Not Reached			Not Reached			Not Reached		

Table 26: HWTT Results for Spanish Spring Type 3 at 50°C.

Spanish Spring Type 3									
Parameters	-2% P200			Control Mix			+2% P200		
Passes	Left	Right	Average 2 Wheels	Left	Right	Average 2 Wheels	Left	Right	Average 2 Wheels
5000	-2.13	-3.67	-2.90	-4.46	-3.20	-3.83	-3.31	-3.45	-3.38
10000	-2.92	-4.37	-3.64	-4.76	-3.70	-4.23	-3.92	-4.16	-4.04
15000	-3.77	-4.87	-4.32	-5.00	-4.14	-4.57	-4.64	-4.88	-4.76
20000	-5.33	-5.11	-5.22	-5.30	-4.67	-4.99	-5.67	-5.94	-5.81
Failure (12.5 mm)	Not Reached			Not Reached			Not Reached		
Stripping Inflection Point, cycles	Not Reached			17350	Not Reached		17140	17538	17339

Table 27: HWTT Results for Mustang Type 2 at 50°C.

Mustang Type 2									
Parameters	-2% P200			Control Mix			+2% P200		
Passes	Left	Right	Average 2 Wheels	Left	Right	Average 2 Wheels	Left	Right	Average 2 Wheels
5000	-2.57	-2.52	-2.54	-1.86	-2.80	-2.33	-2.92	-2.94	-2.93
10000	-2.89	-2.97	-2.93	-2.28	-3.05	-2.66	-3.45	-3.47	-3.46
15000	-3.13	-3.18	-3.16	-2.84	-3.26	-3.05	-3.89	-3.89	-3.89
20000	-3.58	-3.74	-3.66	-3.26	-3.48	-3.37	-4.22	-4.35	-4.29
Failure (12.5 mm)	Not Reached			Not Reached			Not Reached		
Stripping Inflection Point, cycles	Not Reached			Not Reached			Not Reached		

Table 28: HWTT Results for Mustang Type 3 at 50°C.

Mustang Type 3									
Parameters	-2% P200			Control Mix			+2% P200		
Passes	Left	Right	Average 2 Wheels	Left	Right	Average 2 Wheels	Left	Right	Average 2 Wheels
5000	-3.49	-3.45	-3.47	-2.76	-3.47	-3.11	-5.97	-3.73	-4.85
10000	-4.19	-4.18	-4.18	-3.39	-4.29	-3.84	-6.93	-4.56	-5.74
15000	-4.92	-5.21	-5.07	-4.19	-4.75	-4.47	-7.54	-6.04	-6.79
20000	-6.19	-6.53	-6.36	-5.16	-5.25	-5.21	-8.02	-8.41	-8.21
Failure (12.5 mm)	Not Reached			Not Reached			Not Reached		
Stripping Inflection Point, cycles	Not Reached			Not Reached			Not Reached	17625	-

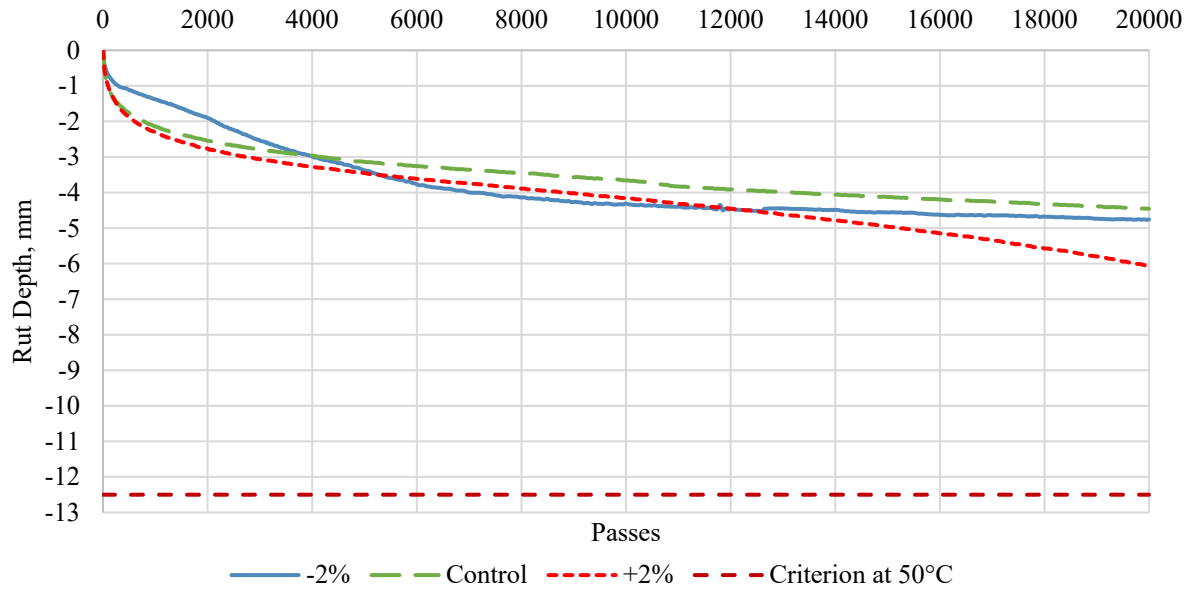


Figure 28. Rut depth (mm) vs number of passes for Lockwood Type 2 mixtures @ 50°C.

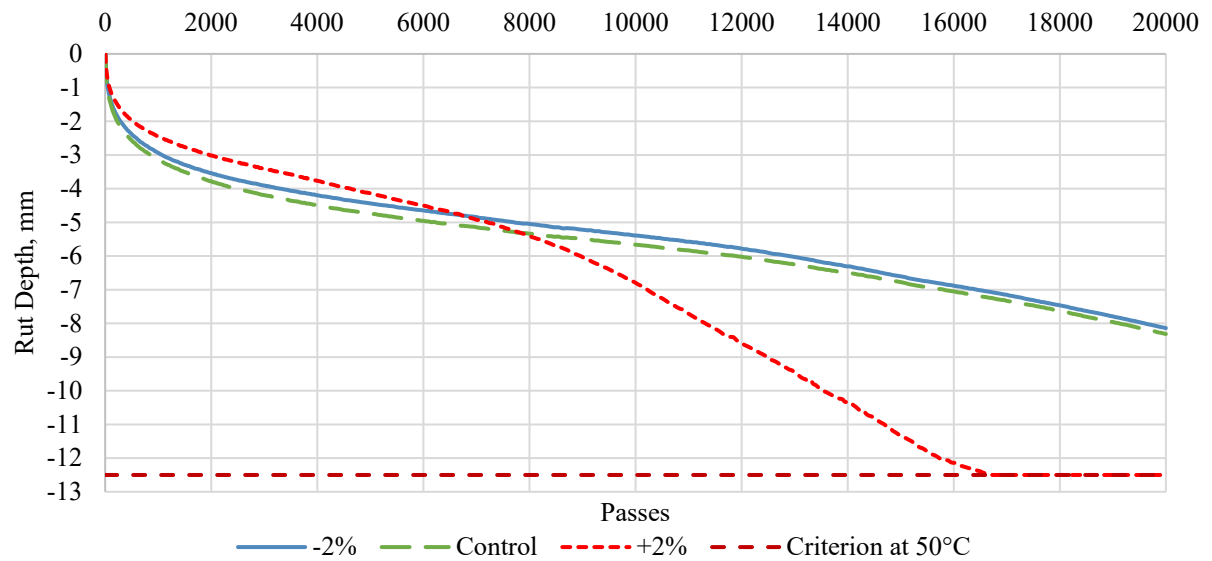


Figure 29. Rut depth (mm) vs number of passes for Lockwood Type 3 mixtures @ 50°C.

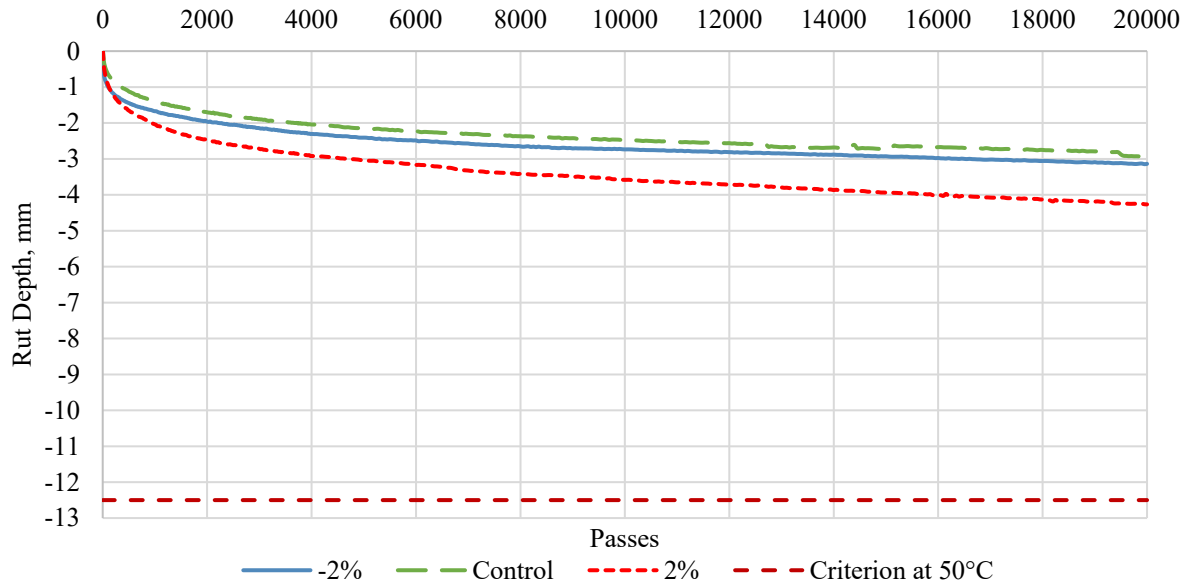


Figure 30. Rut depth (mm) vs number of passes for Spanish Spring Type 2 mixtures @ 50°C.

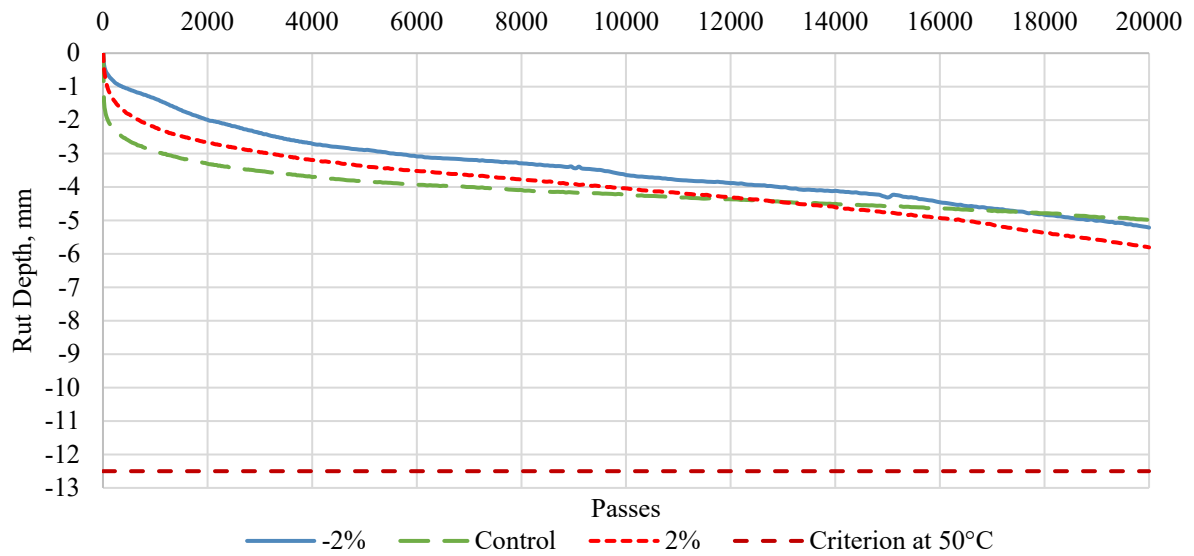


Figure 31. Rut depth (mm) vs number of passes for Spanish Spring Type 3 mixtures @ 50°C.

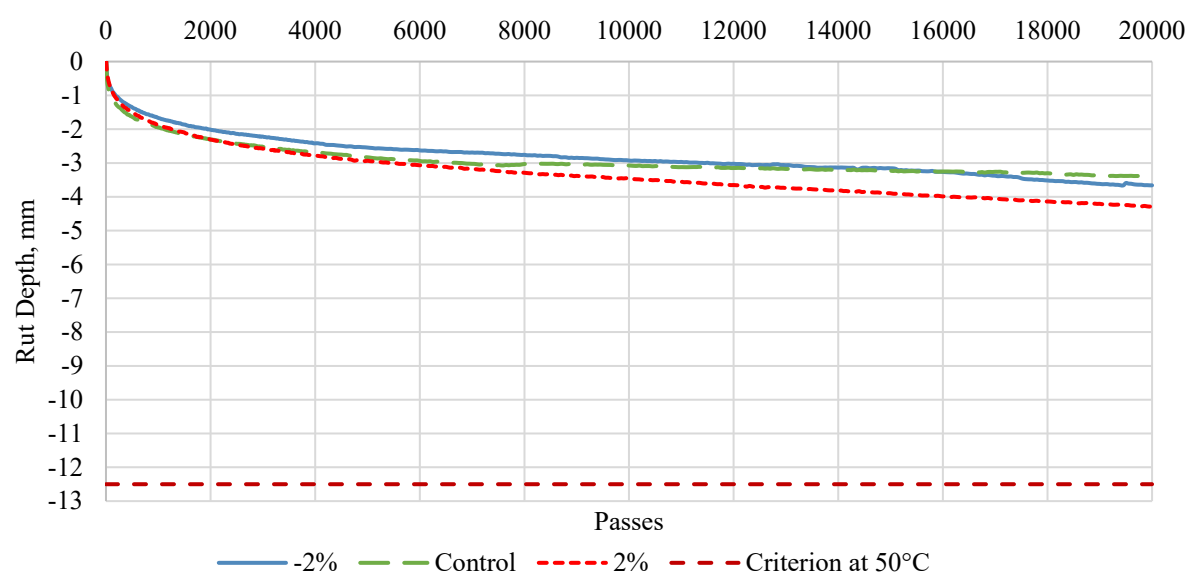


Figure 32. Rut depth (mm) vs number of passes for Mustang Type 2 mixtures @ 50°C.

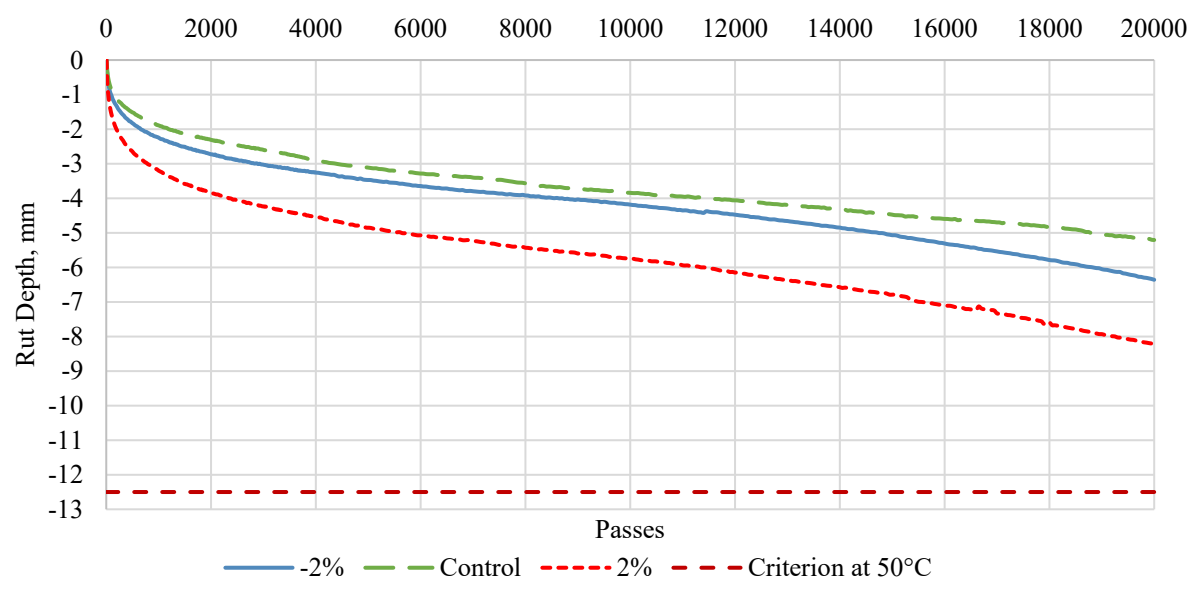


Figure 33. Rut depth (mm) vs number of passes for Mustang Type 3 mixtures @ 50°C.

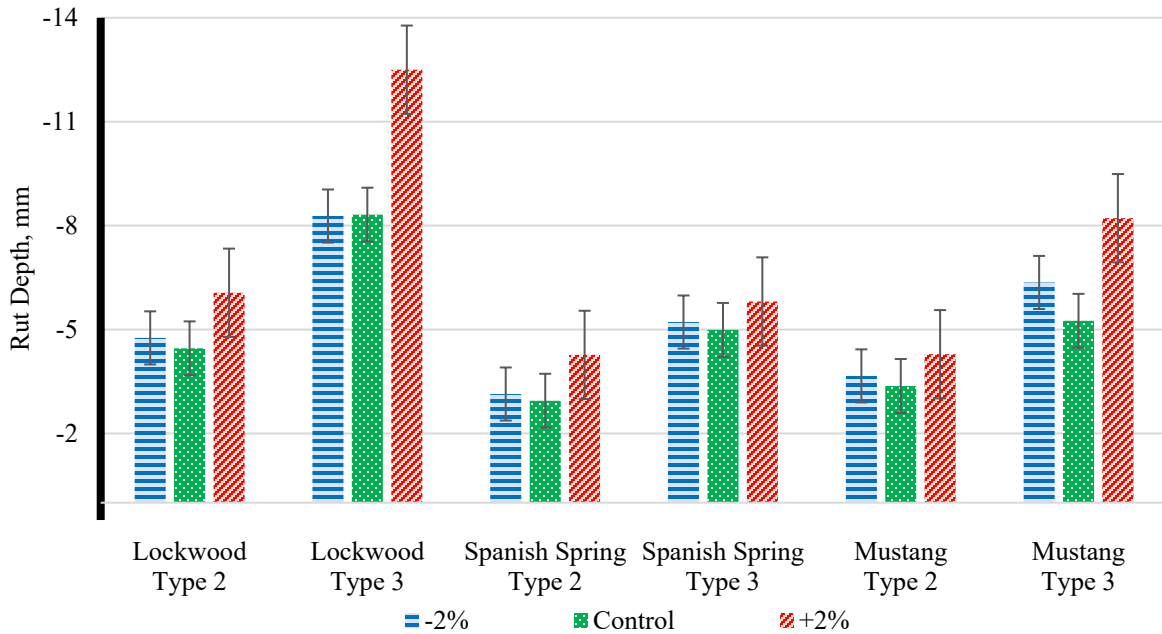


Figure 34. Comparison of rut depth (mm) for -2% p200, control and +2% p200 mixtures at 50°C.

5.3.1 Stripping Inflection Points (SIP)

HWTT simulates repeated wheel loading on asphalt specimens submerged in water, making it particularly effective in assessing both rutting performance and stripping potential (moisture-induced damage). A key performance indicator derived from this test is the SIP, defined as the point on the rut depth vs. number of passes curve where a noticeable change in slope occurs. This inflection marks the transition from rutting-dominated deformation to stripping-induced damage. Prior to the SIP, rutting develops at a relatively stable rate primarily due to shear deformation. Beyond the SIP, the rate of rutting significantly accelerates, indicating the onset of moisture damage and adhesive failure between the binder and aggregates.

In this study, the SIP was determined by analyzing the curvature of the rutting progression curve for each mixture. A steep increase in rut depth after a certain number of load passes signifies moisture-induced stripping failure. The slope before and after the SIP reflects the change in deformation behavior. A higher slope ratio often implies more severe stripping potential.

SIPs were observed in five mixtures, indicating the onset of moisture-induced damage during Hamburg Wheel Tracking Tests. For the Spanish Spring Type 3 Control mixture, a SIP was recorded at 17,350 passes with a stripping slope of 0.71 mm/1,000 passes and a high stripping-to-creep slope ratio of 5.3. The Lockwood Type 2 mixture with 7% P200 exhibited a SIP at 17,060 passes and a lower stripping slope of 0.41 mm/1,000 passes, with a stripping/creep slope ratio of 2.89, reflecting moderate susceptibility. In the Lockwood Type 3 mixture with 7% P200, both left and right wheel paths showed SIPs at 12,061 and 11,859 passes respectively, averaging 11,960 passes, with an average stripping slope of 1.35 mm/1,000 passes and a slope ratio of 3.23, indicating more aggressive post-SIP rutting. The Spanish Spring Type 3 mixture with 7% P200 demonstrated an average SIP at 17,339 passes, a low stripping slope of 0.33 mm/1,000 passes, and a slope ratio of 2.59. Finally, the Mustang Type 3 mixture with 7% P200 showed a SIP at an average of 17,037 passes, with a stripping slope of 0.60 mm/1,000 passes and a stripping-to-creep slope ratio of 3.76. These results will be illustrated in Figure 32 through Figure 37.

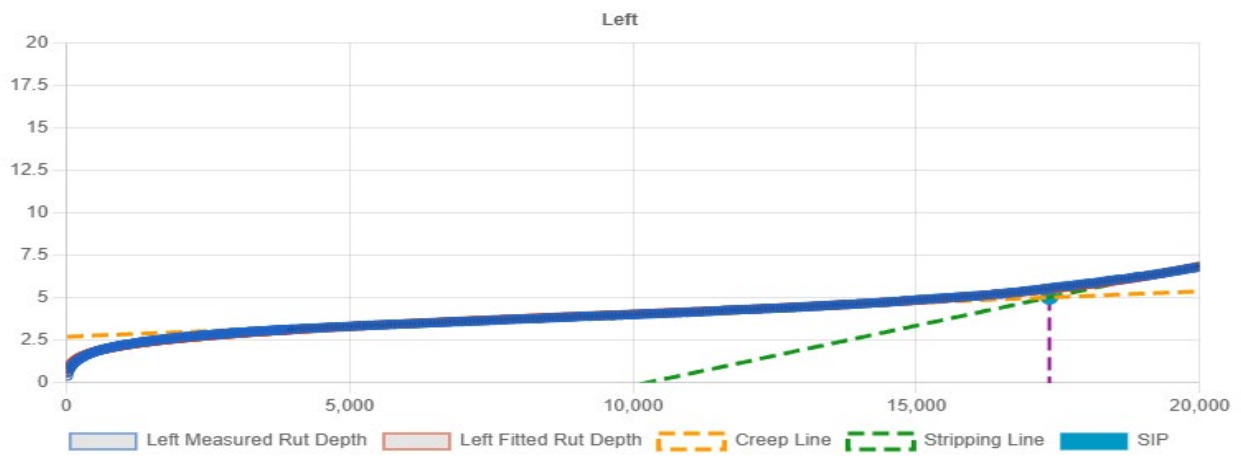
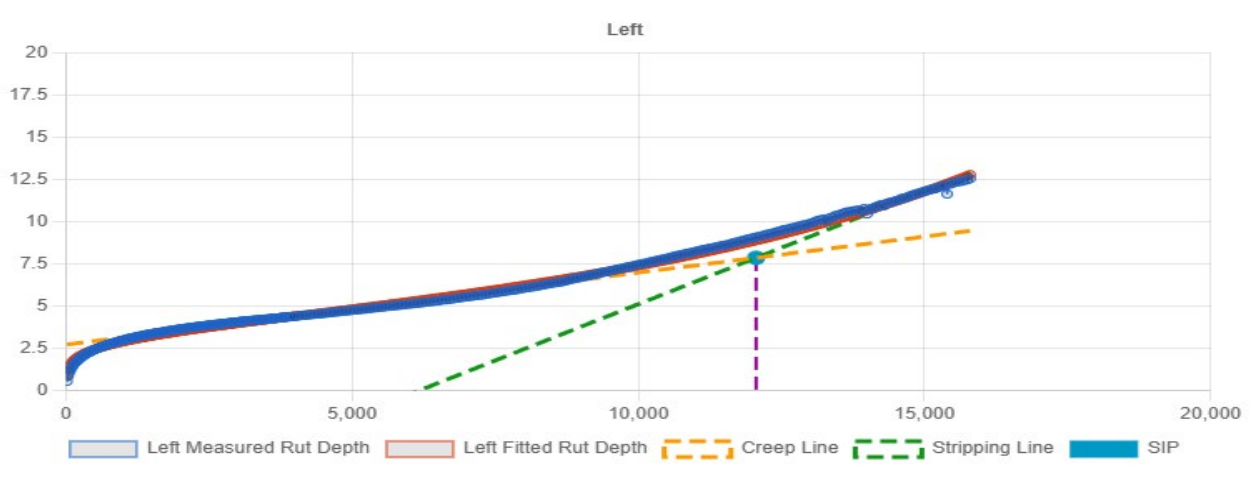


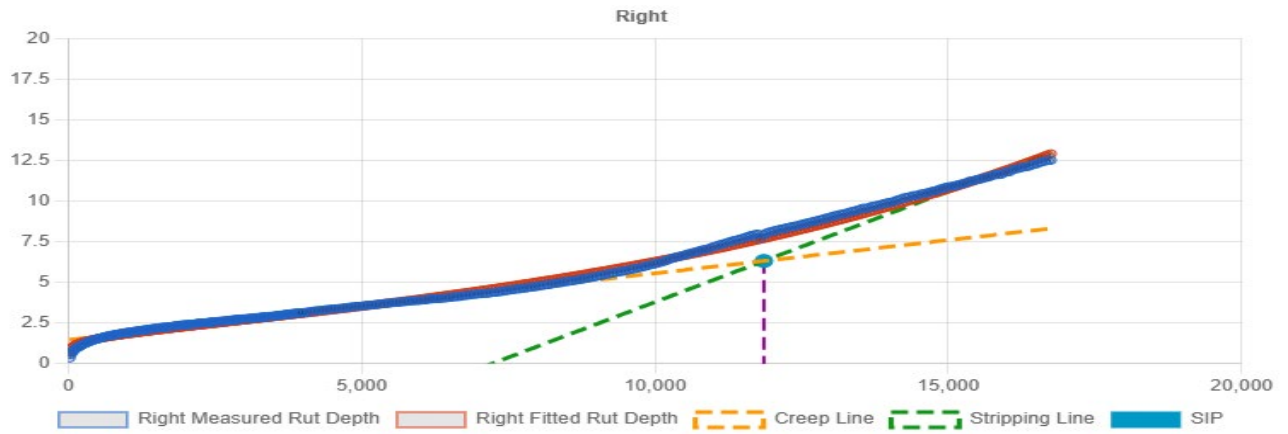
Figure 35. SIP for Spanish Spring Type 3 control mixture left wheel.



Figure 36. SIP for Lockwood Type 2 +2% P200 left wheel.

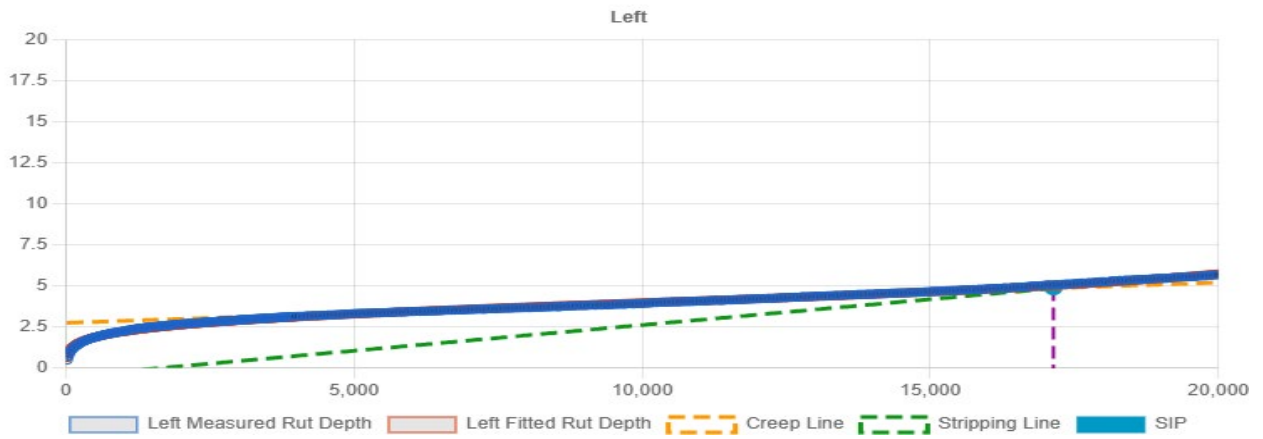


(a)

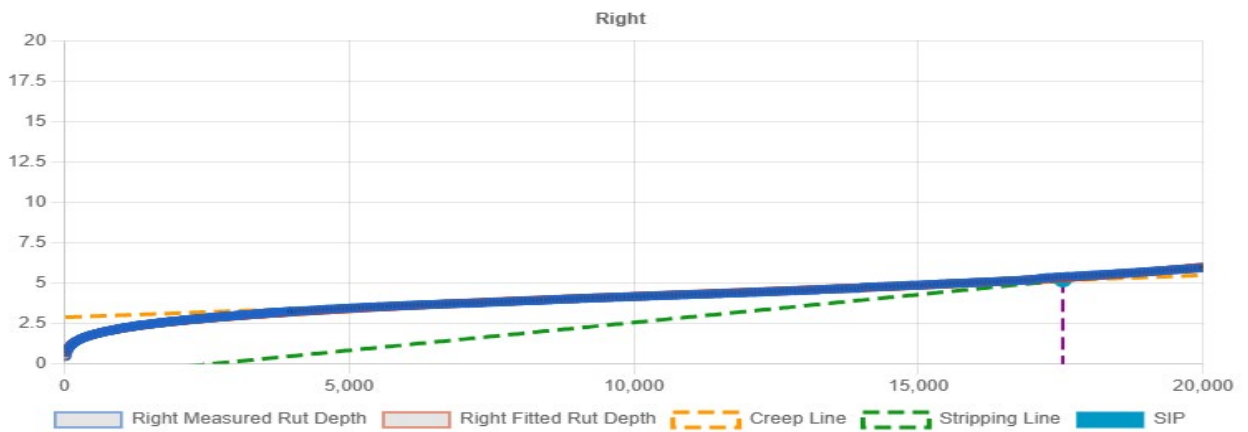


(b)

Figure 37. SIP for Lockwood Type 3 +2% P200 left (a) and right (b) wheel.



(a)



(b)

Figure 38. SIP for Spanish Spring Type 3 +2% P200 left (a) and right (b) wheel.

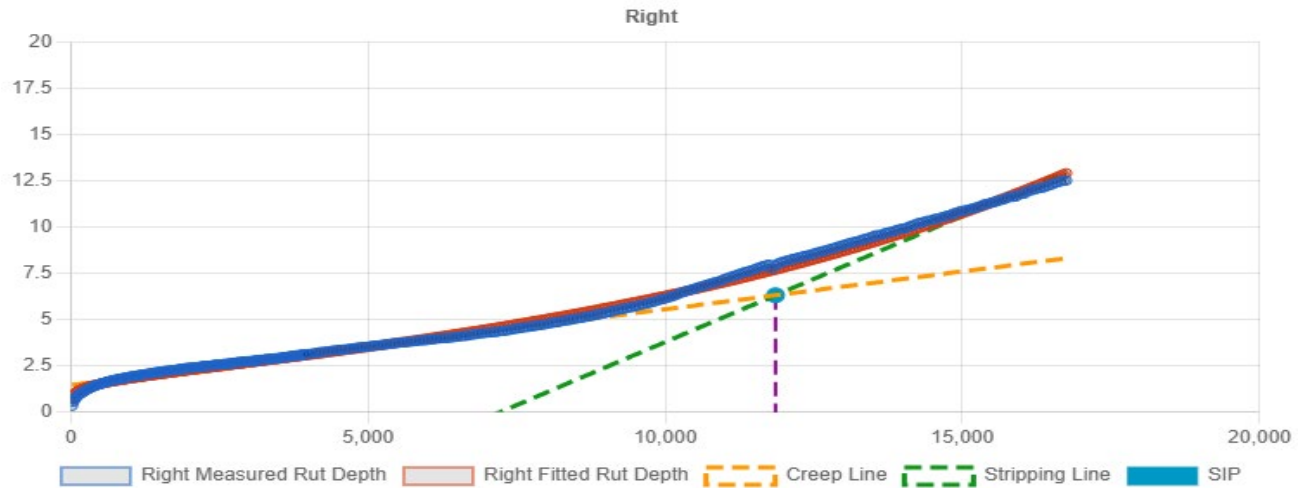


Figure 39. SIP for Mustang Type 3 +2% P200 right wheel.

5.4 Resistance to Cracking: Indirect Tensile Cracking Test (IDEAL-CT)

The IDEAL-CT evaluates the cracking resistance of asphalt mixtures under intermediate temperature conditions. The main output of this test is the Cracking Tolerance Index or CTindex, a numerical measure that characterizes the mixture's ability to resist cracking due to aging, thermal cycles, or traffic loading. The IDEAL-CT test was conducted in accordance with ASTM D8225 [39], and all specimens were tested at a controlled temperature of 77°F (25°C). For each gradation, three replicate specimens were prepared using asphalt mixtures compacted at the OBC.

5.4.1 Conditioning of Specimens

For the IDEAL-CT test, two types of sample aging conditions were used: short-term aging and mid-term aging. Short-term aging followed the standard procedure, where the loose mix was conditioned for 2 hours at the compaction temperature after mixing, simulating the typical aging that occurs during plant production and laydown.

Mid-term aging of asphalt mixtures for the IDEAL-CT test involves simulating the oxidative aging that occurs during mix production and early service life. In this process, the loose asphalt mix is conditioned in a at 212°F (100°C) for 20 hours prior to compaction. This aging step allows the binder to undergo controlled oxidation. After the 20-hour conditioning, the mixture is then reheated and conditioned for an additional 2 hours at the target compaction temperature to ensure uniform workability and temperature consistency before compaction. This procedure is crucial for producing laboratory samples that more accurately represent the in-place behavior of asphalt mixtures shortly after construction, particularly for evaluating cracking resistance under aged conditions.

Prior to compaction, all the loose mixtures were conditioned at the mixing temperature for 2 hours to ensure uniform coating and blending of the aggregates and binder. After compaction, the specimens were further conditioned for 2 hours at the target testing temperature to achieve thermal equilibrium before testing. Load was applied at a constant deformation rate of 2 inches/min. The CTindex is calculated using the load-displacement curve obtained during the indirect tensile loading of the specimen.

Tables 30 – 35 summarize the CTindex properties of the 18 mixtures. Figures 24 and 25 compares the CTindex properties of the various mixtures at the short-term and mid-term aging stages, respectively. The height of the bar represents the average value and the whisker over the bar

represent the 95% confidence interval (95%CI). Overlapping 95%CI indicates the measured CTindex values of the two mixtures are statistically similar. The data indicate that the majority of the mixtures with the three levels of P200 from each source exhibit statistically similar CTindex properties with the exception of the Lockwood mixture Type 3 where the lower P200 exhibited higher CTindex.

Table 29: IDEAL-CT Specifications (ASTM D8225-19).

Specifications Used in Lab Test	
Standard	ASTM D8225-19
Compaction Method	Superpave Gyratory
Test Temperature	25°C
Target Air Voids%	7 ± 0.5 %
Loading Rate	50mm/min (2in/min)
Aging	Short and Mid Term
Mid Term Aging Condition	STA + 20 hours at 100°C
Repeatability (ASTM D8225-19)	13.5

Table 30: IDEAL-CT Results for Lockwood Type 2 @ 25°C.

Lockwood Type 2																		
Properties	-2% P200						Control Mix						+2% P200					
Aging	Short Term Aged			Mid Term Aged (STA + 20hrs at 100°C)			Short Term Aged			Mid Term Aged (STA + 20hrs at 100°C)			Short Term Aged			Mid Term Aged (STA + 20hrs at 100°C)		
Sample ID	1	2	3	1	2	3	1	2	3	1	2	3	1	2	3	1	2	3
Binder Content TWM	4.7						4.7						4.7					
% AV	6.8	7.0	7.3	7.2	7.1	6.9	7.3	6.9	7.0	7.4	7.2	6.6	6.5	6.8	6.7	7.3	7.4	6.8
Water Absorbed	0.9	1.1	1.3	1.3	1.0	1.1	1.4	0.9	1.1	1.4	1.4	0.9	0.7	0.8	0.8	1.1	1.2	0.9
CT _{Index}	111.0	115.6	97.0	72.5	69.4	78.0	96.1	105.1	89.5	55.3	49.7	58.0	111.2	93.5	103.1	87.3	79.0	102.7
CT _{Index} Average	107.9			73.3			96.9			54.3			102.6			89.7		
Repeatability Standard Deviation	9.7			4.4			7.8			4.2			8.9			12.0		
Repeatability Standard Deviation Criteria	13.5						13.5						13.5					

Table 31: IDEAL-CT Results for Lockwood Type 3 @ 25°C.

Lockwood Type 3																		
Properties	-2% P200						Control Mix						+2% P200					
Aging	Short Term Aged			Mid Term Aged (STA + 20hrs at 100°C)			Short Term Aged			Mid Term Aged (STA + 20hrs at 100°C)			Short Term Aged			Mid Term Aged (STA + 20hrs at 100°C)		
Sample ID	1	2	3	1	2	3	1	2	3	1	2	3	1	2	3	1	2	3
Binder Content TWM	5.9						5.9						5.7					
% AV	7.1	7.5	7.0	6.8	7.4	7.2	7.1	7.0	6.6	7.1	7.3	7.3	6.5	6.6	7.1	7.3	6.5	6.7
Water Absorbed	1.1	1.4	1.1	0.9	1.5	1.2	1.1	1.1	0.8	1.0	1.3	1.3	0.7	0.7	1.0	1.2	0.8	0.9
CT _{Index}	285.4	273.0	283.7	224.3	200.8	214.9	210.3	207.2	220.7	132.8	125.7	113.8	273.2	266.5	256.7	133.4	149.6	156.4
CT _{Index} Average	280.7			213.3			212.7			124.1			265.5			146.5		
Repeatability Standard Deviation	6.7			11.8			7.1			9.6			8.3			11.8		
Repeatability Standard Deviation Criteria	13.5						13.5						13.5					

Table 32: IDEAL-CT Results for Spanish Spring Type 2 @ 25°C.

Spanish Spring Type 2																		
Properties	-2% P200						Control Mix						+2% P200					
Aging	Short Term Aged			Mid Term Aged (STA + 20hrs at 100°C)			Short Term Aged			Mid Term Aged (STA + 20hrs at 100°C)			Short Term Aged			Mid Term Aged (STA + 20hrs at 100°C)		
Sample ID	1.0	2.0	3.0	1.0	2.0	3.0	1.0	2.0	3.0	1.0	2.0	3.0	1.0	2.0	3.0	1.0	2.0	3.0
Binder Content TWM	4.4						4.4						4.4					
% AV	7.3	7.0	7.2	6.8	7.2	7.4	7.3	7.5	7.4	7.4	7.4	7.5	6.6	7.2	6.7	7.3	7.0	6.8
Water Absorbed	1.3	1.1	1.3	1.0	1.3	1.4	1.2	1.7	1.2	1.1	1.0	0.9	0.8	1.1	0.9	1.1	1.0	0.8
CT _{Index}	55.7	68.2	57.8	40.6	45.9	39.8	55.0	32.2	43.4	38.5	40.2	29.5	59.3	43.3	55.2	34.3	45.0	41.4
CT _{Index} Average	60.6			42.1			43.5			36.1			52.6			40.2		
Repeatability Standard Deviation	6.7			3.3			11.4			5.8			8.3			5.4		
Repeatability Standard Deviation Criteria	13.5						13.5						13.5					

Table 33: IDEAL-CT Results for Spanish Spring Type 3 @ 25°C.

Spanish Spring Type 3																		
Properties	-2% P200						Control Mix						+2% P200					
Aging	Short Term Aged			Mid Term Aged (STA + 20hrs at 100C)			Short Term Aged			Mid Term Aged (STA + 20hrs at 100C)			Short Term Aged			Mid Term Aged (STA + 20hrs at 100C)		
Sample ID	1	2	3	1	2	3	1	2	3	1	2	3	1	2	3	1	2	3
Binder Content TWM	4.9						4.9						4.7					
% AV	7.5	7.1	7.0	7.2	6.9	7.3	7.0	7.4	6.9	7.2	6.9	7.2	7.0	6.7	6.9	6.7	6.6	7.3
Water Absorbed	1.3	1.0	0.9	1.1	0.9	1.2	1.1	1.1	0.9	1.2	1.0	1.2	1.1	0.9	1.1	1.0	0.8	1.2
CT _{Index}	93.2	116.8	107.8	83.9	91.7	75.6	84.9	98.7	102.9	46.3	57.4	60.9	106.4	118.8	123.5	98.2	90.0	73.2
CT _{Index} Average	105.9			83.7			95.5			54.9			116.2			87.1		
Repeatability Standard Deviation	11.9			8.1			9.4			7.6			8.8			12.7		
Repeatability Standard Deviation Criteria	13.5						13.5						13.5					

Table 34: IDEAL-CT Results for Mustang Type 2 @ 25°C.

Mustang Type 2																		
Properties	-2% P200						Control Mix						+2% P200					
Aging	Short Term Aged			Mid Term Aged (STA + 20hrs at 100C)			Short Term Aged			Mid Term Aged (STA + 20hrs at 100C)			Short Term Aged			Mid Term Aged (STA + 20hrs at 100C)		
Sample ID	1	2	3	1	2	3	1	2	3	1	2	3	1	2	3	1	2	3
Binder Content TWM	4.6						4.6						4.6					
% AV	7.0	7.4	6.9	7.1	6.7	7.0	6.5	6.7	6.5	6.5	7.2	7.1	6.8	7.3	6.9	7.3	7.1	6.7
Water Absorbed	1.1	1.4	1.1	1.2	0.9	1.0	1.0	1.2	1.1	1.5	1.7	1.4	0.9	1.4	1.0	1.2	1.1	0.8
CT _{Index}	60.5	52.3	57.6	39.4	50.1	45.6	50.2	38.1	41.2	44.3	31.0	37.5	49.5	41.0	56.8	38.5	34.7	45.9
CT _{Index} Average	56.8			45.0			43.2			37.6			49.1			39.7		
Repeatability Standard Deviation	4.2			5.4			6.3			6.7			7.9			5.7		
Repeatability Standard Deviation Criteria	13.5						13.5						13.5					

Table 35: IDEAL-CT Results for Mustang Type 3 @ 25°C.

Mustang Type 3																		
Properties	-2% P200						Control Mix						+2% P200					
Aging	Short Term Aged			Mid Term Aged (STA + 20hrs at 100C)			Short Term Aged			Mid Term Aged (STA + 20hrs at 100C)			Short Term Aged			Mid Term Aged (STA + 20hrs at 100C)		
Sample ID	1	2	3	1	2	3	1	2	3	1	2	3	1	2	3	1	2	3
Binder Content TWM	5.6						5.6						5.3					
% AV	6.9	7.3	7.0	6.9	6.8	6.6	6.5	6.7	6.7	7.0	7.3	6.9	6.7	6.7	7.1	6.7	7.2	6.9
Water Absorbed	0.8	1.1	0.9	1.1	0.9	0.9	0.9	0.8	0.9	1.1	1.3	0.9	0.9	1.0	1.0	0.9	1.4	1.0
CT _{Index}	204.3	183.9	201.1	84.5	97.0	89.9	120.2	124.9	110.0	77.2	72.8	75.8	135.8	128.4	123.9	106.7	92.1	115.2
CT _{Index} Average	196.4			90.5			118.4			75.3			129.4			104.7		
Repeatability Standard Deviation	11.0			6.3			7.6			2.2			6.0			11.7		
Repeatability Standard Deviation Criteria	13.5						13.5						13.5					

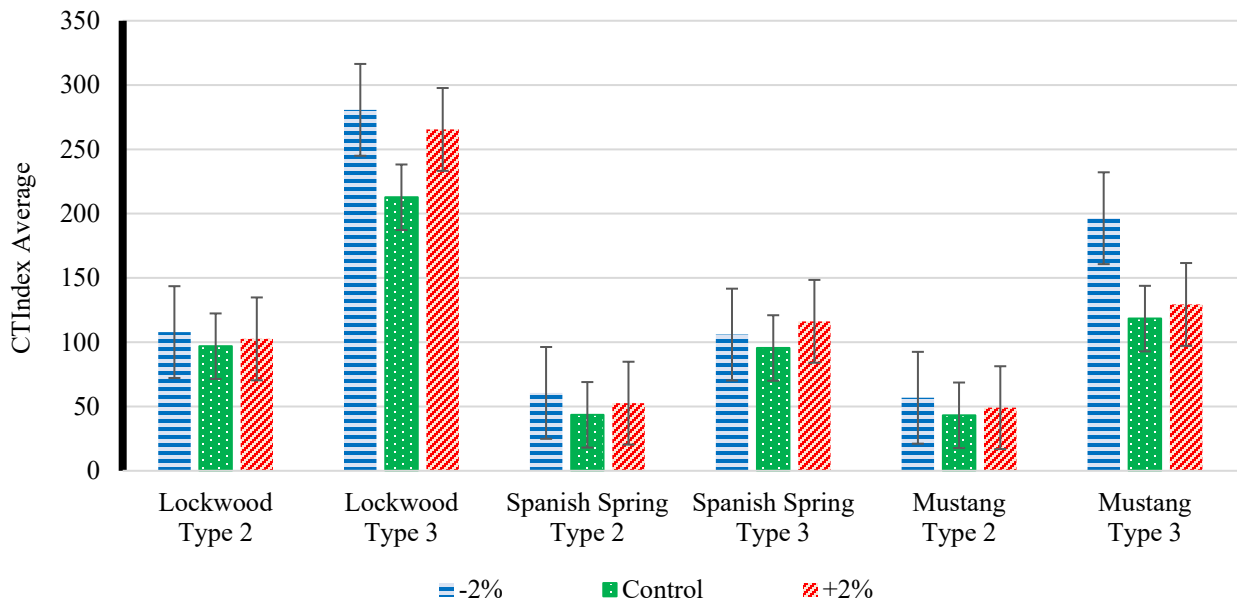


Figure 40. Comparison of Average CTIndex for -2% p200, control and +2% p200 short-term aged mix @ 25°C.

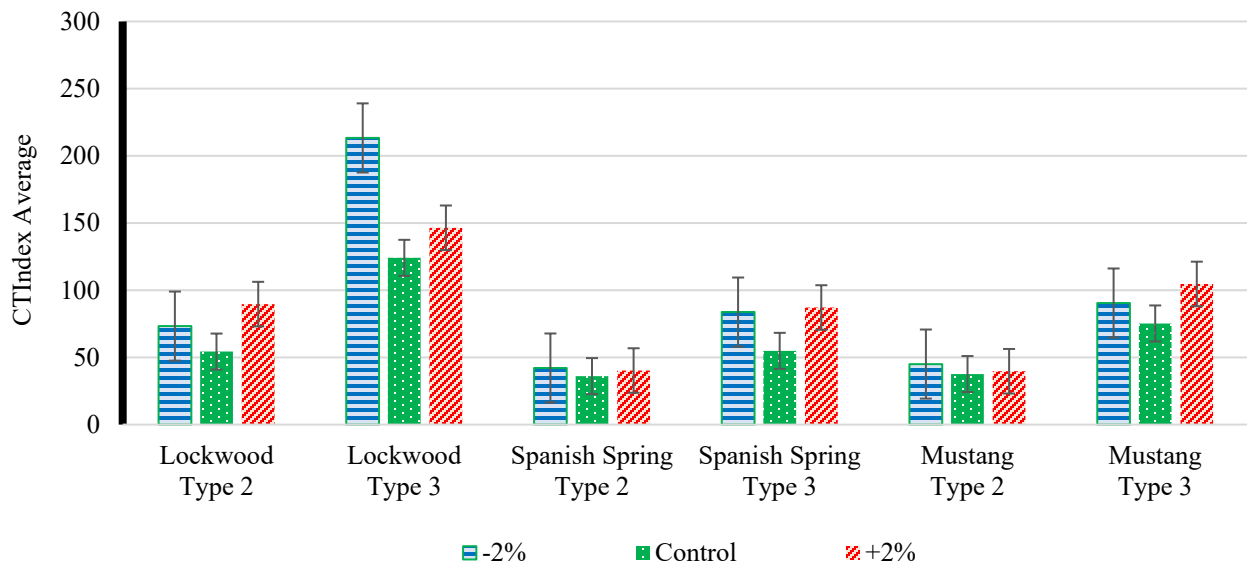


Figure 41. Comparison of Average CTIndex for -2% p200, control and +2% p200 mid-term aged mix @ 25°C.

5.4.2 CTindex after MTOA vs OBC

A linear regression analysis was performed to investigate the relationship between the optimum binder content (OBC) and the CTindex after MTOA of the mixtures. The analysis showed a strong positive correlation between OBC and CTindex values. The regression equation obtained was:

$$\text{CTindex} = 70.9 * \text{OBC} - 273$$

The coefficient of determination ($R^2 = 0.68$) indicates that approximately 68% of the variability in CTindex values can be explained by changes in OBC. The adjusted R^2 value of 0.66 accounts for the sample size of $n = 18$. The regression model was found to be statistically significant, with an F-statistic of 33.7 and a corresponding p-value of $2.7 * 10^{-5}$, confirming that the observed relationship is highly unlikely to have occurred by chance.

The slope coefficient (70.9) suggests that for every 1% increase in OBC, CTindex increases by approximately 71 units, indicating a substantial improvement in cracking resistance with increased binder content. Both the slope and intercept were statistically significant ($p < 0.05$). The standard error of the estimate was 26.9, reflecting the typical deviation of the observed CTindex values from the predicted regression line.

These findings provide strong evidence that higher binder contents lead to improved cracking resistance, supporting the hypothesis that binder film thickness plays a critical role in mixture performance. However, approximately 32% of the variability remains unexplained, which may be attributed to material heterogeneity, measurement variability or other influencing factors not accounted for in this model. The CTindex vs OBC plot is represented in figure 42.

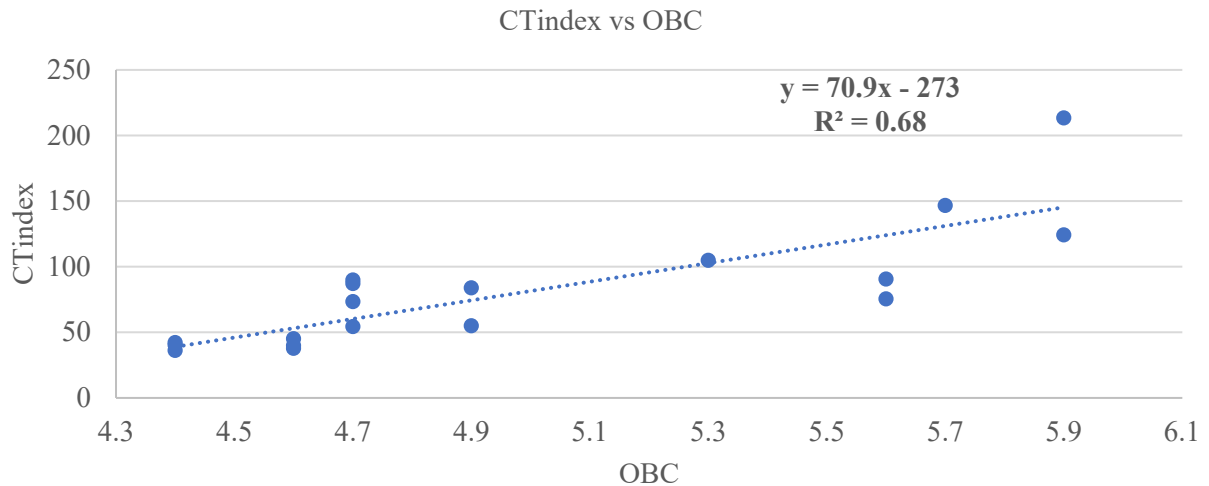


Figure 42. CTindex vs OBC.

5.4.3 CTindex after MTOA vs VMA

A linear regression analysis was conducted to evaluate the relationship between Voids in Mineral Aggregate (VMA) and the CTindex values of the asphalt mixtures. The regression equation obtained was:

$$\text{CTindex} = 56.0 * \text{VMA} - 693.6$$

The analysis showed a strong positive correlation, with a coefficient of determination ($R^2 = 0.74$) indicating that approximately 74.4% of the variation in CTindex values could be explained by changes in VMA. The adjusted R^2 value is 0.73 for the considering the sample size ($n = 18$). The standard error of the estimate was 24.0, indicating the average deviation of observed CTindex values from the predicted regression line.

The regression model was found to be statistically significant, with an F-statistic of 46.6 and a corresponding p-value of $4 * 10^{-6}$, indicating that the observed relationship between VMA and CTindex is highly unlikely to have occurred by chance.

The slope coefficient (56.0) suggests that for every 1% increase in VMA, the CTindex increases by approximately 56 units, highlighting the influence of VMA on improving cracking resistance. Both the slope and intercept were statistically significant ($p < 0.05$), as demonstrated by strong t-statistic values.

These findings indicate increasing VMA positively influences cracking resistance, likely due to the resulting increase in binder film thickness and enhanced mixture flexibility. However, it was noted that excessively high VMA potentially compromised mixture stability, emphasizing the importance of achieving an optimum VMA range for balanced performance.

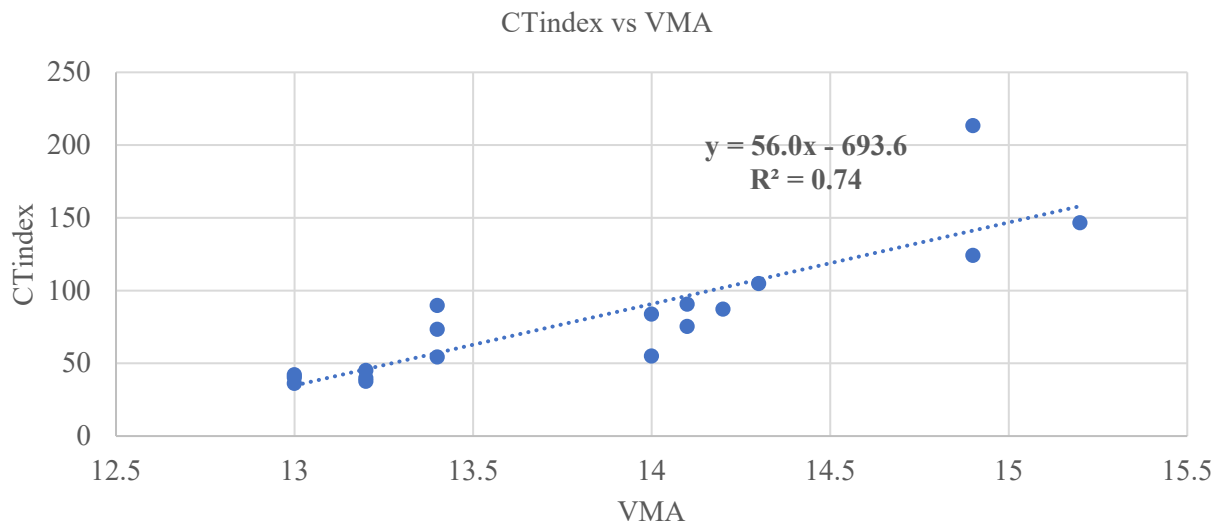


Figure 43. CTindex vs VMA.

5.4.4 CTindex after MTOA vs DP

A linear regression analysis was conducted to investigate the relationship between DP (Dust Proportion) and CTindex values of the asphalt mixtures. The resulting regression equation was:

$$\text{CTindex} = -410.0 \cdot \text{DP} + 562.8$$

The model showed a weak correlation, with a coefficient of determination $R^2 = 0.07$, indicating that only about 7.1% of the variation in CTindex values could be explained by changes in DP. The adjusted R^2 was 0.01.

The standard error of the estimate was 0.03, and the regression model was not statistically significant. The F-statistic was 1.2 with a p-value of 0.29 (>0.05), indicating that the relationship between DP and CTindex is not statistically meaningful at the 95% confidence level.

The slope coefficient (-0.0002) suggests a negligible negative trend, where an increase in DP slightly reduces CTindex. However, the t-statistic for the slope was -1.1 with a p-value of 0.29, indicating that this result is statistically insignificant.

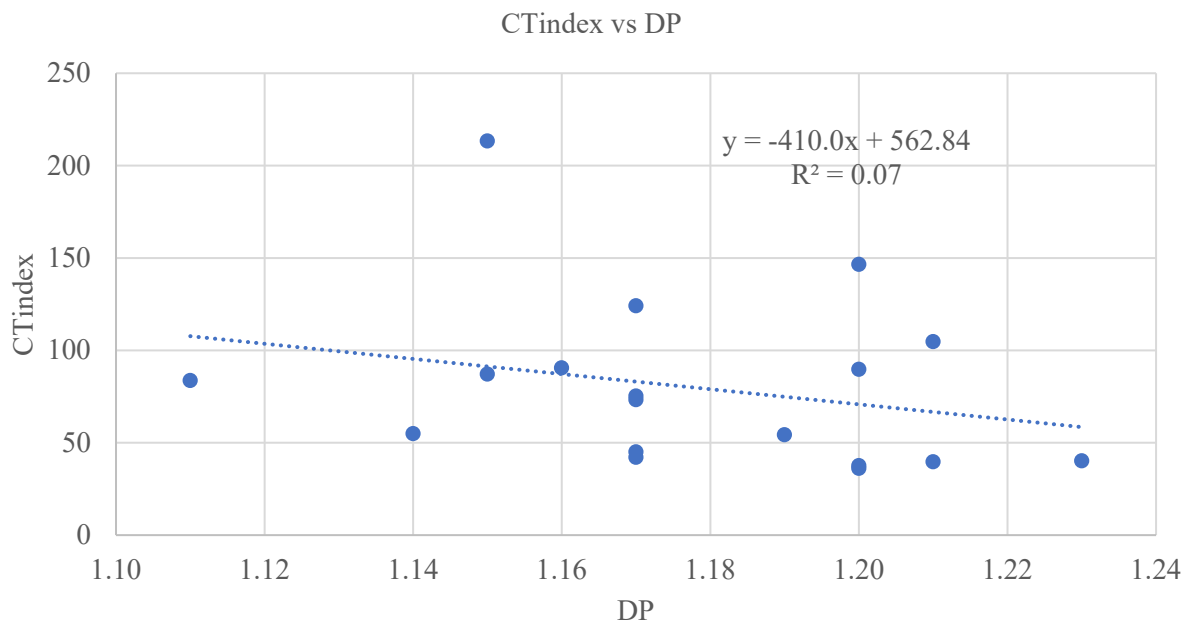


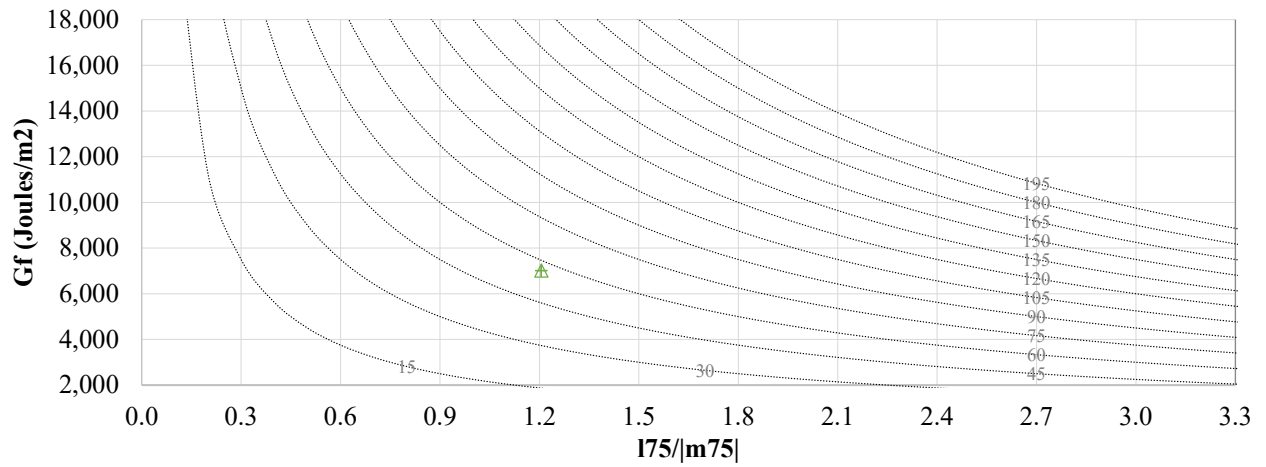
Figure 44. CTindex vs DP.

5.4.5 Interaction Plot for IDEAL-CT Test

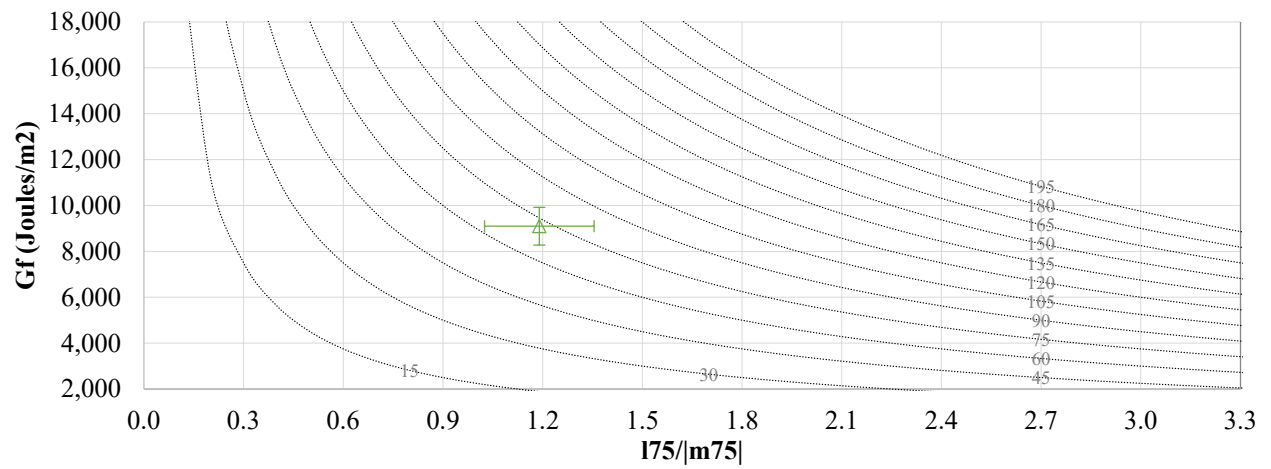
The interaction plot is a graphical tool used to visualize the relationship between fracture energy (G_f) and the load ratio at 75% of peak load (denoted as l_{75}/m_{75}) obtained from the IDEAL-CT test. This plot helps in evaluating and comparing the cracking behavior of asphalt mixtures by simultaneously considering both the energy absorption capacity and the shape of the load-displacement curve.

In this study, interaction plots were developed by plotting G_f (J/m^2) on the x-axis and l_{75}/m_{75} on the y-axis for each replicate. The G_f value represents the area under the load-displacement curve, reflecting the total energy required to fracture the specimen. The l_{75}/m_{75} ratio gives insight into the post-peak cracking behavior, lower values typically indicate more brittle failure, while higher values suggest more gradual, ductile cracking.

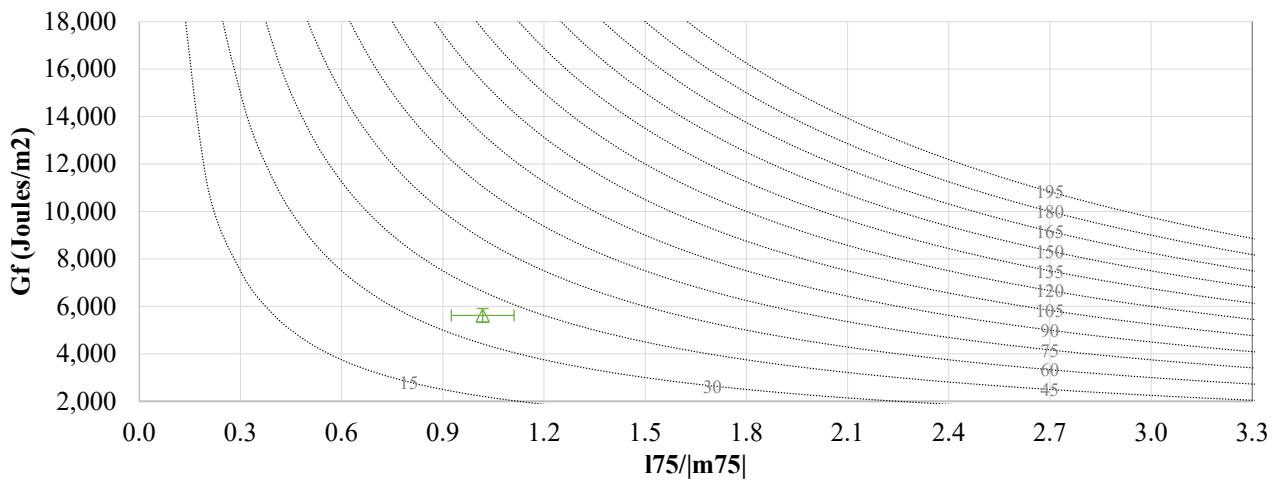
The interaction plot allows for easy identification of mixtures with balanced cracking resistance. Mixtures located in the upper right portion of the graph (i.e., high G_f and high l_{75}/m_{75}) demonstrate both good energy absorption and favorable post-peak behavior, indicating enhanced cracking resistance. Conversely, points in the lower left corner reflect low fracture energy and brittle response, typically associated with poor cracking performance. This type of analysis is particularly useful for distinguishing between mixtures that may have similar CT_{index} values but differ in underlying fracture mechanisms. In this study, only MTOA (Medium-Term Oven-Aged) samples were included in the interaction plots to focus on long-term performance trends. The interaction plots are represented in figure 34-36.



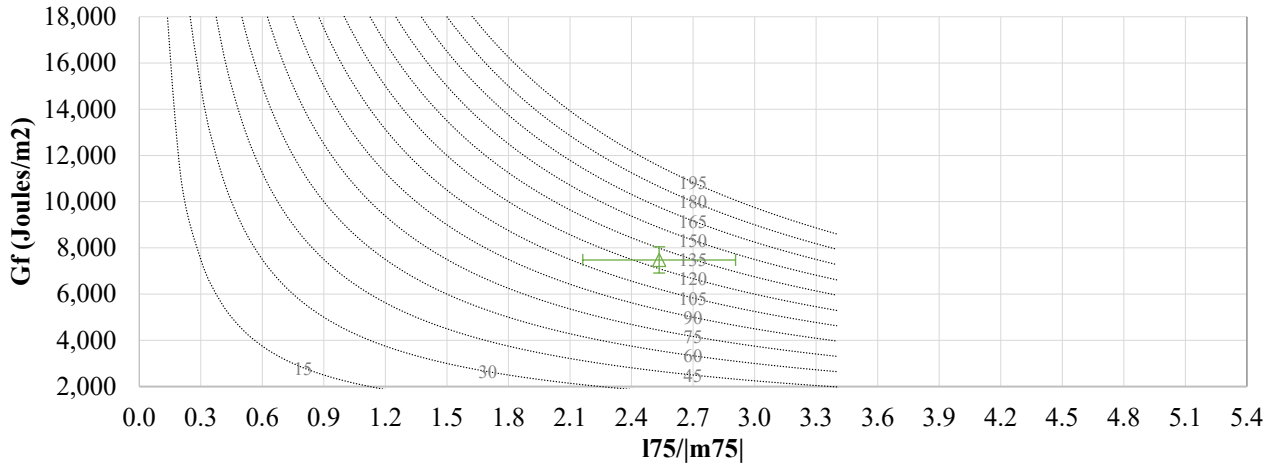
a. Lockwood Type 2 control.



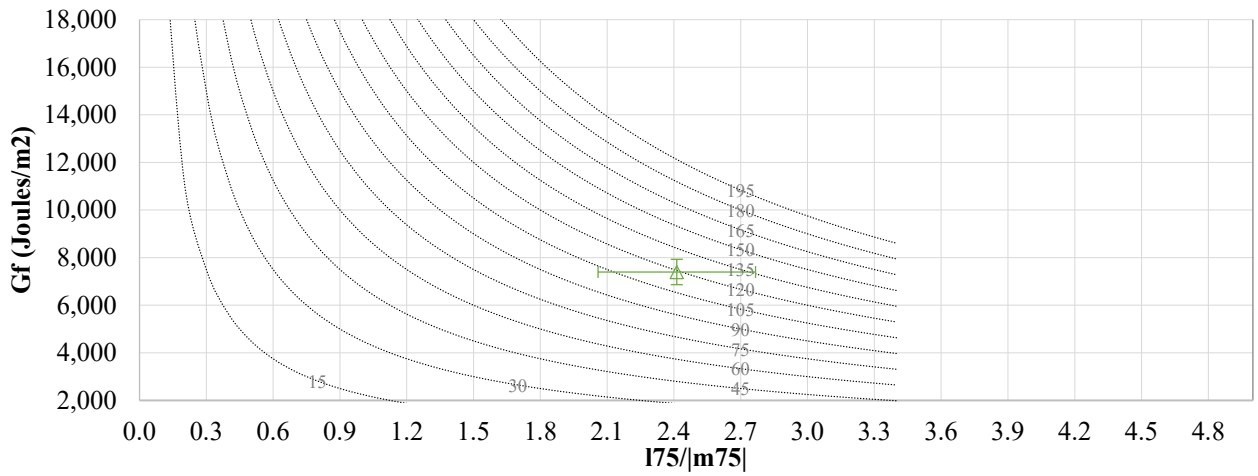
b. Lockwood Type 2 -2% P200.



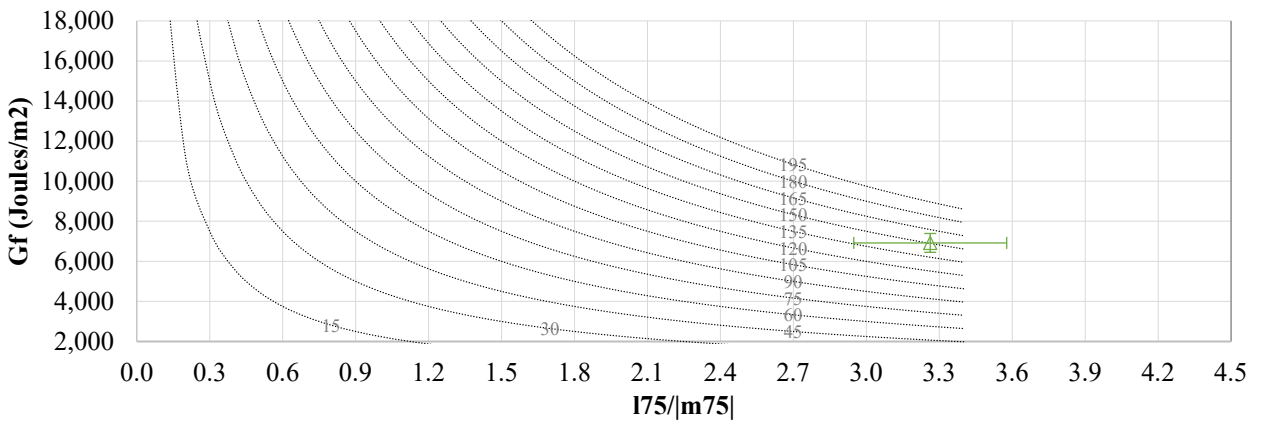
c. Lockwood Type 2 +2% P200.



d. Lockwood Type 3 control.

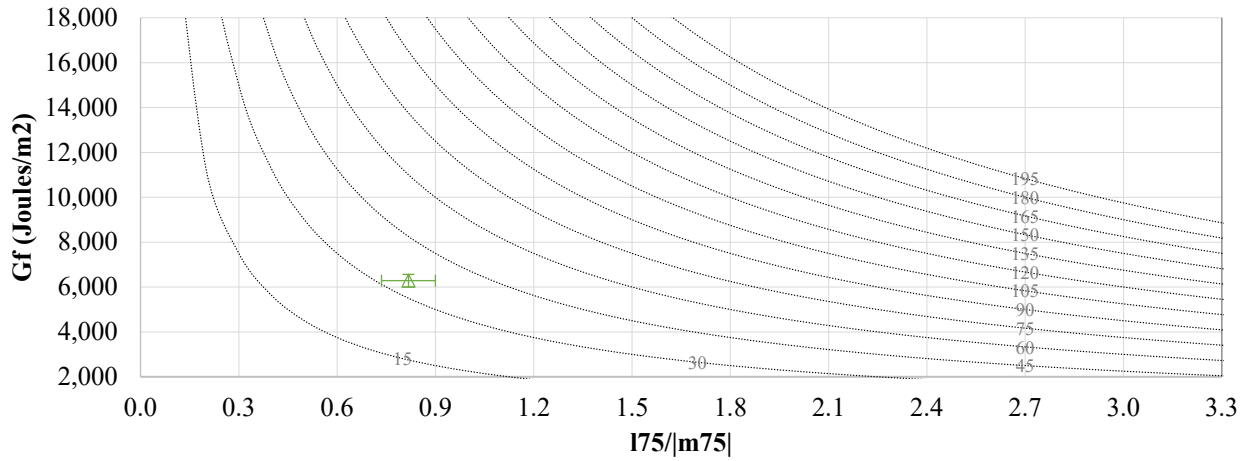


e. Lockwood Type 3 -2% P200.

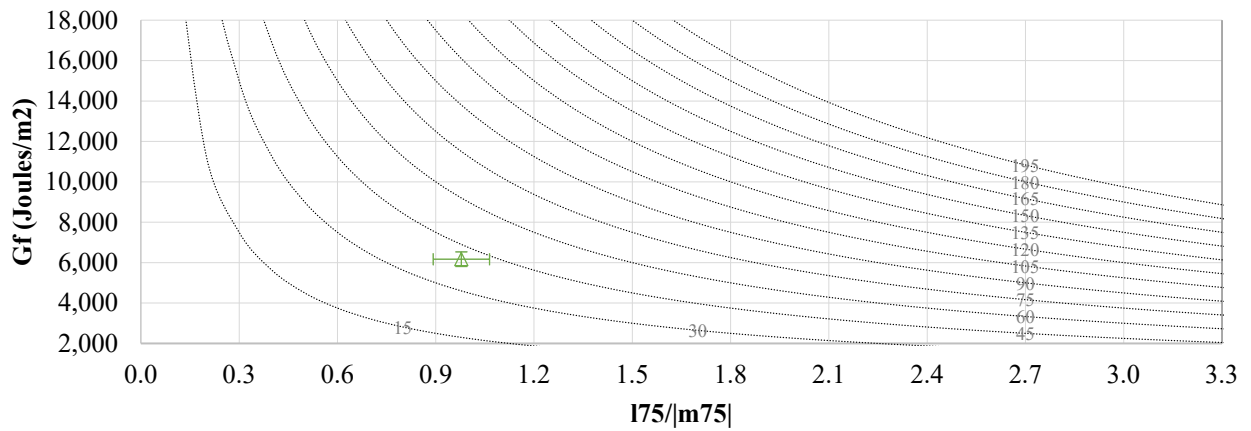


f. Lockwood Type 3 -7% P200.

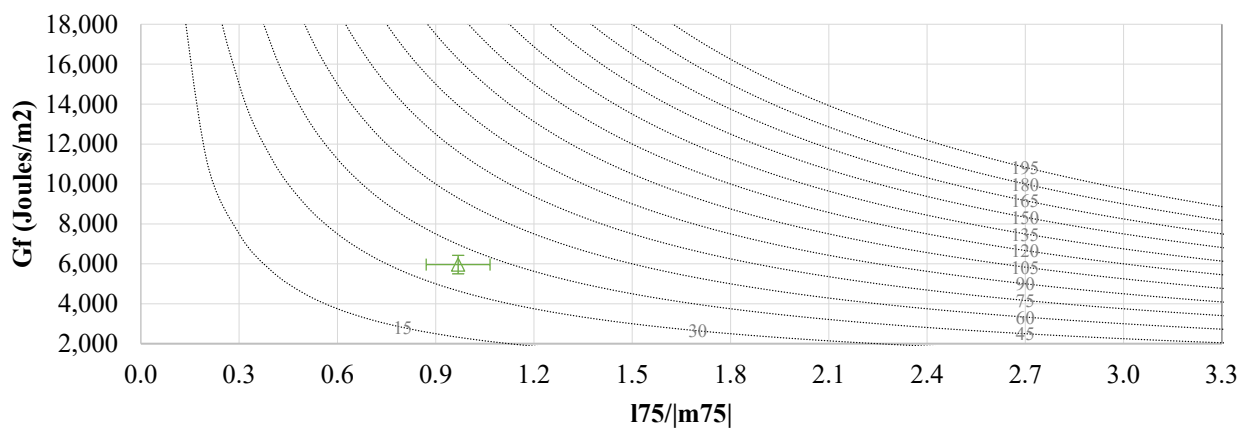
Figure 45. Interaction plots for Lockwood mid-term aged mix @ 25°C.



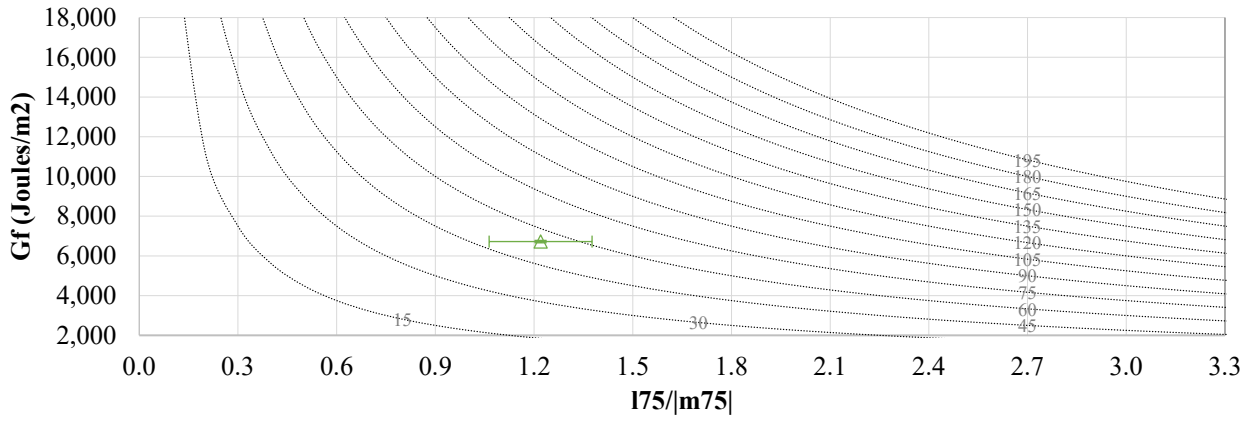
a. Spanish Spring Type 2 control.



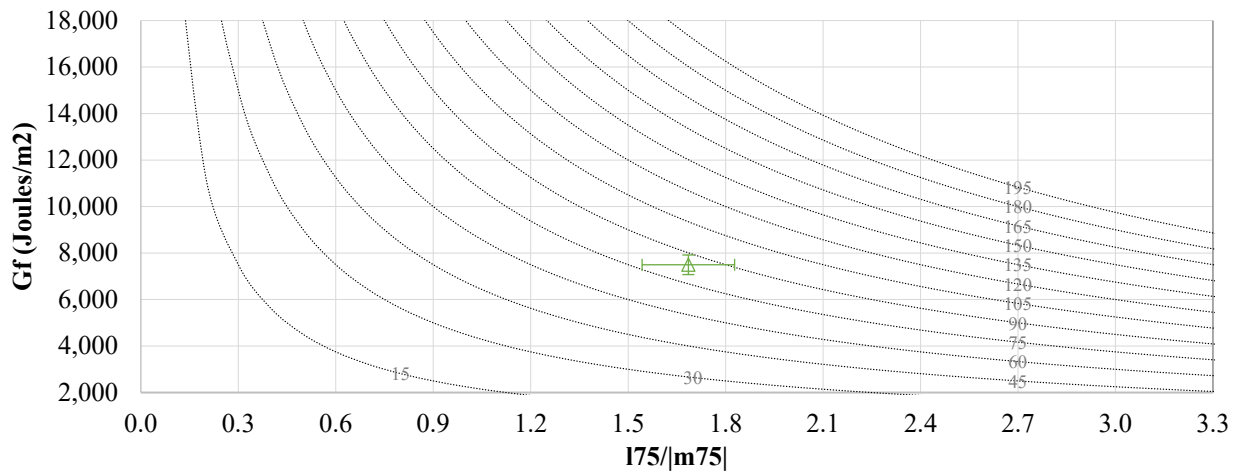
b. Spanish Spring Type 2 -2% P200.



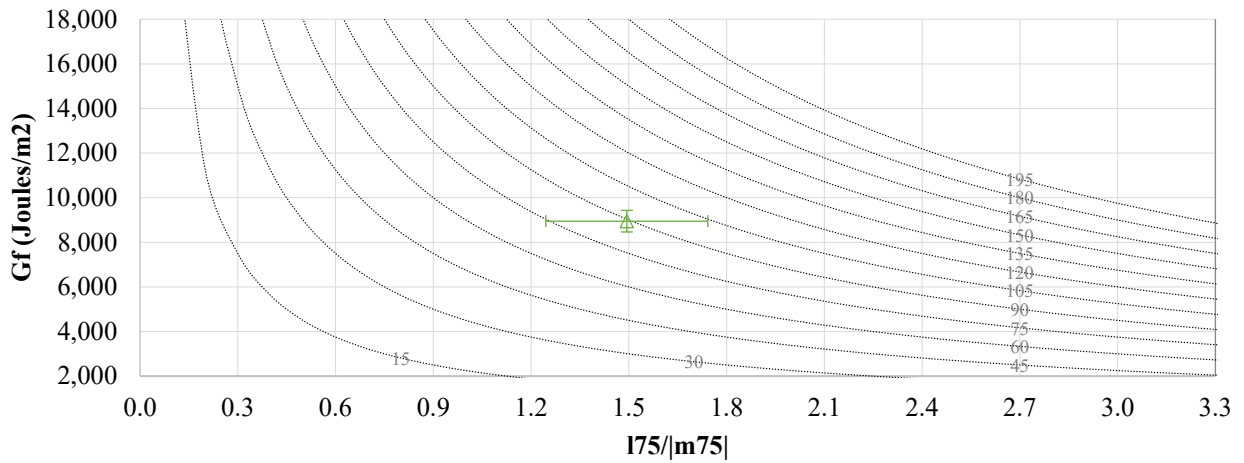
c. Spanish Spring Type 2 +2% P200.



d. Spanish Spring Type 3 control.

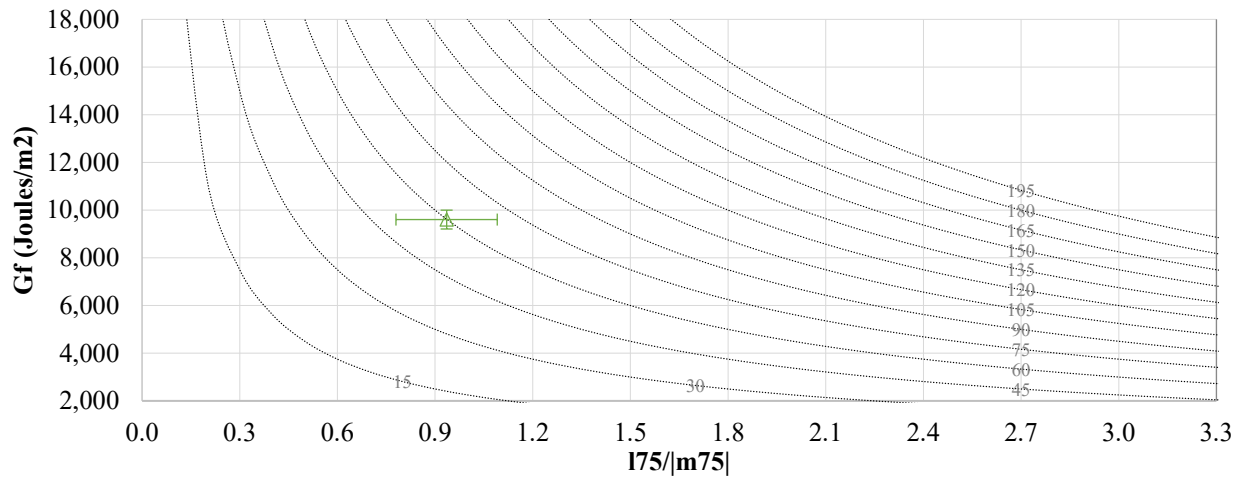


e. Spanish Spring Type 3 -2% P200.

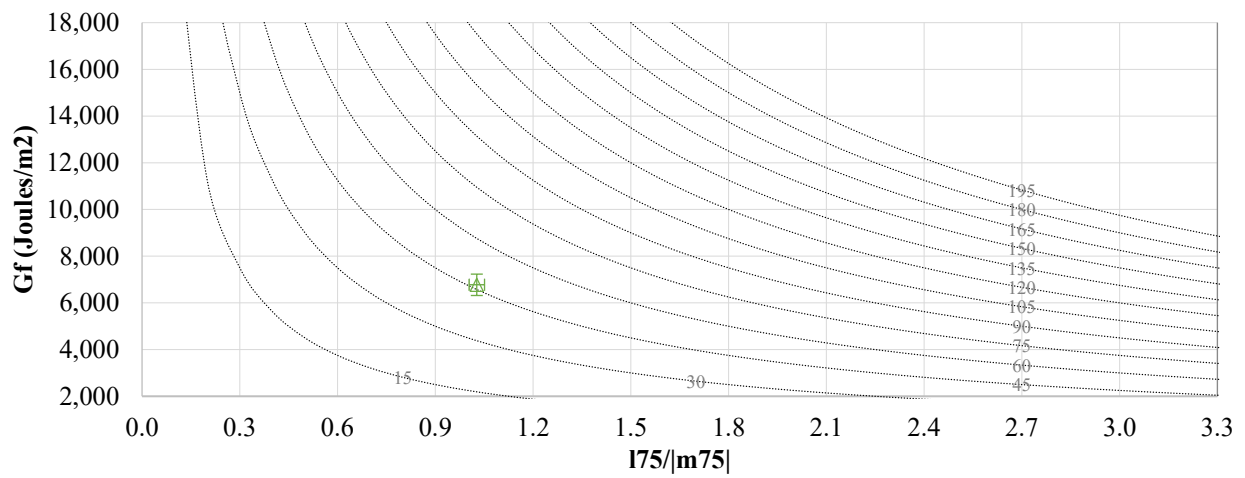


f. Spanish Spring Type 3 +2% P200.

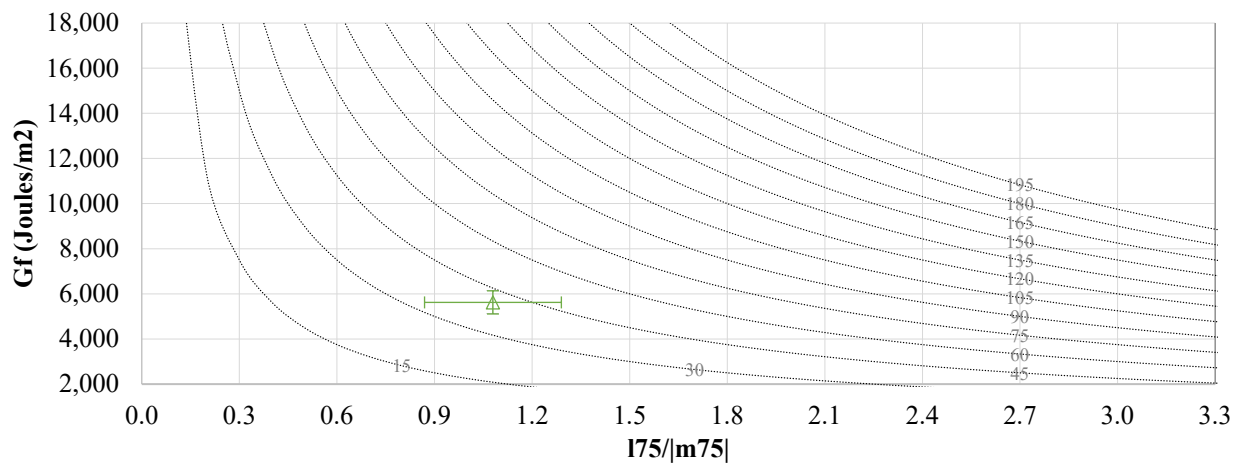
Figure 46. Interaction plots for Spanish Spring mid-term aged mix @ 25°C.



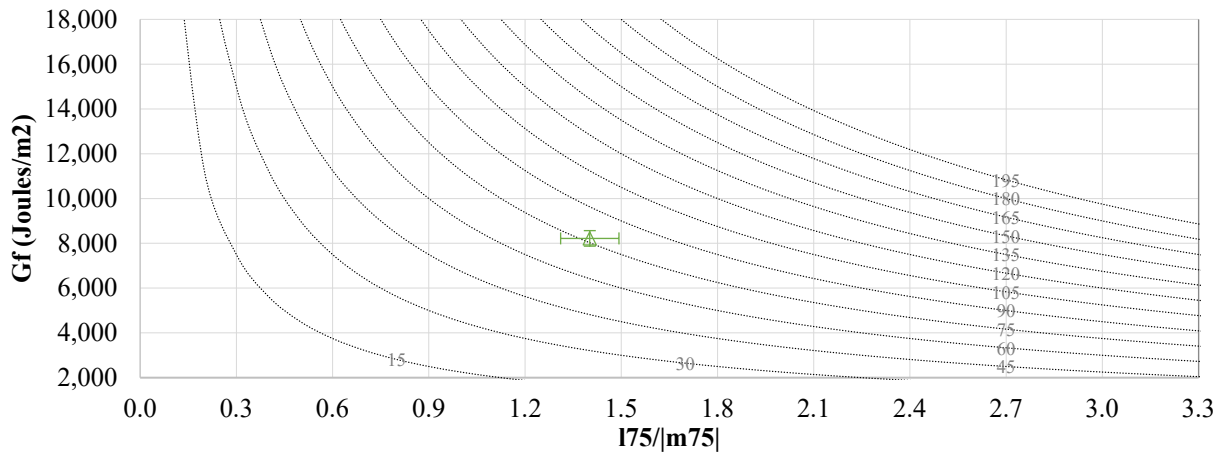
a. Mustang Type 2 control.



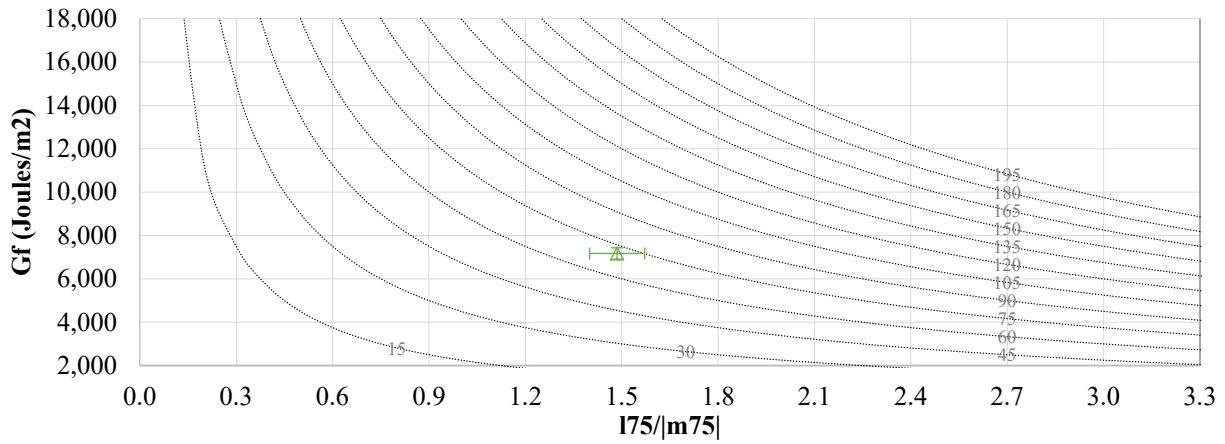
b. Mustang Type 2 -2% P200.



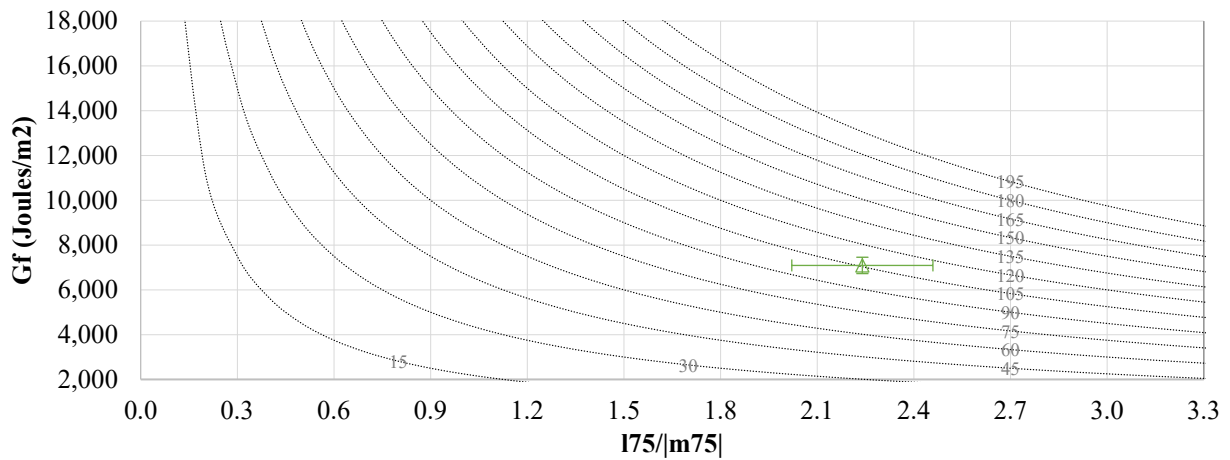
c. Mustang Type 2 +2% P200.



d. Mustang Type 3 control.



e. Mustang Type 3 -2% P200.



f. Mustang Type 2 +2% P200.

Figure 47. Interaction plots for Mustang mid-term aged mix @ 25°C.

Chapter 6: Mechanistic Empirical Pavement Modeling

6.1 Introduction to Pavement ME Design

The Mechanistic-Empirical Pavement Design Guide (MEPDG) [45] implemented through the AASHTOWare Pavement ME Design software, is a cutting-edge tool used for predicting pavement performance under specific environmental, traffic, and material conditions. Unlike empirical-based methods, the ME framework combines mechanistic modeling of pavement responses (stresses, strains, deflections) with empirical transfer functions derived from long-term field performance data. This allows for a more reliable prediction of key distresses such as rutting, fatigue cracking, and thermal cracking.

In this study, the Pavement ME Design software was used to evaluate the long-term performance implications of varying P200 content in AC mixtures. By simulating field conditions, the software provided a means to relate laboratory findings with real-world performance expectations.

6.2 AASHTOWare Pavement ME Design Software

The Pavement ME software, developed under the guidance of AASHTO includes a variety of inputs to model pavement life and distress over time. This includes:

- Climatic data derived from the Modern-Era Retrospective Analysis for Research and Applications (MERRA), which provides hourly weather information from the closest station to the project site.
- Traffic input based on actual axle load spectra and vehicle classifications, replacing outdated ESAL-based approaches.
- Material properties, entered based on a hierarchical input system (Levels 1–3), depending on the availability of test data.

For this project, a Level 1 input approach was followed where possible, using laboratory-generated data from dynamic modulus (E^*) testing, HWTT, and IDEAL-CT tests. The software accounted for layer-specific modulus, binder properties, and volumetric characteristics for each mix variant (Control, -2% P200, and +2% P200).

6.3 Model Calibration for Nevada Conditions

Although Pavement ME includes nationally calibrated models, these often require regional adjustment to reflect local materials and environmental conditions. To address this, the Nevada Department of Transportation (NDOT), in collaboration with the University of Nevada, Reno, developed state-specific calibration factors and material property databases [47]. These were documented in the “Manual for Designing Flexible Pavements in Nevada Using AASHTOWare Pavement ME Design.”

In this study, District 2 calibration factors were applied to ensure the results accurately represent the performance of mixtures produced using regional materials such as Lockwood, Spanish Spring, and Mustang aggregates. The use of a PG64-28NV SBS polymer-modified binder and 15% RAP further aligns with standard Nevada paving practices and ensures the modeling inputs reflect real construction scenarios.

6.4 Simulation of Mix Performance

Each of the 18 mix designs developed in the laboratory, representing combinations of mix type (Type 2 and Type 3) and varying P200 content, were individually modeled in Pavement ME. Key objectives of the modeling phase included:

- Assessing the impact of P200 on rutting depth over time under typical Nevada loading conditions.

- Predicting fatigue cracking potential due to increased brittleness from excessive fines.
- Evaluating thermal cracking behavior, especially for mid- to long-term aged conditions.

Inputs included:

- Dynamic modulus master curves generated from lab data across multiple temperatures and frequencies.
- Volumetric properties such as air voids, VMA, and effective binder content.
- 3 pavement layers: Subgrade, Crushed Aggregate Base Course (CAB), and Asphalt layer.
AC layer thickness: 7 inches over an aggregate base of 12 inches with 20,000 psi modulus with a subgrade of 8,000 psi at an Average Annual Daily Truck Traffic (AADTT) of 700.
- Structural composition reflecting typical asphalt pavement structures used in Nevada.

6.5 Key Modeling Insights

The comparison between Pavement ME simulation outputs and laboratory test results reveal a consistent trend with respect to P200 content. Mixtures with higher P200 content exhibited increased predicted rut depths, aligning with the rutting behavior observed in the Hamburg Wheel Tracking Test (HWTT). The control mixtures consistently demonstrated better performance, with an average predicted service life of 3 to 5 years, outperforming both reduced and increased P200 mixtures. These findings indicate the importance of maintaining proper control over P200 content during both mix design and field production, as deviations can significantly impact long-term pavement durability and rutting resistance.

Table 36: Comparison of Average Performance Test Results Between Pavement ME Output and Laboratory Test.

Measured Parameters		P200 Content		
		-2%	Control	2%
Rutting of Pavement (in)	Pavement ME Output	2.3	1.8	3.5
	Lab Test (HWTT) Average	5.2	4.9	6.9
Fatigue Cracking	Pavement ME Output, %lane	1.7	2.5	2.6
	Lab Test (IDEAL-CT) Average	134.7	101.7	119.2

Preliminary modeling results showed strong alignment with laboratory findings. The following performance trends were observed:

- Higher P200 content was associated with increased predicted rut depths, particularly in Type 3 mixtures, confirming HWTT trends.
- Control mixtures performed better overall, showing an average life span of 3 to 5 years, higher than reduced or increased P200 mixtures.
- These simulations support the hypothesis that proper control of P200 content during mix design and field production is crucial for optimizing pavement durability and performance.

6.6 Future Application of Pavement ME in Fine Content Research

The use of Pavement ME Design in this study illustrates its value in extending laboratory results into long-term performance predictions. Future work could enhance this application by:

- Incorporating climate change scenarios to assess how future temperature increases might affect high-fine-content mixtures.
- Expanding simulations to include different subgrade types or alternative binder grades.
- Using traffic growth projections to evaluate the robustness of different fine content designs under increased axle load repetitions.

The evaluation was primarily based on the volumetric properties and dynamic modulus values of the developed gradations. However, to accurately assess the long-term performance and predicted service life of each mix, it is essential to obtain mix-specific calibration factors. These localized calibration parameters help to relate laboratory-based performance indicators and actual field behavior. Moreover, the analysis revealed that top-down fatigue cracking emerged as the dominant distress mechanism influencing the pavement's lifespan, especially in gradations with higher stiffness and reduced flexibility. By leveraging regionally calibrated models, this approach provides realistic insight into how P200 variations impact the long-term behavior of asphalt pavements and can be used to guide future mix design specifications and construction practices in Nevada and similar regions.

Chapter 7: Findings, Conclusions, and Recommendations

7.1 Findings and Conclusions

This research investigated the effects of fine aggregate content, specifically the percentage passing the No. 200 sieve on the performance of asphalt concrete (AC) mixtures. The study involved designing mixtures using the Marshall Method with three varying P200 levels (-2%, control, and +2%) in accordance with RTC specifications. Performance evaluation was conducted through dynamic modulus testing, Hamburg Wheel Track Testing (HWTT), and the IDEAL-CT cracking test. Mixtures were developed using two standard gradation types (Type 2 and Type 3) and three different aggregate sources (Lockwood, Spanish Spring, and Mustang), with 15% RAP content and a PG64-28NV SBS polymer-modified binder.

Based on the mix design process, laboratory performance testing, and data analysis, the following key findings and conclusions are drawn:

Effect of P200 on Stiffness: Increasing P200 content consistently resulted in lower dynamic modulus (E^*) values, especially at lower frequencies (0.1 Hz and 0.01 Hz), suggesting a significant reduction in structural stiffness and load-bearing capacity of the AC mixtures.

Rutting Resistance: HWTT results showed a direct correlation between higher P200 content and increased rutting susceptibility. This trend was particularly noticeable in Type 3 mixtures, indicating that excess fines compromise resistance to permanent deformation under repeated loading.

Cracking Resistance: The IDEAL-CT results revealed that mixtures with higher P200 content became stiffer and more brittle, particularly after mid-term aging, leading to lower cracking

resistance. Conversely, lower P200 mixtures showed improved flexibility and better performance against cracking.

Air Voids and Binder Adjustments: Some modified mixtures failed to meet the $4\pm 1.5\%$ air voids specification, highlighting that changes in P200 content impact volumetric properties. Adjustments in binder content were necessary to bring these mixtures back into specification, indicating a need for careful control of binder content alongside fines during mix design.

Material Variability: Aggregate source played a role in performance outcomes, with variations in stiffness, rutting depth, and cracking resistance observed across the Lockwood, Spanish Spring, and Mustang aggregates. This suggests source-specific behavior of fine materials must be considered during design and construction.

Durability Considerations: Mid-term aged samples demonstrated that the adverse effects of excessive fines are amplified over time, indicating the need for precise control of fine aggregate content during production and placement.

In summary, the study confirms that the P200 content has a critical influence on AC mixture performance. Proper control of fine materials is essential for ensuring balance between durability, flexibility, and resistance to deformation.

7.2 Recommendations

Based on the results of this study, the following recommendations are proposed to optimize asphalt mix performance and guide future research.

Construction and Quality Control

- **Tighter Control on P200 During Construction:** Field production should include regular monitoring of P200 content to ensure it remains within a narrow and optimized range. Real-time adjustments to maintain mix uniformity and performance targets are strongly recommended.
- **Binder Content Adjustments:** When modifying P200 content, corresponding binder adjustments must be made to maintain air voids within specifications and preserve mixture workability and cohesion.

Mix Design Enhancements

- **Re-Evaluation of Specifications:** RTC and similar standard-setting agencies may consider revisiting P200 tolerances in Type 2 and Type 3 gradations to better account for modern performance-based mix designs.
- **Source-Specific Calibration:** Since aggregate source affects the behavior of fines, regional calibration of mix designs using locally available materials is suggested for more accurate performance predictions.

Future Research Recommendations

- **Long-Term Aging Studies:** Extend laboratory aging protocols to simulate long-term field conditions to assess the evolution of fatigue cracking and stiffness degradation across varying P200 levels.
- **Mechanistic-Empirical Modeling:** Incorporate the experimental data into pavement design software (e.g., MEPDG) to validate lab-based findings under real-world traffic and climate conditions.

- Alternative Fine Materials and Additives: Explore the use of modified fillers, fibers, or nano-materials to improve mix durability and performance while minimizing the negative impacts of excess fines.
- Moisture Sensitivity Evaluation: While not a focus of this study, future work could include moisture susceptibility testing such as Tensile Strength Ratio (TSR) to further understand P200's influence on water damage resistance.

In conclusion, this study demonstrates that small changes in P200 content can significantly influence the performance of asphalt mixtures. As pavement design continues to transition toward performance-based specifications, controlling P200 content, will be crucial for optimizing both short-term constructability and long-term durability of asphalt pavements.

Chapter 8: References

- [1] J. C. Nicholls, M. J. McHale, and R. D. Griffiths., “Best practice guide for durability of asphalt pavements.” TRL Limited, 2008, ISBN: 978-1-84608-709-7.
- [2] N. Badreddine, "Analysis of fine asphalt concrete mixture gradations from various sources to enhance durability," M.S. thesis, Dept. of Civil and Environmental Engineering, Univ. of Nevada, Reno, 2024.
- [3] Regional Transportation Commission of Washoe County (RTC), Standard Specifications for Public Works Construction – Revision No. 9, Reno, NV, USA, 2016. [Online]. Available: <https://rtcwashoe.com/wp-content/uploads/2023/10/2016-Version-Revision-No.-9.pdf>
- [4] A. Golalipour, E. Jamshidi, Y. Niazi, Z. Afsharkia, and M. Khadem, "Effect of aggregate gradation on rutting of asphalt pavements," *Procedia - Social and Behavioral Sciences*, vol. 53, pp. 440–449, 2012.
- [5] P. E. Sebaaly and G. Bazi, "Impact of construction variability on pavement performance," Univ. of Nevada, Reno, Reno, NV, USA, Final Rep., 2005.
- [6] A. H. M. Afaf, "Effect of aggregate gradation and type on hot asphalt concrete mix properties," *Journal of Engineering Sciences*, vol. 42, no. 3, pp. 567–574, May–Jun. 2014.
- [7] P. S. Kandhal and S. Chakraborty, "Effect of asphalt film thickness on short and long-term aging of asphalt paving mixtures," *Transportation Research Record*, vol. 1535, no. 1, pp. 83–90, 1996.
- [8] P. S. Kandhal, "Evaluation of Baghouse Fines for Hot Mix Asphalt- Part I," National Asphalt Pavement Association, Lanham, MD, Information Series 127, 1999.
- [9] J. A. Musselman, B. Choubane, and P.B. Upshaw, “Superpave Field Implementation: Florida’s Early Experience,” *Transportation Research Board*, vol. 1609, no. 1, 1998.

- [10] B. A. Chadbourn, E. L. Skok and D. E. Newcomb, "The Effect of Voids in Mineral Aggregate (VMA) on Hot-Mix Asphalt Pavements," Minnesota Department of Transportation, Minnesota, 1999
- [11] ASTM International, ASTM D6927-15: Standard Test Method for Marshall Stability and Flow of Asphalt Mixtures. ASTM International, West Conshohocken, PA, USA, 2015. Available: <https://www.astm.org/d6927-15.html>
- [12] F. Hierholzer and A. Hand, "Investigation of the Current Levels of Dust-to-Binder Ratio on Durability of Asphalt Mixtures," University of Nevada, Reno, 2021.
- [13] P. B. D. Brian D, Z. Jingna and B. E Ray, "Aggregate Properties and the Performance of Superpave-Designed Hot Mix Asphalt - NCHRP Report 539," Transportation Research Board, 2005.
- [14] F. Zhou et al., "Experimental Design for Field Validation of Laboratory Tests to Assess Cracking Resistance of Asphalt Mixtures, Project Final Report, National Cooperative Highway Research Program, Transportation Research Board, National Academies of Science," 2016.
- [15] D. Park, W.-J. Seo, J. Kim, and H. V. Vo, "Evaluation of moisture susceptibility of asphalt mixture using liquid anti-stripping agents," *Construction and Building Materials*, vol. 148, pp. 399–405, 2017.
- [16] N. Raveendran and A. Hand, "Investigation of Fine Asphalt Concrete Mixture Gradations with Improved Durability," University of Nevada, Reno, Reno, NV, USA, Final Report 2023.
- [17] F. L. Roberts, P. S. Kandhal, E. R. Brown, D. Y. Lee, and T. W. Kennedy, *Hot Mix Asphalt Materials, Mixture Design, and Construction*, 2nd ed. Lanham, MD, USA: National Asphalt Pavement Association Research and Education Foundation, 1996.

- [18] W. Li, W. Cao, X. Ren, S. Lou, S. Liu, and J. Zhang, "Impacts of aggregate gradation on the volumetric parameters and rutting performance of asphalt concrete mixtures," *Materials*, vol. 15, no. 14, p. 4866, 2022.
- [19] Y. Yue, M. Abdelsalam, and M. S. Eisa, "Aggregate gradation variation on the properties of asphalt mixtures," *Coatings*, vol. 12, no. 11, p. 1608, 2022.
- [20] E. R. Brown, J. L. McRae, and A. B. Crawley, "Effect of aggregates on performance of bituminous concrete," in *Implication of Aggregates in the Design, Construction, and Performance of Flexible Pavements*, ASTM STP 1016, Philadelphia, PA, USA: American Society for Testing and Materials, pp. 34–63, 1989.
- [21] J. Wang et al., "Crack resistance investigation of mixtures with reclaimed SBS modified asphalt pavement using the SCB and DSCT tests," *Construction and Building Materials*, vol. 265, p. 120365, 2020.
- [22] E. R. Brown and J. E. Haddock, "A study of fine aggregate angularity using a modified flow test," *Journal of the Association of Asphalt Paving Technologists*, vol. 84, pp. 545–568, 2015.
- [23] Brown, E. R., & Haddock, J. E. (2015). A study of fine aggregate angularity using a modified flow test. *Journal of the Association of Asphalt Paving Technologists*, 84, 545-568. [Blank]
- [24] R. C. West, D. H. Timm, and J. R. Willis, "Investigation of the relationship between dust proportion and performance of asphalt mixtures," National Center for Asphalt Technology (NCAT), Auburn University, Auburn, AL, USA, Report 18-03, 2018.
- [25] American Association of State Highway and Transportation Officials (AASHTO), AASHTO M 320-22: Standard Specification for Performance-Graded Asphalt Binder, in

- Standard Specifications for Transportation Materials and Methods of Sampling and Testing, 42nd ed., Washington, DC, USA: AASHTO, 2024.
- [26] American Association of State Highway and Transportation Officials, AASHTO M 332-22: Standard Specification for Performance-Graded Asphalt Binder Using Multiple Stress Creep Recovery (MSCR) Test. In Standard Specifications for Transportation Materials and Methods of Sampling and Testing, 42nd Edition. Washington, D.C.: AASHTO, 2024.
- [27] AASHTO T 11-22: American Association of State Highway and Transportation Officials. (2024). Standard Method of Test for Materials Finer Than 75- μm (No. 200) Sieve in Mineral Aggregates by Washing (AASHTO Designation: T 11-22). In Standard Specifications for Transportation Materials and Methods of Sampling and Testing, 42nd Edition.
- [28] AASHTO T 27-22: American Association of State Highway and Transportation Officials. (2022). Standard Method of Test for Sieve Analysis of Fine and Coarse Aggregates (AASHTO Designation: T 27-22). In Standard Specifications for Transportation Materials and Methods of Sampling and Testing, 42nd Edition.
- [29] National Asphalt Pavement Association, RAP Benefits for Pavement Owners, Nov. 2021. [Online]. Available: https://www.asphalt pavement.org/uploads/documents/Sustainability/NAPA_RAP_Benefits_for_Pavement_Owners_1121.pdf
- [30] American Association of State Highway and Transportation Officials (AASHTO). (2023). Standard Method of Test for Quantitative Extraction and Recovery of Asphalt Binder from Asphalt Mixtures (AASHTO T 319-23). In Standard Specifications for Transportation Materials and Methods of Sampling and Testing and Provisional Standards (43rd Edition). Washington, D.C.: AASHTO.

- [31] ASTM D6926-20: ASTM International. (2020). Standard Practice for Preparation of Asphalt Mixture Specimens Using Marshall Apparatus (ASTM D6926-20). West Conshohocken, PA: ASTM International.
- [32] AASHTO T 245-22: American Association of State Highway and Transportation Officials. (2022). Standard Method of Test for Resistance to Plastic Flow of Asphalt Mixtures Using Marshall Apparatus (AASHTO T 245-22). Washington, D.C.: AASHTO.
- [33] L. Santucci, "Minimizing Moisture Damage in Asphalt Pavements," *Pavement Technology Update*, vol. 2, no. 2, Oct. 2010.
- [34] American Association of State Highway and Transportation Officials (AASHTO), Standard Method of Test for Resistance of Compacted Asphalt Mixtures to Moisture-Induced Damage, AASHTO T 283-22, Washington, D.C.: American Association of State Highway and Transportation Officials, 2024.
- [35] American Association of State Highway and Transportation Officials (AASHTO), Standard Method of Test for Determining the Dynamic Modulus and Flow Number for Asphalt Mixtures Using the Asphalt Mixture Performance Tester (AMPT), AASHTO T 378-22, Washington, D.C., USA: AASHTO, 2024.
- [36] AASHTO, Standard Practice for Developing Dynamic Modulus Master Curves for Asphalt Mixtures Using the Asphalt Mixture Performance Tester (AMPT), AASHTO R 84-17, American Association of State Highway and Transportation Officials, Washington, D.C., 2023.
- [37] AASHTO, Standard Method of Test for Hamburg Wheel-Track Testing of Compacted Asphalt Mixtures, AASHTO T 324-19, American Association of State Highway and Transportation Officials, Washington, D.C., 2019.

- [38] P. Tavassoti and H. Baaj, "Moisture Damage in Asphalt Concrete Mixtures: State of the Art and Critical Review of the Test Methods," presented at the Transportation Association of Canada (TAC) Annual Conference, Vancouver, BC, Canada, Oct. 2020.
- [39] ASTM International, ASTM D8225-19: Standard Test Method for Determination of Crack Resistance of Asphalt Mixtures Using the Indirect Tensile (IDT) Test at High Temperatures, ASTM International, West Conshohocken, PA, 2019.
- [40] T. Bennert, E. Haas, and E. Wass, "Indirect Tensile Test (IDT) to Determine Asphalt Mixture Performance Indicators during Quality Control Testing in New Jersey," *Transportation Research Record*, vol. 2672, no. 28, pp. 394–403, Aug. 2018, doi: 10.1177/0361198118793276.
- [41] R. West, J. Moore, and A. Taylor, "Balanced Mix Design for Surface Asphalt Mixtures: Phase I," Virginia Transportation Research Council, VTRC 20-R15, Apr. 2020.
- [42] F. Hierholzer and A. Hand, "Investigation of the Current Levels of Dust-to-Binder Ratio on Durability of Asphalt Mixtures," University of Nevada, Reno, 2021.
- [43] P. Romero-Zambrana, "Variability of the IDEAL-CT Test for Pavement Cracking to Achieve a Balanced Asphalt Mix Design," Mountain-Plains Consortium, MPC-589, Feb. 2023.
- [44] D. N. Little and J. A. Epps, "The Benefits of Hydrated Lime in Hot Mix Asphalt," National Lime Association, 2001.
- [45] American Association of State Highway and Transportation Officials, *Mechanistic-Empirical Pavement Design Guide: A Manual of Practice*. Washington, D.C.: AASHTO, 2008.

- [46] E. Y. Hajj, P. E. Sebaaly, M. Piratheepan and P. Nabhan, "Manual for Designing Flexible Pavements in Nevada Using the AASHTOWare Pavement ME - WRSC- 201504," Nevada Department of Transportation, Carson City, 2019.
- [47] Nevada Department of Transportation, "Characterization of Unbound Materials for Mechanistic-Empirical Pavement Design for NDOT Districts 2 and 3," 2020.